PB-251 587

OZONE AND PARTICULATE FORMATION IN PHOTOCHEMICAL REACTIONS

Chi-Hung Shen, et al

Michigan University

Prepared for:

Environmental Protection Agency

April 1975

DISTRIBUTED BY

NTIS

National Technical Information Service
U. S. DEPARTMENT OF COMMERCE

100172

PB 251 587

EPA-460/3-76-005
April 1975

OZONE AND PARTICULATE FORMATION IN PHOTOCHEMICAL REACTIONS

U.S. ENVIRONMENTAL PROTECTION AGENCY
Office of Air and Waste Management
Office of Mobile Source Air Pollution Control
Emission Control Technology Division
Ann Arbor, Michigan 48105

REPRODUCED BY
NATIONAL TECHNICAL
INFORMATION SERVICE
U.S. DEPARTMENT OF COMMERCE
SPRINGFIELD, VA. 22161

EPA-460/3-76-003

OZONE AND PARTICULATE FORMATION IN PHOTOCHEMICAL REACTIONS

by

Chi-Hung Shen and George T. Springer

The University of Michigan
Ann Arbor, Michigan 48104

Grant No. R-801176

EPA Project Officer: Gordon J. Kennedy

Prepared for

U.S. ENVIRONMENTAL PROTECTION AGENCY
Office of Air and Waste Management
Office of Mobile Source Air Pollution Control
Emission Control Technology Division
Ann Arbor, Michigan 48105

April 1976

ABSTRACT

Experiments were performed to investigate the photochemical formation of nuclei and aerosols in sulfur dioxide-air mixtures and the photochemical formation of ozone, nuclei, and aerosols in cyclohexene-nitrogen dioxide-air mixtures. The mixtures were irradiated by ultraviolet fluorescent lamps while flowing at a steady speed through a 3.12 m long and 15.2 cm I.D. Pyrex tube. The amounts of ozone, nuclei, and aerosols generated in the gas-air mixtures were measured at various points along the tube by a chemiluminescent analyzer, a condensation nuclei counter, and an aerosol counter, respectively.

Photooxidation experiments with sulfur dioxide-air mixtures were performed for five different initial sulfur dioxide concentrations (0.2, 0.3, 0.5, 0.7, and 1 ppm) and for four relative humidities (25, 50, 75, and 100%). The data showed that the maximum number of nuclei produced is directly proportional to the initial sulfur dioxide concentration and to the square of the relative humidity. There were no measurable amounts of aerosols observed during the tests.

Experiments with cyclohexene-nitrogen dioxide-air mixtures were performed with the initial cyclohexene concentration ranging from 0.5 to 50 ppm and the initial nitrogen dioxide concentration from 0.6 to 10 ppm. The relative humidity was kept constant at 50%. The amount of ozone produced depended on the initial concentrations of cyclohexene and nitrogen dioxide as well as on the light intensity. On the basis of the present measurements and the data obtained by previous investigators, the maximum amount of ozone was found to be given by the expression

$$[O_3]_{max} = 0.13 \sqrt{k_1} \sqrt{[HC]_0}$$

and

$$[O_3]_{max} = 0.13 \sqrt{k_1 R} \sqrt{[NO_2]_0}$$

Here, k_1 represents the nitrogen dioxide photodissociation rate constant in s^{-1} and is proportional to the light intensity. R is the concentration ratio of the hydrocarbon to nitrogen dioxide at which the ozone content is maximum. The value of R was found to be related to the relative hydroxyl rate constant $\hat{k}_g$ by $R = 5.1/\sqrt{\hat{k}_g}$.

The maximum number of nuclei produced varied directly with the square root of both the cyclohexene concentration and the nitrogen dioxide concentration.

The maximum number of aerosols produced appeared to depend only on the concentration ratio of cyclohexene to nitrogen dioxide and seemed to be insensitive to the initial cyclohexene and nitrogen dioxide concentrations. The aerosol size distributions were also measured and followed closely Friedlander's universal self-preserving curve.

TABLE OF CONTENTS

	Page
LIST OF FIGURES	vi
LIST OF TABLES	ix
LIST OF APPENDICES	x
CHAPTER	
I. INTRODUCTION	1
1.1 Literature Survey	2
1.2 Objective	5
II. EXPERIMENTAL APPARATUS	7
2.1 Test Section	7
2.2 Gas Supply System	14
2.3 Measuring Instruments	18
III. EXPERIMENTAL PROCEDURE	28
IV. PHOTOCHEMICAL PARTICULATE FORMATION IN SULFUR DIOXIDE-AIR MIXTURES	40
V. OZONE AND PARTICULATE FORMATION IN CYCLOHEXENE-NITROGEN DIOXIDE-AIR MIXTURES	52
5.1 The Effects of Mixture Composition on Ozone Formation	53
5.2 The Effects of Mixture Composition on Particulate Formation	77
VI. CONCLUDING REMARKS	94
APPENDIX	98
REFERENCES	122

List of Figures

Figure		Page
2.1	Schematic of experimental apparatus	8
2.2	Schematic of the sampling probes	9
2.3	Spectral energy of the ultraviolet light as specified by the manufacturer	13
2.4	Correspondence between the aerosol diameter and the channel number on the multichannel analyzer	20
2.5	Typical aerosol size distribution in room air and in the tunnel	21
2.6	Size distribution of aerosols in room air	25
3.1	Variation of ozone and nuclei contents with time along the tunnel	29
3.2	Variation of ozone, nuclei, and aerosol contents with time along the tunnel	30
3.3	Spectral energy of the light inside the tunnel	32
3.4	Ozone content along the tunnel in various nitrogen dioxide-air mixtures	35
3.5	Relationship between the photostationary content of ozone and the initial concentration of nitrogen dioxide	36
4.1	Number of nuclei formed as a function of irradiation time in sulfur dioxide-air mixtures	41
4.2	Number of nuclei formed in sulfur dioxide-air mixtures	43
4.3	Number of nuclei formed in sulfur dioxide-air mixtures	44
4.4	Number of nuclei formed in sulfur dioxide-air mixtures. Correlation of the data for various initial sulfur dioxide concentrations $[SO_2]_0$ and initial relative humidities ϕ_0	46
4.5	Formation of sulfuric acid in sulfur dioxide-air mixtures	50
4.6	Amount of light scattered from sulfur dioxide-air mixtures	51

LIST OF FIGURES (continued)

Figure		Page
5.1	Typical variations of ozone, nuclei, and aerosol contents along the tunnel in cyclohexene-nitrogen dioxide-air mixtures	54
5.2	Ozone content in cyclohexene-nitrogen dioxide-air mixtures	58
5.3	Ozone content in cyclohexene-nitrogen dioxide-air mixtures	59
5.4	Normalized ozone content in cyclohexene-nitrogen dioxide-air mixtures	64
5.5	Normalized ozone content in hydrocarbon-nitrogen oxides-air mixtures	65
5.6	Maximum amount of ozone M as a function of the concentration ratio R at which M occurs	69
5.7	Maximum amount of ozone as a function of the initial hydrocarbon concentration	70
5.8	Maximum amount of ozone as a function of the initial nitrogen oxides concentration	72
5.9	Variation in the concentration ratio R (at which the ozone content is maximum) with the reactivity k_y	75
5.10	Ozone content in cyclohexene-nitrogen dioxide-air mixtures	76
5.11	(a) Oxidant content in the atmosphere, and (b) ozone content in propylene-nitric oxide-air mixtures	78
5.12	Nuclei content in cyclohexene-nitrogen dioxide-air mixtures	80
5.13	Nuclei content as a function of the initial concentration ratio in cyclohexene-nitrogen dioxide-air mixture	82
5.14	Aerosol content in cyclohexene-nitrogen dioxide-air mixtures	85
5.15	Aerosol content as a function of the initial concentration ratio in cyclohexene-nitrogen dioxide-air mixtures	86

LIST OF FIGURES (continued)

Figure		Page
5.16	Light scattering from aerosols produced in cyclohexane-nitrogen dioxide-air mixtures	80
5.17	Aerosol size distribution obtained in the tunnel for cyclohexane-nitrogen dioxide-air mixtures	81

LIST OF TABLES

Table		Page
2.1	Flowrates of the Flowmeters used in the Experiments	16
3.1	Rates of Photodissociation of Nitrogen Dioxide in the Lower Atmosphere in the Wavelength Range 29[1] to 430 nm	38
3.2	Summary of values of k_1 used in Differerent Experiments	39
4.1	Summary of Experimental Conditions used by Different Investigators	47
5.1	The Reaction Mechanism Proposed by Eschenroeder and Martinez [19]	56
5.2	Reactivities of Different Hydrocarbons ($\bar{k} = k/KC\ gm_p$)	74

LIST OF APPENDICES

Appendix		Page
A.	LITERATURE SURVEY	98
B.	CERTIFIED CONCENTRATION OF TEST GASES	106
C	ESTIMATION OF PARTICLE LOSSES DUE TO SETTLING, COAGULATION, AND DIFFUSION	107
	C.1 Loss due to Settling	107
	C.2 Loss due to Coagulation	109
	C.3 Loss due to Diffusion	109
D.	TABULATION OF EXPERIMENTAL DATA	112
	D.1 Ozone Content along the Tunnel	112
	D.2 Nuclei and Aerosol Contents along the Tunnel	116
E.	ESTIMATED PEAK VALUES OF OZONE, NUCLEI AND AEROSOLS FOR DIFFERENT INITIAL MIXTURE CONDITIONS	120

CHAPTER I

INTRODUCTION

It is well recognized that ozone and particulate matter contribute to the problem of air pollution. Excessive amounts of ozone in the atmosphere accelerate the degradation processes of elastomers and textiles, and adversely affect the growth of plants [69]. High concentrations of particulate matter in the atmosphere reduce visibility [66]. Ozone and particulate matter are also major constituents of smog [66,69]. In order to determine the amounts of ozone and particulates in the atmosphere, and to establish effective means for controlling the production of these pollutants, it is necessary to understand in detail the processes by which ozone and particulates are generated. This study is addressed to one aspect of the problem, namely, the formation of ozone and particulates due to photochemical reactions.

Ozone is formed photochemically in the atmosphere when a mixture of nitrogen oxides (nitrogen dioxide or nitric oxide) and certain types of hydrocarbons is irradiated by sunlight [3,8,31,53,69]. Nitrogen oxides and hydrocarbons are usually introduced into the atmosphere by automotive vehicles [68,70]. Hence, large amounts of ozone are produced in areas where the traffic is heavy and where the weather conditions are such that there is much sunshine but little chance for the automobile exhaust to disperse rapidly.

Particulates* are formed photochemically when air containing sulfur dioxide, or nitrogen oxides and hydrocarbons is irradiated [3,8,28,51,61,66].

* In reference [66], NAS has suggested that "particle" or "particulate" be defined as any dispersed matter, solid or liquid (except uncombined water), in which the individual aggregates are larger than single molecules ($\sim$ 0.2 μm dia.) but smaller than about 500 μm in diameter.

Since automotive vehicles may emit considerable quantities of sulfur dioxide, nitrogen oxides and hydrocarbons, photochemical particulates may form whenever there is heavy traffic. Sulfur dioxide is also introduced into the atmosphere by power plants burning high sulfur content fuels [67]. In the vicinity of such plants, the amount of particulates produced due to photooxidation of sulfur dioxide may also be significant.

In view of the importance of the ozone and the particulates formed by photochemical reactions, the mechanisms by which they are produced need to be understood and the amounts generated need to be known. Although this problem has been investigated widely, many facets of the problem still remain unclear. The overall objective of this study was to perform experiments with the aim of obtaining information which will contribute to the general understanding of the photochemical formation of ozone and particulates, and provide quantitative data on the amounts of ozone and particulate matter formed. The specific goals of this study are listed at the end of this section. First, however, a brief survey is given of the previous relevant investigations. A detailed survey of past research efforts is presented in Appendix A.

1.1 Literature Survey

In most previous experiments studying photochemical reactions, the procedure normally employed was the following. The gas-air mixture to be studied was introduced into a chamber. The chamber was then irradiated by sunlight or artificial ultraviolet light, and selected reaction products were monitored.

The production of ozone during the photooxidation of hydrocarbon-nitrogen oxides-air mixtures has been studied by several investigators

[2,5,6,7,10,25,31,41,50,51,58]. The data are generally presented in one of three ways: 1) the initial ozone formation rate [25], 2) the ozone dosage (i.e. the integral of the ozone content versus time curve [6,7,10], and 3) the amount of ozone produced [2,5,31,41,50,51]. Of these three types of measurements, the last one is of the greatest interest to us, because only this type of measurement provides data which gives directly the maximum amount of the ozone generated.

The production of ozone in the presence of nitrogen oxides and several different types of hydrocarbons has been studied. Ozone measurements with paraffins were reported in references [6,31,50], with olefins in references [2,5,10,25,31,51,58], with aromatics in references [7,25,31], and with aldehydes in reference [41]. Unfortunately, the information provided by many of the available data were limited, because most measurements were made only for a few selected initial concentrations of the hydrocarbon and the nitrogen oxides. Consequently, it is difficult to extend the applicability of the data to conditions beyond which they were obtained, to correlate the results of the various experiments, and to draw general conclusions from the existing data. In order to provide additional insight into the photochemical formation of ozone, a series of tests would be needed in which the initial concentrations of the hydrocarbon and the nitrogen oxides were varied systematically over a wide range.

The particulate formation in hydrocarbon-nitrogen oxides-air mixtures and hydrocarbon-nitrogen oxides-sulfur dioxide-air mixtures has also been investigated [27,29,47,49,51,59]. In most of the previous particulate experiments, the initial concentrations of the hydrocarbon and the nitrogen oxides were kept constant and only the type of hydro-

carbon was varied. Experiments have been performed with the following types of hydrocarbons: paraffins [29,47,49], olefins [27,29,47,49,53,59], cyclo-olefins [28,29,47,49,59], diolefins [29,47,49,51], and aromatics [28,29,39]. The results of these investigations indicate that certain types of hydrocarbons produce particles under certain experimental conditions. The results, however, do not provide information for those concentrations which have not been tested. In order to obtain a better understanding of the particulate formation process, a comprehensive experiment would be necessary in which the initial concentrations of the hydrocarbon and the nitrogen oxides were varied over a range.

Several experiments have been performed in the past for measuring particulates in sulfur dioxide-air mixtures [13,14,17,24,40,48,49]. The major goal of these experiments was to determine the effects of the initial sulfur dioxide concentration and the relative humidity on the number of particles formed. Most results indicate that the number of particles formed increased with increasing amounts of initial sulfur dioxide concentration. However, the relationship between the amount of particulate matter and the initial sulfur dioxide concentration is not yet well established. The effect of humidity on the amount of particulate matter formed is also subject to debate. For example, Gerhard and Johnstone [24] and Owon et. al. [48] found that the humidity had no effect on the amount of particles formed; Renzetti and Doyle [49], demonstrated that humidity influenced significantly the formation of particles. Thus, a need for further study of the effects of the initial sulfur dioxide concentration and the relative humidity on particulate formation is evident.

1.2 Objective

The foregoing survey indicates the need for further work on the photochemical formation of ozone and particulates in mixtures of hydrocarbon-nitrogen oxides-air mixtures in which the initial concentrations of the hydrocarbon and the nitrogen oxides are varied over a wide range. Particulate formation in sulfur dioxide-air mixtures also require further investigation. Therefore, the major goals of this study were: 1) to design and build an apparatus suitable for studying photochemical reactions in gas mixtures, and 2) to determine the amounts of ozone and particulates formed in selected mixtures. In particular, experiments were performed to investigate the following problems.

1) Particulate formation in sulfur dioxide-air mixtures and the evaluation of the amount of particulates produced as a function of a) the length of time the mixture is irradiated, b) the initial sulfur dioxide concentration, and c) the relative humidity.

2) Ozone formation and particulate formation in a hydrocrabon-nitrogen dioxide-air mixture, and the determination of the amounts of ozone and particulates formed for different initial concentrations of the hydrocarbon and the nitrogen dioxide. In the present study, cyclohexene was selected as the hydrocarbon because it has been shown to produce large quantities of particulates in photochemical reactions [29,47,49,59].

The ozone concentration was measured by a chemiluminescent analyzer. The particles were examined in two different categories. The first category contained those particles whose diameters were between 2 nm and 0.1 μm. These particles were designated as condensation nuclei and were measured by a condensation nuclei counter. In the second category

were those particles whose diameters were greater than about 0.3 μm. These particles were designated as aerosols, and were measured by a Royco Particle Counter. The number concentrations (no. per cm^3) of the condensation nuclei and of the aerosols, as well as the size distribution of the aerosols were all measured in the present experiment.

CHAPTER II

EXPERIMENTAL APPARATUS

The experiment was performed in a flow type apparatus which consisted of: 1) the test section, 2) the gas supply system, and 3) various measuring instruments (Fig. 2.1).

2.1 Test Section

The test section had three major components, the irradiation tunnel, the gas mixing chamber, and the lighting system (Fig. 2.1).

The photochemical reactions were generated in the irradiation tunnel. This tunnel was made from six identical Pyrex glass tubes joined together. The tubes were arranged horizontally in a straight line. Pyrex glass was selected because of its excellent chemical resistance and constant ultraviolet transmissivity [39,5P]. Each tube was 1.52 m long and 15.2 cm I.d. with a wall thickness of 0.84 cm. The tubes were connected by compression couplings lined with teflon gaskets. The six sections together were 9.12 m long and had a total volume of approximately 0.166 m^3. Two openings were made in the wall of each tube, through which the sampling probes were inserted. These openings were located on top of the irradiation tunnel. The first opening was 23 cm from the entrance of the tunnel. The distance between any two successive openings was 76 cm. A 5 cm long standard 10/30 outer ground glass joint was welded to each opening (Fig. 2.2).

Two types of sampling probes were used in the experiments, one for sampling particulates and one for sampling ozone (Fig. 2.2). The probes for the particulates were made from 0.636 cm o.d. stainless steel tubing with a wall thickness of 0.075 cm. Each probe was 30 cm long.

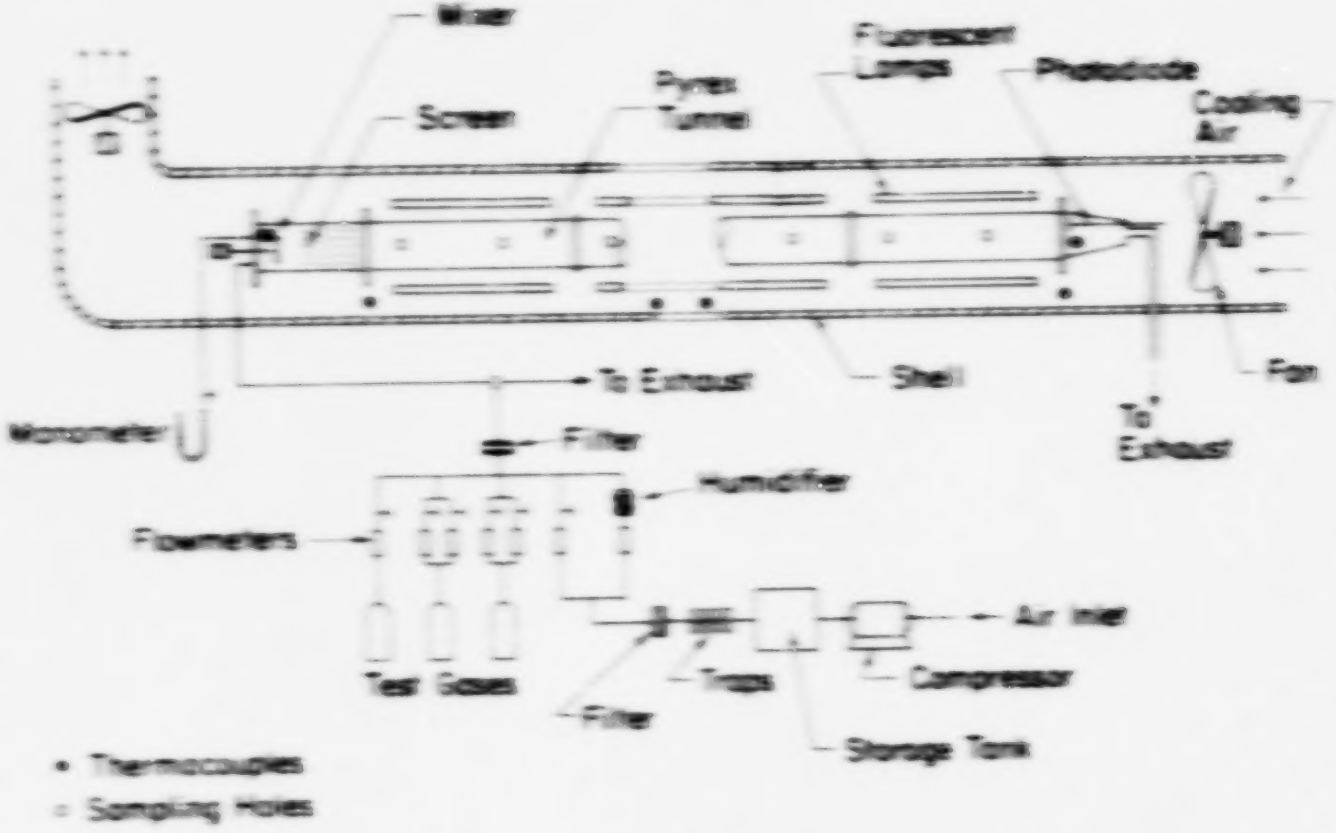
Mixer
Screen
Pyrex Tunnel
Fluorescent Lamps
Photodiode
Cooling Air
Fan
To Exhaust
Shell
To Exhaust
Manometer
Filter
Humidifier
Flowmeters
Air Inlet
Test Gases
Traps
Compressor
Filter
Storage Tank
• Thermocouples
○ Sampling Holes

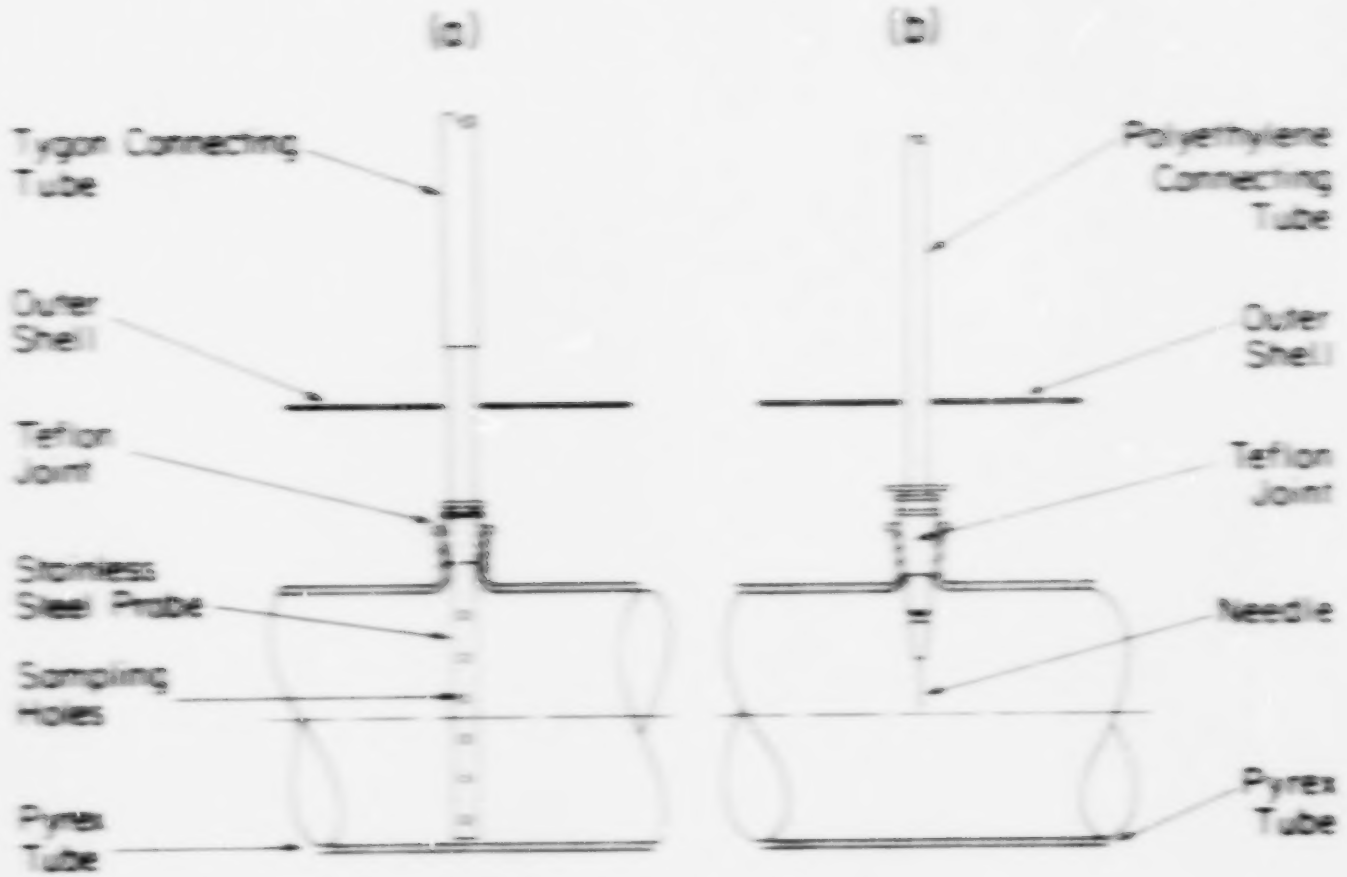

Fig. [illegible] Schematic of the sampling probes (a) Probe for sampling particulates. (b) Probe for sampling water.

One end of each probe was sealed. Twelve 0.221 cm diameter holes were drilled into each probe. The holes were arranged in pairs, six holes being on one side of the probe and six on the opposite side. The first two holes were 1.27 cm from the sealed tip of the probe. The distance between each subsequent pair of holes was 2.54 cm. The probes were inserted into the irradiation tunnel through the ground glass openings, and were held in place by standard 10/18 teflon adaptor joints fitted with Viton-A O-rings. The probes were mounted vertically so that the closed tips were touching the bottom of the tunnel. The axes of the holes were normal to the direction of the flow, i.e., the holes faced the walls of the tunnel. The open end of each probe was outside the tunnel and was connected to a straight bore teflon stopcock by a 15 cm long tygon tube.

The ozone sampling probes were 26 gauge (0.02 cm i.d. and 1.27 cm long) hypodermic needles. The needles were connected to 1 cm^3 nominal capacity syringes (9 cm long and 0.46 cm i.d.). The stems of the syringes were mounted in the glass joints using standard 10/18 teflon adaptors fitted with Viton-A O-rings. The needles were placed vertically, with the openings about 4 cm deep inside the irradiation tunnel. The plungers inside the syringes were removed, and one end of a 60 cm long polyethylene intramedic tubing (0.376 cm i.d.) was inserted into each syringe. The other end of the tubing was either connected directly to the ozone analyzer (during measurements) or was sealed with a C-clamp.

The mixing chamber, made from a 30.4 cm long, 15.2 cm i.d. and 15.46 cm o.d. stainless steel tube, was connected to the upstream end of the irradiation tunnel (Fig. 2.1). The upstream end of the chamber

was covered by a stainless steel plate fitted with three 0.536 cm Swagelok connectors. One of the connectors was connected to the gas supply system and one to a mercury manometer. The third connector served as a thermocouple feedthrough for a copper-constantan thermocouple placed about 2 cm inside the mixing chamber.

The gas-air mixture inside the chamber was stirred by a 12.7 cm diameter fan rotating at 500 rpm. The fan was located 5 cm from the cover plate with its axis coinciding with the axis of the chamber. The fan was driven by a variable speed motor placed outside the mixing chamber and connected to the fan shaft by a rotary feedthrough.

Six stainless steel screens, serving as flow straighteners, were placed downstream of the fan. These screens were made of 0.08 cm thick perforated plates. The perforations were 0.316 cm diameter holes arranged uniformly in square arrays 0.48 cm apart from each other. The plates were cut into 15.2 cm diameter circles, and were fitted inside the mixing chamber so that the holes faced the flow. The screens were placed side by side with 2.5 cm between each screen. The last screen was at the end of the chamber.

The downstream end of the irradiation tunnel was connected to a 15.2 cm long hollow stainless steel cone (15.2 cm i.d. at upstream end, 10.2 cm i.d. at downstream end and 0.13 cm wall thickness). The downstream end of the cone was covered by a stainless steel plate, which had three openings in it. The first was 2.54 cm in diameter and was connected either to an exhaust vent or a vacuum pump. The second served as a feedthrough for a copper-constantan thermocouple probe placed 5 cm inside the tunnel. The third was used to insert a light intensity detector into the tunnel.

The ultraviolet radiation was produced by forty-eight F40BL (General Electric) fluorescent lamps. The initial spectral distribution of the lamps, provided by the manufacturer, is shown in Fig. 2.3. Each lamp was 1.22 m long and 3.8 cm in diameter. The lamps were arranged in six clusters along the tunnel, each cluster illuminating one section of the tunnel. Each cluster contained eight lamps placed around the tunnel systematically on a 31.7 cm diameter circle. The lamps in each cluster were mounted on two semi-circular (18.5 cm radius) galvanized metal shells. The insides of the shells were covered with aluminum foils. The shells thus served both as light fixtures and reflectors. The shells also provided ducting for the cooling air as explained below. The shells were hinged together and could be opened to install the lamps and the sampling probes. There were small holes along the upper edges of the shells to allow the sampling probes to pass through.

The ultraviolet lamps generated a large amount of heat. To minimize the temperature rise of the gas-air mixture inside the tunnel [9], room air was blown through the annulus between the irradiation tunnel and the shell. This air was blown by a 45 cm fan in the direction opposite to the flow inside the tunnel. The cooling air flowed along the entire length of the tunnel and was then discharged into an exhaust vent. The temperature of the cooling air was monitored by four copper-constantan thermocouples placed inside the annulus at equal intervals along the tunnel. The average temperature rise of the cooling air was 7°C. The temperature rise of the gas-air mixture in the tunnel (i.e. the temperature difference between the gas-air mixture in the sliding chamber and at the exhaust port) was always less than 4°C.

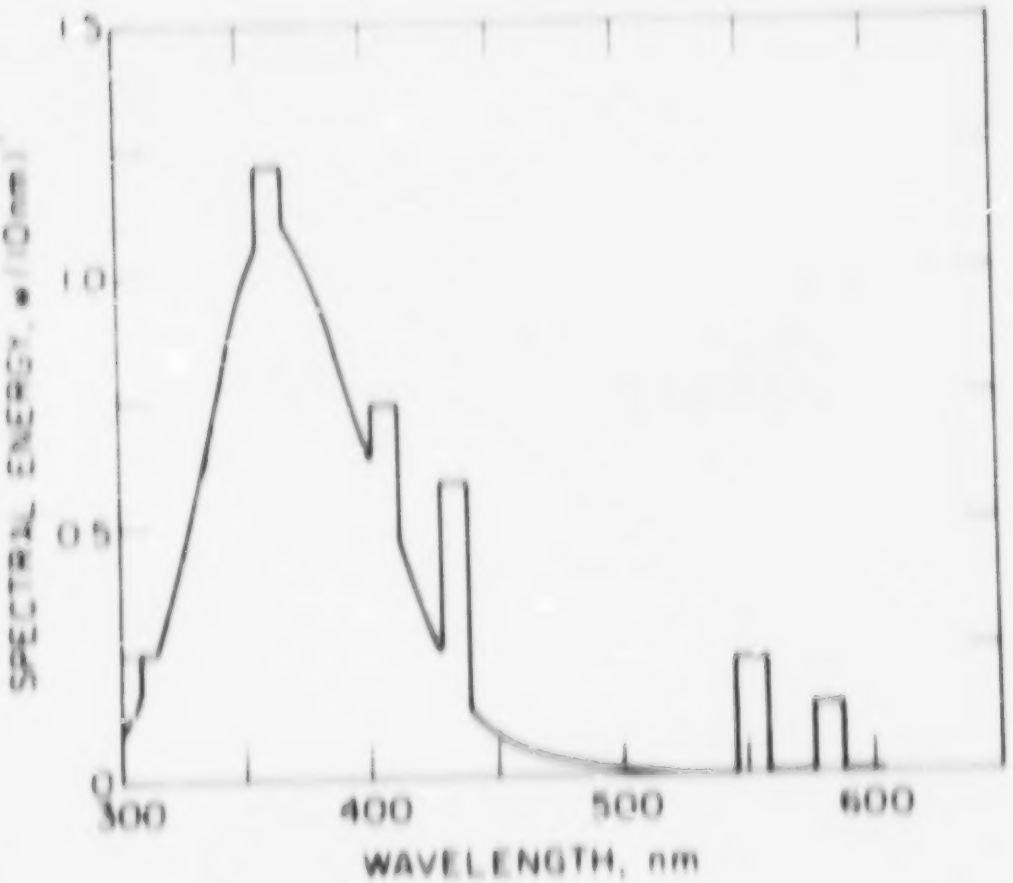

Fig. 2.1. Spectral energy of the ultraviolet light as specified by the manufacturer (General Electric Fluorescent Lamp Manual)

2.2 Gas Supply System

The air used in the experiments was supplied from an air-conditioned room kept at a constant temperature (20°C) and at a constant relative humidity (75%). The air was compressed by an oil-free, diaphragm type compressor (Sears; Model No. 15122) into a 0.03 m^3 storage tank. The air pressure inside the tank was maintained between 110 kN m^{-2} and 165 kN m^{-2} gauge pressures. The air stream from the tank passed through four traps connected in series. The first trap, consisting of 0.45 kg of activated carbon in a Plexiglas container, was installed to remove trace gases present in the air. The second trap was a 1.5 m long, 1.9 cm i.d. tygon tubing filled with anhydrous calcium chloride. The third trap was 0.45 kg of "indicating" anhydrous calcium sulfate packed in a glass jar. These latter two traps were intended to absorb the water vapor in the air stream. A change in color in the calcium sulfate from blue to pink indicated that the calcium chloride had been saturated and needed replacement. The fourth trap was a Gelman type A glass fiber filter for removing atmospheric aerosols from the air stream. After these four stages of purification, the air was branched into two streams. One stream, designated as "dry air", passed through a flowmeter and a needle valve. The other stream, which was to be saturated with water vapor, passed through a flowmeter, a needle valve, and a humidifier. The humidifier was made from a 13 cm high and 12.7 cm i.d. cylindrical Plexiglas chamber. The chamber was packed three-quarters full with 0.4 cm diameter glass spheres and filled with double-distilled water so that the water level was about 1 cm above the glass spheres. The temperature of the humidifier was kept constant (±0.5 °) by electrical heating tapes surrounded

by thermal insulation. The air was bubbled through the humidifier. The air, thus saturated with water vapor (100% relative humidity), was led through a water trap consisting of a 10 cm high and 4 cm i.d. cylindrical Plexiglas chamber. After passing through the trap and a needle valve, the saturated air was reunited with the dry air stream. The relative humidity of the test air was controlled by adjusting the flowrates of the two streams of air. For example, equal flowrates of the dry and saturated stream would result in an air of 50% relative humidity. The air stream was led through a 0.636 cm o.d., 0.486 cm i.d., and 60 cm long stainless steel tube until it was mixed with the test gases.

The test gases were supplied as special blends and were pre-diluted with pure dry nitrogen to approximately 200 ppm by the manufacturers. Nitrogen dioxide was obtained from the Air Products and Chemicals Company. Sulfur dioxide and cyclohexene were supplied by the Matheson Gas Company. The composition of each gas was individually analyzed and certified by the supplier (see Appendix B). The supply line of the test gases were made of 0.636 cm o.d. and 0.486 cm i.d. stainless steel tubing. The flowrates of each gas were regulated by stainless steel needle valves and were measured by two flowmeters connected in parallel. These flowmeters operated at different ranges of flowrates (see Table 2.1), allowing accurate measurements of the flowrates (and consequently the concentration of the test gases) over a wide range of values. After the flowmeters, the gas lines were joined with the line containing the humidity-controlled air. The entire gas-air mixture then passed through another Gelman type A glass fiber filter and a three-way stainless steel ball valve. This valve was used to admit the mixture either directly into the mixing chamber or into an exhaust vent.

Table 2.1 Flowrates of the Flowmeters Used in the Experiments
(all flowmeters were manufactured by Kontes Glass Company)

Gas	Flowmeter Size No.	Flowrate, $cm^3 s^{-1}$
Dry Air	1221	12-130
Moist Air	1221	12-130
Sulfur Dioxide	1123	0.08-1.75
Nitrogen Dioxide	1123	0.08-1.75
	1423	0.33-17.9
Cyclohexene	1123	0.08-1.75
	1423	0.33-17.9

It is noted here that the lengths of the gas supply lines from the tanks to the flowmeters were about 4 m, from the flowmeters to the connection with the air 0.6 m, and from this connection to the mixing chamber 1.5 m.

After the apparatus was assembled, the downstream end of the tunnel was connected to a mechanical vacuum pump, and the entire system was tested for leakage. The lowest pressure obtained in the system (including the gas lines, the mixing chamber, and the irradiation tunnel) was 66 N m^{-2}. The leak rate of the system was 3 mN m^{-2} s^{-1}.

During the experiments, the tunnel was not connected to the vacuum pump, but to an exhaust vent. The pressure in the vent was atmospheric. The pressure in the air supply line ahead of the traps was kept at 35 kN m^{-2} gauge. The pressure decreased considerably along the supply line till it became practically atmospheric in the mixing chamber, as indicated by the mercury manometer. The pressure drop inside the tunnel was less than 0.7 mN m^{-2}, so that the pressure throughout the tunnel was practically atmospheric during the tests.

The flowrate in the tunnel could be varied from 46 $cm^3 s^{-1}$ to 184 $cm^3 s^{-1}$. The average velocities corresponding to these flowrates were 0.26 cm s^{-1} and 1.04 cm s^{-1}. The Reynolds numbers, based on these velocities, were approximately 24 and 96, respectively. At such low Reynolds numbers the flow was expected to be laminar in the tunnel.

An estimate of the number of particles lost along the tunnel due to various mechanisms is presented in Appendix C. It was found that, in general, the loss of particles in the tunnel was negligible except when the particle diameter was either smaller than 0.01 μm or greater than 1 μm.

2.3 Measuring Instruments

In this investigation, measurements of the following parameters were of major concern: nuclei concentration, aerosol concentration, ozone concentration, total light intensity, and spectral distribution of the light.

The concentration of the condensation nuclei was measured by a "Small-Particle Detector" manufactured by Gardner Associates, Inc. In this instrument, the sample was drawn into a chamber lined with wet blotting paper. The pressure was then suddenly reduced in the chamber, resulting in water condensing on the nuclei present in the sample. A light beam was directed through the sample, and the decrease in light intensity (which is proportional to the number of nuclei) was measured by a photomultiplier. The output of the photomultiplier was displayed on a meter. The reading on this meter, together with a calibration chart supplied by the manufacturer, gave the number of nuclei per cm^3. The instrument could measure nuclei whose diameters were between 2 nm and 0.1 μm. The measurable concentration range was from 200 to $1x10^7$ nuclei cm^{-3}. The fluctuation of the instrument was within ±10% when the nuclei count was above 1000 per cm^3. The fluctuation became higher (±20%) when the nuclei count was smaller than 1000 per cm^3. The calibration chart provided by the manufacturer is accurate within ±20%. Thus the maximum percentage error in the nuclei measurement was about ± 30%. All condensation nuclei measurements presented in sections IV and V were the averages of at least three readings.

The concentrations of the aerosols (i.e. particles having diameters greater than 0.3 μm) were measured by a Royco Particle Counter (Model 225) coupled with a Royco plug-in unit (Module 507). This instrument

operated as follows: The sample was drawn into a chamber and a light was passed through it. The light scattered in the near-forward direction by the aerosols in the sample was measured by a photomultiplier. The output of this photomultiplier was calibrated by the manufacturer to indicate directly the number of aerosols in a certain size range. Although the unit could be used to measure the aerosol content in five different size ranges, in the present experiment, it was always set to measure the concentration of all the aerosols larger than 0.3 μm in diameter. The measured particle concentration was displayed digitally and was also recorded by a five-digit printer.

In order to measure the size distribution of the aerosols, a multichannel (128 channels) analyzer (Nuclear Data Inc., Model ND 555) was attached to the Royco Particle Counter. The output of the Royco Instruments was fed directly into the analyzer with each channel corresponding to a given particle size. The particle size corresponding to a particular channel was obtained by comparing the particle count on the Royco Instrument with the particle count given by the analyzer. This calibration was performed at the five particle size ranges available on the Royco Instruments (particle diameter greater than 0.3, 0.7, 1.4, 3, and 5 μm) (Fig. 2.4). The calibration could not be done accurately for particles between 0.7 and 1.4 μm because, in this size range, the output of the Royco Instruments varied with the particle size in a complex manner.

During the test, the output of the analyzer was displayed on a Tektronix oscilloscope (type 565 Dual-Beam). A typical result obtained with room air is shown in Fig. 2.5. Each bright dot in the picture

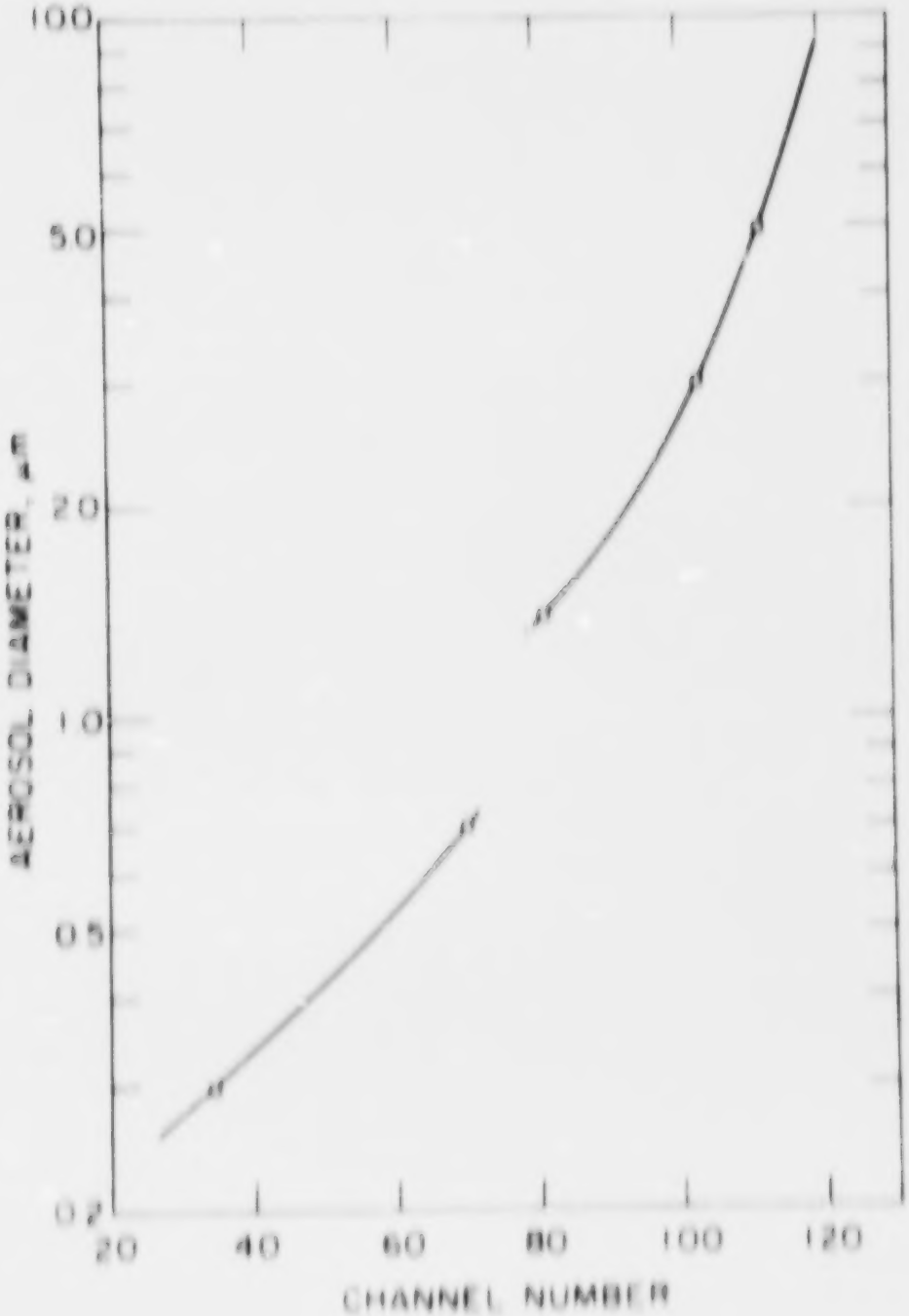
100
50
20
10
0.5
0.2
AEROSOL DIAMETER, μm
20
40
60
80
100
120
CHANNEL NUMBER

(b)

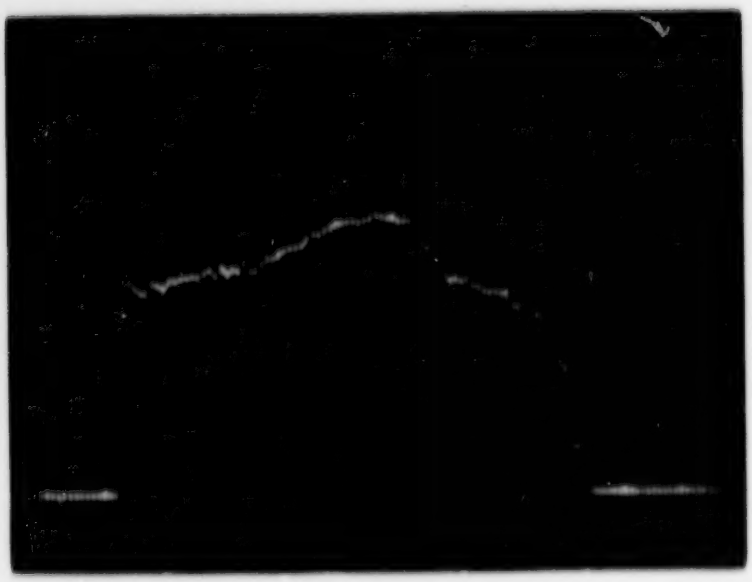

Fig. 2.5 Typical aerosol size distributions in a) room air and b) in the tunnel. Vertical axis represents the voltage output from the multichannel analyzer (0.1 volt per division). Voltage is proportional to the number of particles (eq. 2.1). Horizontal axis represents channel number and, correspondingly, particle size.

corresponds to a channel, with the first dot on the right hand side corresponding to channel #128. The correspondence between the channel number and the aerosol size is given in Fig. 2.4. The vertical axis in Fig. 2.5 has the units of volts and is proportional to the number of aerosols counted in a particular channel (i.e. in a given size range) during a given period of time. The relationship between the voltage and the number of aerosols counted was determined by a selector switch on the multichannel analyzer. The selector switch has 8 positions. At positions 10^2, 10^3, 10^4, or 10^5 the output of 1 volt per channel corresponded to 10^2, 10^3, 10^4, or 10^5 counts, respectively. When the selector switch was at positions 4×10^2, 4×10^3, or 4×10^4, the output of 2.5 volts per channel corresponded to 4×10^2, 4×10^3, or 4×10^4 counts, respectively. For these seven selector switch settings, the voltage was linearly proportional to the number of aerosols counted. There was an eighth setting in which the output voltage for each channel, v, was related to the number of aerosols counted, n, by the expression

$$v = c \log_{10} n + v_0 \qquad (2.1)$$

where c and v_0 were undetermined constants. These constants were evaluated by sampling a mixture, and by measuring the number of aerosols in a particular channel using one of the seven settings for which n was linearly proportional to v. The selector switch was then turned to the logarithmic scale and the voltage was measured for the same channel. Repeating this procedure twice, two sets of v and n values for the logarithmic setting were obtained. Substituting these values into eq. 2.1, c and v_0 could be calculated. In practice, the procedure was repeated for several sets of v and n values in order to obtain representative

average values for ϵ and v_0. The ϵ and v_0 values were found to be 0.14 and 0.06 volts, respectively.

From the results displayed in pictures such as fig. 2.5, the number of aerosols per channel could be determined to within 20% accuracy. However, the inaccuracy in the aerosol results (both the size distribution and the total number count) was considerably larger due to the statistical nature of the measurement. The actual number of aerosols fluctuated and this was manifested in the fluctuations in the outputs of the Royco Particle Counter and the multichannel analyzer. Characteristically, the fluctuation was of the order of ±30%. All the results presented in Section V for the total number of aerosol count and for the size distribution were the averages of at least three measurements.

The Royco Particle Counter could be operated at sampling rates of 47 $cm^3\ s^{-1}$ and 4.7 $cm^3\ s^{-1}$. The lower sampling rate (which was about one tenth of the flowrate in the tunnel) was used in the experiments. At this flowrate the lowest and highest detectable aerosol concentrations were 0 and 3.5×10^3 particles cm^{-3}, respectively. It is noted here, that neither the Small Particle Detector nor the Royco Particle Counter was calibrated in our laboratory. The results reported were based on the calibrations provided by the manufacturers.

In order to test the instruments, the size distribution of the atmospheric aerosols in the room were determined. The data were presented in terms of the dimensionless parameters

$$\eta = \frac{r}{(\nu/n)^{1/3}} \tag{2.2}$$

$$\psi = \frac{\Delta n \Delta r}{n/(\nu/n)^{1/3}} \tag{2.3}$$

ΔN is the number per unit volume of aerosols whose radii lie within the range of r and $r + \Delta r$. N is the total number of the aerosols per unit volume

$$N = \sum \Delta N \tag{2.4}$$

and V is the total aerosol volume per unit sample volume

$$V = \sum \tfrac{4}{3} \pi r^3 \Delta N \tag{2.5}$$

The parameters η and ψ were used in presenting the results because, as has been shown by Friedlander [21], and by Liu and Whitby [45], with the use of these parameters, all the data reduce to a common curve. Moreover, it has been demonstrated both experimentally [11,22,38,45] and analytically [45] that in the size range where the aerosol is in a state of dynamic equilibrium (i.e. where the rate of gain of aerosols due to coagulation is equal to the rate of loss of aerosols due to coagulation, diffusion and sedimentation) ψ varies inversely with the fourth power of η, i.e.

$$\psi \propto \eta^{-4} \tag{2.6}$$

The results of the measurements are given in Fig. 2.6. The data follow quite closely a line whose slope equals -4. The present results also fall within the size range observed by other investigators [11,22, 38,45].

The ozone content was measured by a Thermo Electron Corporation Model 12A Chemiluminescent Analyzer. This instrument operated on the principle that light was produced during the reaction of ozone with nitric oxide [56]. Therefore, the reaction

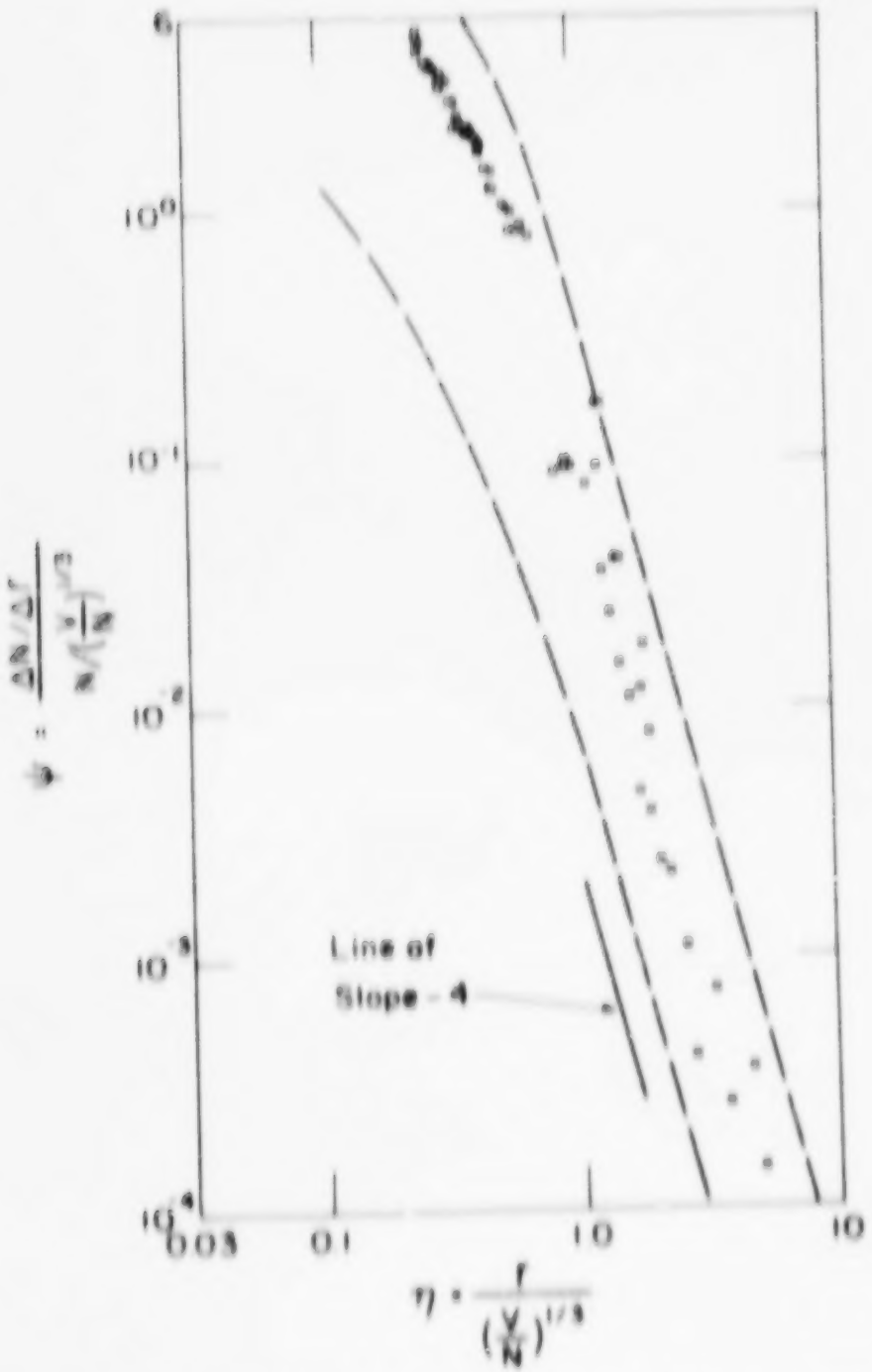

Fig. 1.1. Size distribution of aerosols in room air. • present data, ---- range of data from Cartwright et. al. [1], Friedlander and Pescott [2], Junge [3], and Liu and Whitby [4].

$$\text{[illegible]} \qquad (2.7)$$

was generated inside the instrument and the emitted light was measured by a photomultiplier. The photo current produced by the photomultiplier was a measure of the ozone content in the sample. A linear, full scale meter on the instrument indicated directly the ozone concentration in the sampled gas stream. Eight concentration ranges were provided with the instrument: 0-0.01, 0-0.025, 0-0.1, 0-0.25, 0-1, 0-10, 0-100, and 0-1000 ppm. Within each of these ranges the ozone concentration could be assessed to within two percent precision, while the fluctuations in the measurements were less than 1%.

The total intensity of the ultraviolet light inside the irradiation tunnel was monitored by a silicon Schottky PIN-5 photodiode (United Detector Technology, Inc.). This photodiode was 0.915 cm in diameter and had an active area of 0.64 cm^2. The photodiode was cemented onto one end of a 40 cm long, 0.636 cm o.d. stainless steel tube. The tube with the photodiode at its tip was then inserted about 30 cm deep inside the irradiation tunnel through one of the Swagelok connectors at the downstream end of the tunnel. The electrical leads of the photodiode were led through the tube to the outside of the tunnel. The signal from the photodiode was processed by an electrical circuit recommended by the manufacturer, and was displayed on a digital voltmeter. The relationship between the output voltage and the light intensity was not determined directly. Nevertheless, the voltage output indicated any change in the light intensity in the tunnel, and any possible deterioration in the intensity of the fluorescent lamp. It is noted, however

that a measure of the total light intensity in the tunnel was obtained as described in Section III.

The spectral distribution of the ultraviolet radiation was measured with a EGA/McPherson Monochromator and an RCA photomultiplier tube 1P28-A. The light was collected by a 30 cm long, 2.5 cm i.d. and 3 cm o.d. brass tube which passed through the shell surrounding the tunnel. One end of the tube was attached to the monochromator. The other end, machined to the shape of the outer surface of the tunnel, was attached to the outer wall of the tunnel. All openings were carefully sealed so that only light from the tunnel could reach the monochromator. The spectral distribution of the ultraviolet light, as given by the output of the monochromator, was recorded on a strip chart recorder. The output was not calibrated to give the value of the light intensity at different wavelengths. However, the output indicated the magnitudes of the light intensities and showed any change in those magnitudes. Therefore, this measurement sufficed in the present experiments where the only concern was to ascertain that the spectral distribution remained constant throughout the tests.

CHAPTER III

EXPERIMENTAL PROCEDURE

The experimental procedures used in studying the photochemical reactions in sulfur dioxide-air and in cyclohexene-nitrogen dioxide-air mixtures were similar.

At the start of each experiment, the ultraviolet lamps were turned on, the flow of the cooling air was started, and 50% relative humidity air (without any of the test gases) was fed through the system continuously at a flowrate of 35 $cm^3 s^{-1}$. The temperatures inside the tunnel and in the cooling air were recorded. The system required three to four hours to reach thermal equilibrium. The particulate contents were also measured along the entire length of the tunnel. This procedure continued until both the nuclei and aerosol counters indicated zero readings (i.e., a "clean" system) at every sampling station. This condition was usually reached in four to seven days. Once the system was thus "cleaned", the required gas-air mixture was introduced into the tunnel. After about four hours, both the ozone and particulate contents reached a constant value ("steady state") in the entire tunnel. This is demonstrated in Figs. 3.1 and 3.2 where the ozone, nuclei and aerosol contents are shown as a function of time at different sampling stations. When the conditions had reached steady state, the ozone and particulate contents were measured, and the gas-air mixture was changed to a new value.

The composition of the gas-air mixture was not measured along the tunnel. The mixture composition was known only at the entrance of the tunnel. Therefore, in the subsequent discussions, the specified

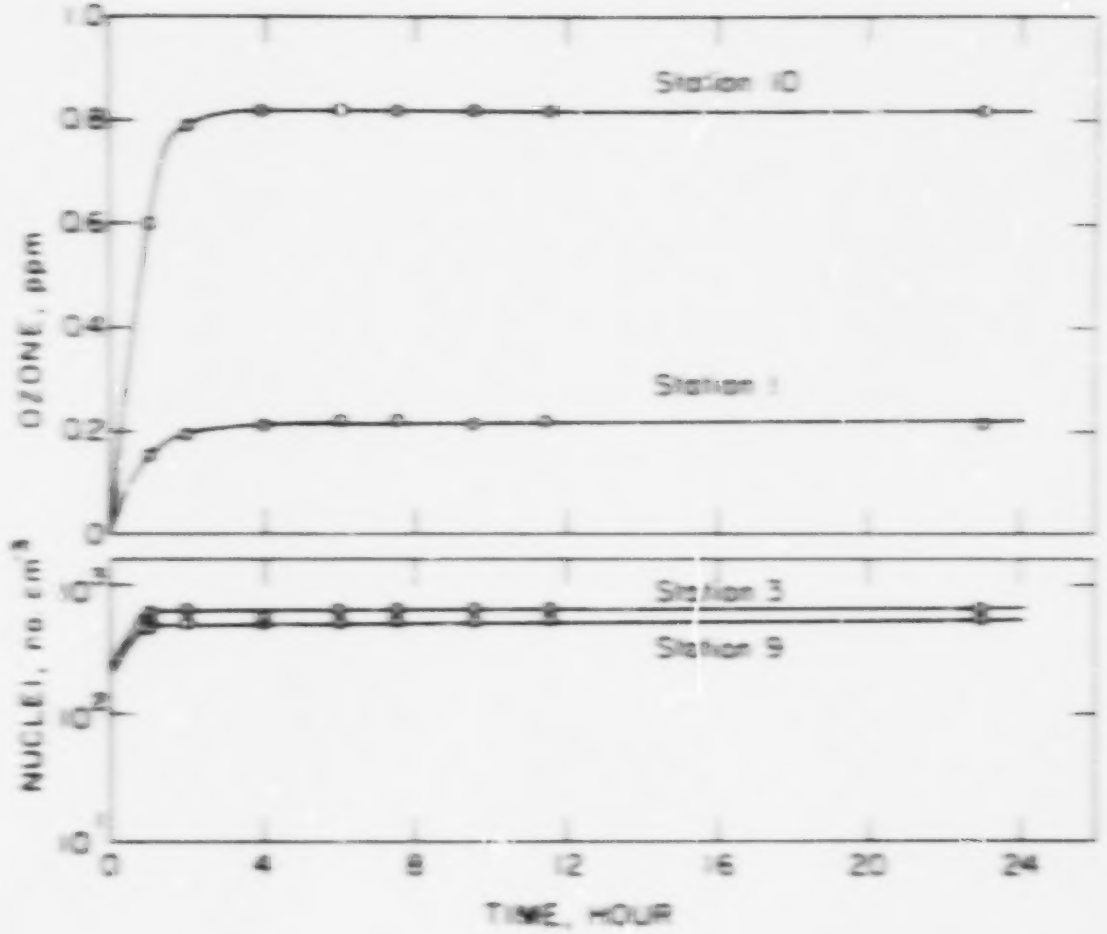

Fig. 2.1. Variation of ozone and nuclei contents with time given the typical mixture composition: cyclohexene 1.25 pphm, nitrogen dioxide 1.5 pphm, relative humidity 34%, rear flow velocity 0.152 m sec⁻¹

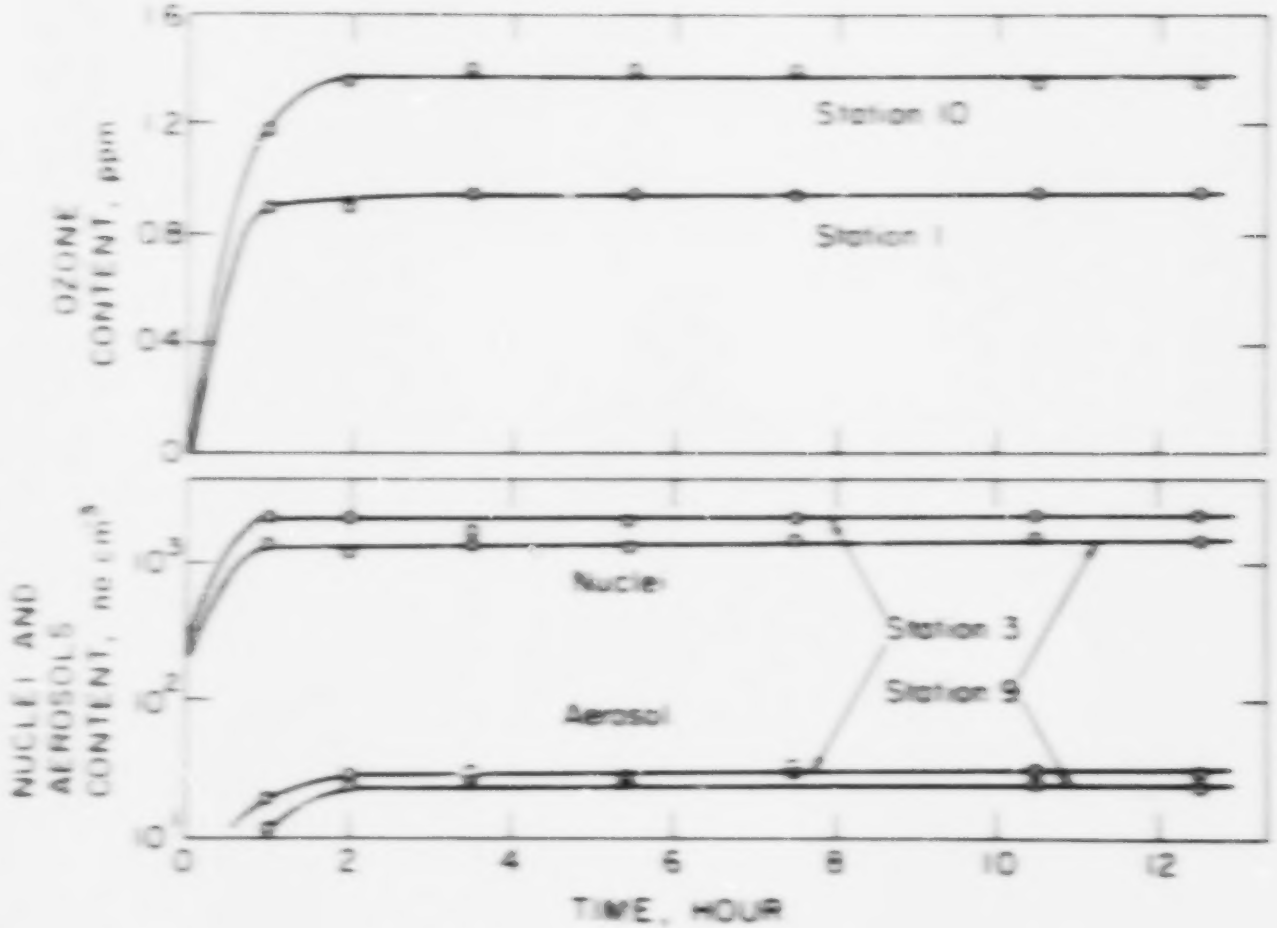
OZONE CONTENT, ppm
1.6
1.2
0.8
0.4
0
Station 10
Station 1
NUCLEI AND AEROSOLS CONTENT, no. cm⁻³
10³
10²
10¹
Nuclei
Aerosol
Station 3
Station 9
0
2
4
6
8
10
12
TIME, HOUR

test gas concentration refers to the amount of test gas in the air prior to exposure to the ultraviolet light. This condition is denoted by the subscript 0.

The spectral distribution of the ultraviolet light and the total light intensity was monitored throughout the tests. The spectral distribution of the light did not vary regardless of the compositions or concentrations of the mixture in the tunnel. Typical spectra taken with just air in the tunnel (i.e. no photochemical reactions) and with a cyclohexene-nitrogen dioxide-air mixture (in which photochemical reactions were taking place) are shown in Fig. 3.3.

The total light intensity also remained constant throughout the tests, as indicated by the steady voltage output of the photodiode. As mentioned in Section II, the output of the photodiode was not calibrated. Thus, while the output indicated that the intensity remained constant, it did not provide the actual value of the light intensity in the tunnel.

The light intensity, I, may be related to the photolysis rate constant (k_1) of nitrogen dioxide by the expression [43]

$$k_1 = \sum_{\lambda} 2.303\, \phi_{\lambda}\, \sigma_{\lambda}\, I_{\lambda} \qquad (3.1)$$

where ϕ is the primary quantum yield of nitrogen dioxide photolysis and σ is the absorption coefficient of nitrogen dioxide. The subscript λ refers to a particular wavelength.

The light intensity in a system may be specified either by the total light intensity $I = \sum I_{\lambda}$, or by the value k_1. In many experiments the light intensity is characterized by k_1. Therefore, the value of k_1 was determined for the present apparatus as follows.

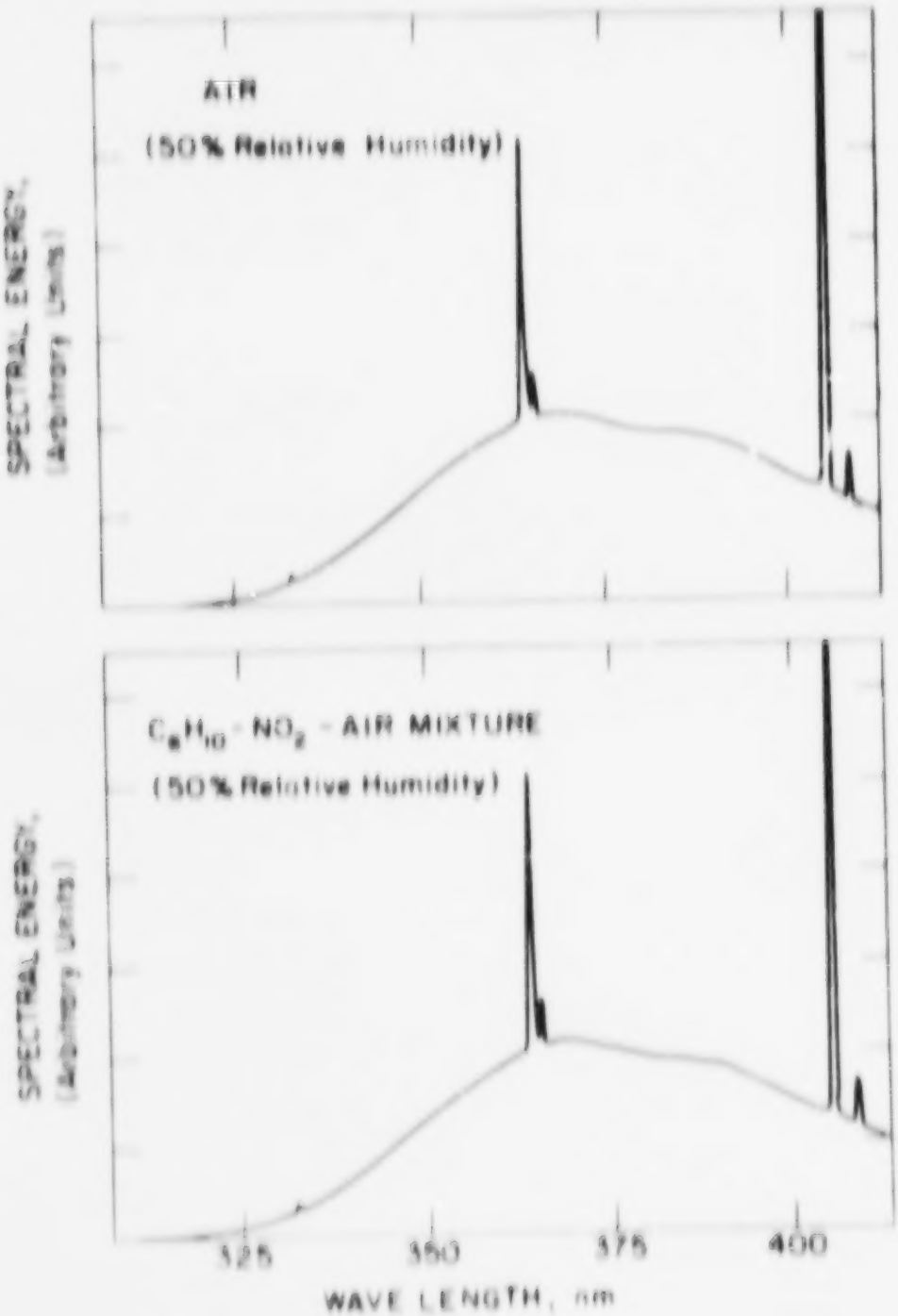
AIR
(50% Relative Humidity)
SPECTRAL ENERGY
(Arbitrary Units)
C_8H_{10} - NO_2 - AIR MIXTURE
(50% Relative Humidity)
SPECTRAL ENERGY
(Arbitrary Units)
325
350
375
400
WAVE LENGTH, nm

The dominant reactions at the initial stage of the photochemical reactions in a nitrogen dioxide-dry air mixture are [8,43,54,57]

$$NO_2 + h\nu \xrightarrow{k_1} NO + O \tag{3.2}$$

$$O + O_2 + M \xrightarrow{k_2} O_3 + M \tag{3.3}$$

$$O_3 + NO \xrightarrow{k_3} NO_2 + O_2 \tag{3.4}$$

where k_1, k_2 and k_3 are the respective rate constants. The rate equation for the nitrogen dioxide may be written as

$$\frac{d[NO_2]}{dt} = -k_1[NO_2] + k_3[O_3][NO] \tag{3.5}$$

A nitrogen mass balance at any instant gives

$$[NO_2]_0 = [NO_2] + [NO] \tag{3.6}$$

where $[NO_2]_0$ is the initial nitrogen dioxide concentration (i.e. the concentration supplied to the system). Some time after the start of the photochemical reaction, the "photostationary state" is reached in the system, at which the concentrations of nitrogen dioxide, nitric oxide, ozone and oxygen atom do not change with time, i.e.:

$$\frac{d[NO_2]}{dt} = \frac{d[O_3]}{dt} = \frac{d[NO]}{dt} = \frac{d[O]}{dt} = 0 \tag{3.7}$$

Depending upon the initial nitrogen dioxide concentration, this state was reached in the tunnel in 120-300 seconds. Equations (3.5) and (3.7) yield

$$k_3[O_3]_{max}[NO]_{max} = k_1[NO_2]_{max} \tag{3.8}$$

where the subscript pss denotes photostationary state. For low initial nitrogen dioxide concentrations ($[NO_2]_0$ less than 2 ppm), $[NO]_{pss}$ may be approximated by $[O_3]_{pss}$ [54,57]

$$[NO]_{pss} \approx [O_3]_{pss} \tag{3.9}$$

From eqs. (3.6), (3.8) and (3.9), we obtain

$$[O_3]^2_{pss} = \frac{k_1}{k_3}\left\{[NO_2]_0 - [O_3]_{pss}\right\} \tag{3.10}$$

According to the above equation, a plot of $[O_3]^2_{pss}$ against $\left\{[NO_2]_0 - [O_3]_{pss}\right\}$ should result in a straight line, the value of k_1/k_3 being given by the slope of this line. Knowing the slope of the $[O_3]^2_{pss}$ versus $\left\{[NO_2]_0 - [O_3]_{pss}\right\}$ curve and the value of k_3, the parameter k_1 can be calculated readily. The value of k_3 has been determined by several investigators, the reported values of k_3 ranging from 0.35 to 1.71 $ppm^{-1}\ s^{-1}$ [12,20,37,52]. The value $k_3 = 0.425\ ppm^{-1}\ s^{-1}$ has been adopted here as recommended by Stedman and Niki [57].

In order to generate the $[O_3]_{pss}$ versus $\left\{[NO_2]_0 - [O_3]_{pss}\right\}$ curve, the ozone concentration was measured at different points inside the tunnel using dry air and three different initial nitrogen dioxide concentrations. Since the flowrate in the tunnel was constant, the distance along the tunnel could be related to a time scale, as shown on the top of Fig. 3.4. The maximum values of the ozone concentration curves were taken as the photostationary state values at these maximum points satisfy the condition $d[O_3]/dt = 0$ (see eq. 3.7). The data thus generated was used to plot a $[O_3]^2_{pss}$ versus $\left\{[NO_2]_0 - [O_3]_{pss}\right\}$ curve (Fig. 3.5). From the slope of this plot, and for $k_3 = 0.425\ ppm^{-1}\ s^{-1}$, the value of k_1 was found to be $0.33\ s^{-1}$. Typical values of k_1 for the

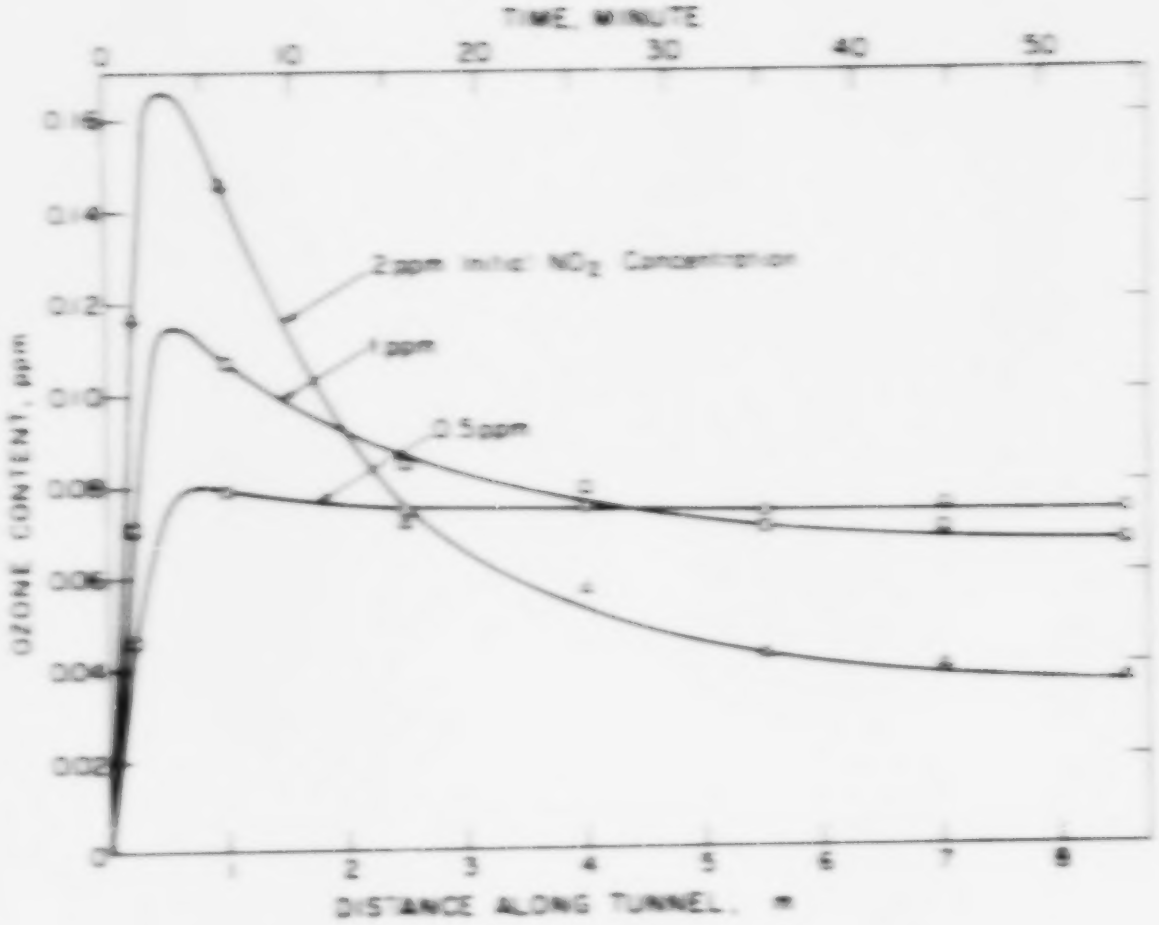

Fig. 2.4. Ozone content along the tunnel in various nitrogen dioxide-air mixtures. The axis represents irradiation time

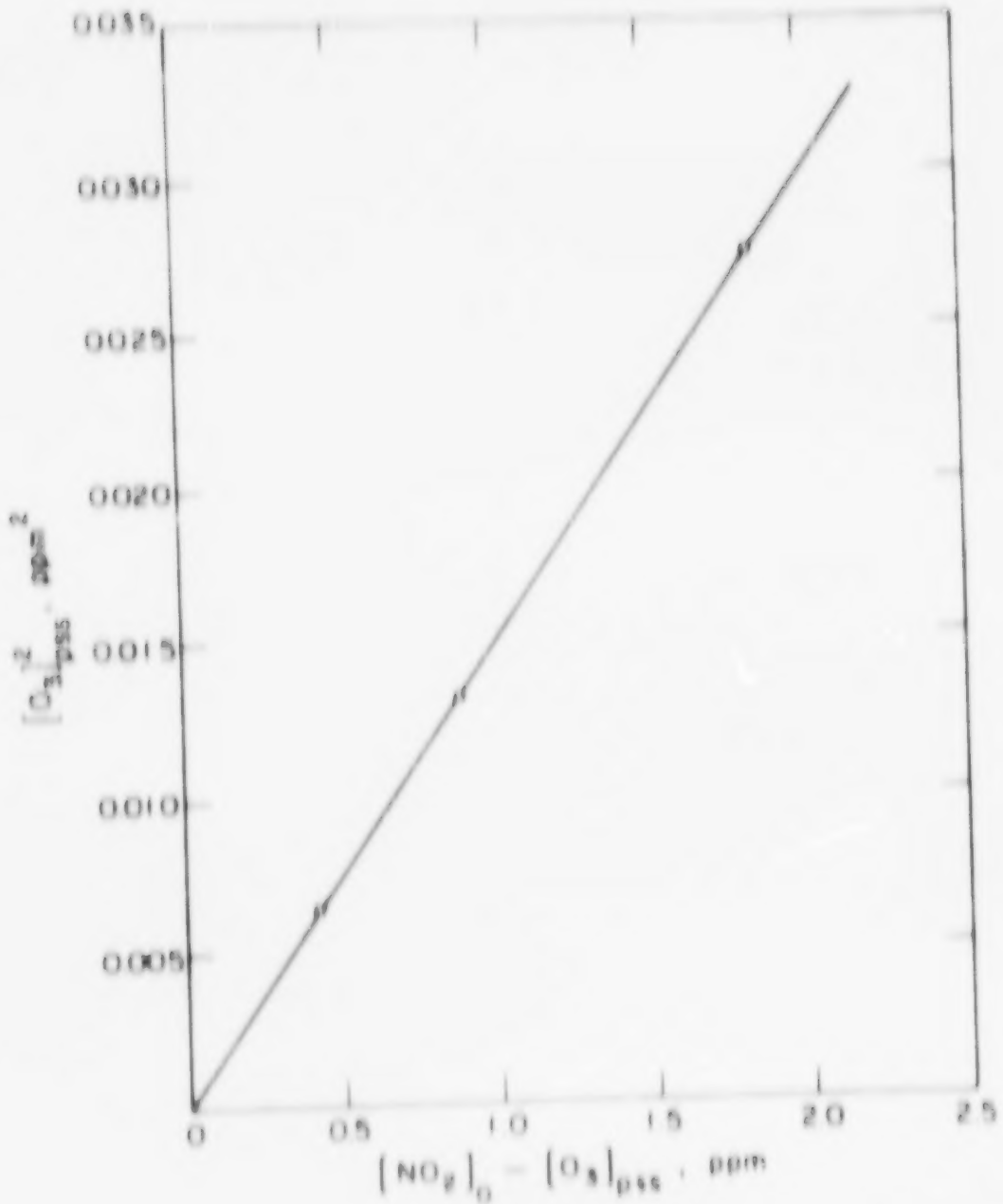

Figure 2. Relationship between the initial stationary concentration of ozone and the initial concentration of nitrogen dioxide. ○ data, ——— fit to data

photodissociation of nitrogen dioxide in the lower atmosphere are presented in Table 3.1. As can be seen, the k_1 values of the present experiment compare well with those which exist in the atmosphere. It is noted that k_1 values obtained in other experimental apparatus range from 0.78 ks^{-1} to 9.17 ks^{-1} (Table 3.2). The present k_1 = 6.33 ks^{-1} falls in this range.

Table 3.1 Rates of Photodissociation of Nitrogen Dioxide in the Lower Atmosphere in the Wavelength Range 290 to 430 nm

Solar zenith angle Z, degree	Photodissociation Rate $k_1 = \sum_{\lambda} 2.303\ \phi_\lambda\ \alpha_\lambda\ J_\lambda$, ks^{-1}
0	9.51
20	9.17
40	8.02
60	5.60
80	1.68

Values of ϕ_λ from table A-II, reference [15]

Values of α_λ from table 14, reference [43]

Values of J_λ from table 6, reference [43]

Table 1.1 Summary of Values of $k_{1,1}$ Used in Different Experiments

Volume, m^3	Experimental Apparatus Material	Type of Experiment	$k_{1,1}$, atm^{-1}	Reference
0.166	Pyrex tube	F	6.33	Present investigation
0.15	Teflon bag	S	0.78	Miller [44]
0.944	Pyrex jar	S	2.33	Stedman & Niki [57]
0.333	Pyrex flask	S	3.67	Leighton [42]
0.141	Pyrex tube	F	3.83	Stephens & Price [56]
0.24	Stainless steel chamber	S	4.17	Gradishar & Kerker [24]
1.67	Aluminum, Pyrex, Teflon and stainless steel removable surfaces	S	5.0	Jaffe & Senum [36]
0.24	Pyrex flask	S	5.33	Holmes et. al. [34]
0.801	Aluminum chamber, Teflon window	S	6.33	Doerbrinder [16]
0.48	Aluminum chamber, polyvinylfluoride window	F	6.67	Altshuller et. al. [5]
0.24	Mylar and Teflon bags	S	6.67 (Teflon) 5.0 (Mylar)	Altshuller & Cohen [7]
0.2	Pyrex jar	F	6.33	Wilson et. al. [65]
———	1-m base path multiple reflection infrared cell	S	6.17	Tuesday [60]

S Static type experiment
F Flow type experiment

CHAPTER IV

PHOTOCHEMICAL PARTICULATE FORMATION IN SO_2-AIR MIXTURES

It has been demonstrated by several investigators that particulates form when a mixture of sulfur dioxide and air is exposed to ultraviolet light [11,17,24,48,49]. However, the number of particulates formed and the dependence of this number on the initial sulfur dioxide concentration and the humidity of the air are not well established. The objectives of the present experiments were, therefore, to measure the number of particulates formed in sulfur dioxide-air mixtures, and to determine the relationships between the number of particulates formed, the initial sulfur dioxide concentration and the humidity of the air.

When a sulfur dioxide-air mixture was exposed in the tunnel to ultraviolet radiation, the number of particulates formed increased with time, reaching a maximum value. The number of particulates then remained nearly constant for some time at the maximum value (see Fig. 4.1) before it decreased due to coagulation, diffusion, and deposition on the walls. Here we were interested in the maximum number of particulates formed in the mixture. In order to determine the exposure time required to reach the maximum number of particulates, the number of nuclei and aerosols were measured at sampling station #1 at different flowrates ranging from 16 $cm^3\ s^{-1}$ to 184 $cm^3\ s^{-1}$. Since sampling station #1 was 23 cm from the entrance to the tunnel, the exposure times corresponding to these flowrates ranged from 90 s to 22.7 s. The experiments were repeated for different sulfur dioxide concentrations and different humidities (Fig. 4.1). There were no measurable amounts of aerosols in any of the experiments. There were, however, nuclei formed in the mix-

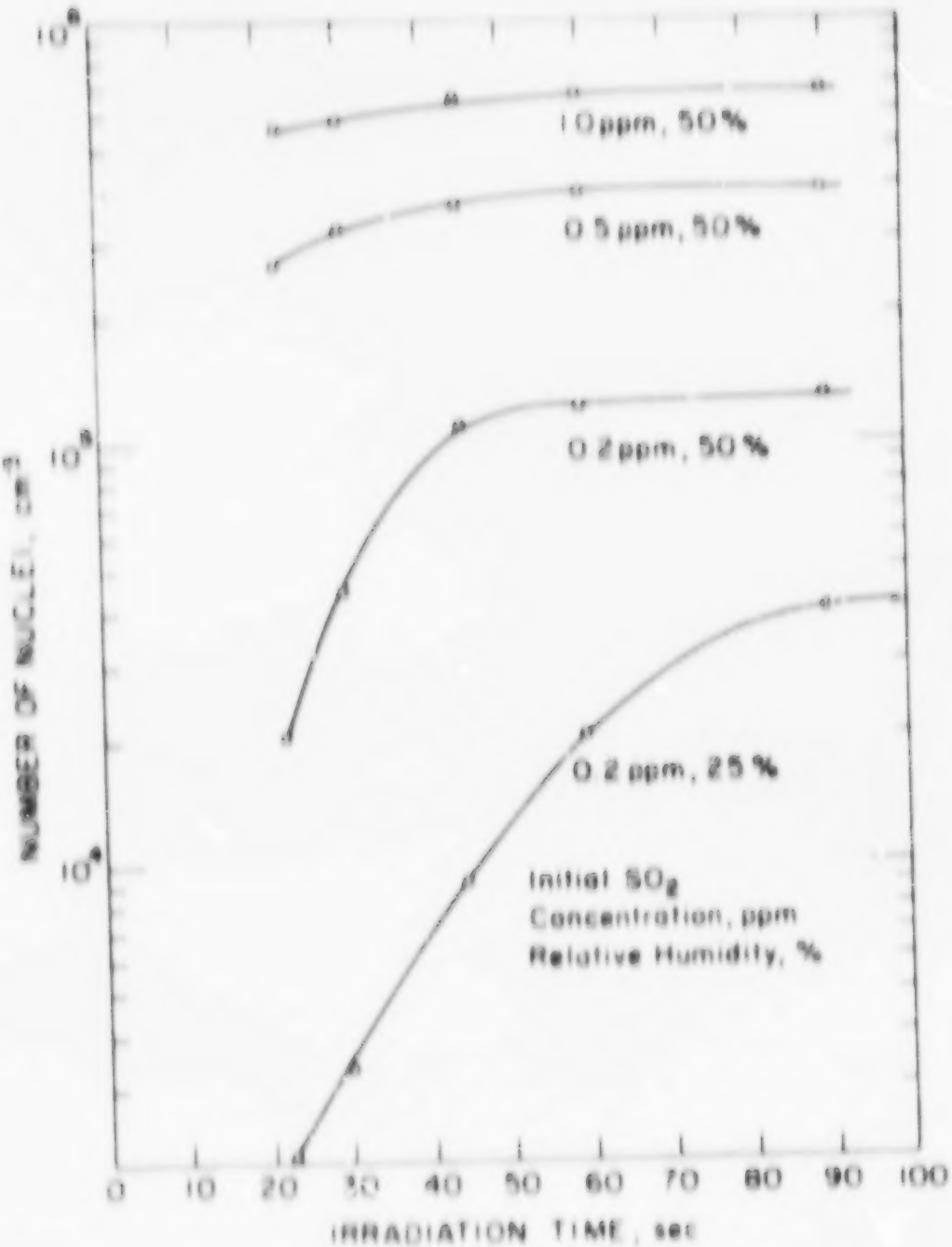
10 ppm, 50 %
0 5 ppm, 50 %
0 2 ppm, 50 %
0 2 ppm, 25 %
Initial SO_2
Concentration, ppm
Relative Humidity, %
NUMBER OF NUCLEI, cm^{-3}
IRRADIATION TIME, sec
0
10
20
30
40
50
60
70
80
90
100

ture. The amount of nuclei formed depended on the exposure time, as shown in Fig. 4.1. The time required to reach the maximum number of nuclei increased as both the initial sulfur dioxide concentration and the humidity in the air decreased.

The lowest initial sulfur dioxide concentration used in the experiment was 0.2 ppm, and the lowest relative humidity was 25%. For this condition, the tests showed that the time required to form the maximum number of nuclei was about 90 s. Therefore, to ensure that the maximum number of nuclei formed was achieved in all the tests, the 90 s exposure time was used throughout the subsequent experiments. The number of nuclei per cm^3 given below correspond to the maximum value obtained in the manner just discussed.

The effects of the initial sulfur dioxide concentration and the relative humidity on the nuclei formation were measured for five different sulfur dioxide concentrations ($[SO_2]_0$ = 0.2, 0.3, 0.5, 0.7, and 1 ppm), and four different relative humidities ($[\phi]_0$ = 25, 50, 75, and 100%). The data are presented in Fig. 4.2, and indicate that the number of nuclei formed vary linearly with the initial sulfur dioxide concentration in the air.

The results in Fig. 4.2 were cross plotted in order to obtain directly the variation of the number of nuclei with relative humidity. As shown in Fig. 4.3, the number of nuclei varies with the square of the relative humidity. Thus, according to the results of Fig. 4.2 and 4.3, the maximum number of nuclei formed may be expressed as

$$N = \alpha [SO_2]_0 [\phi]_0^2 \qquad (4.1)$$

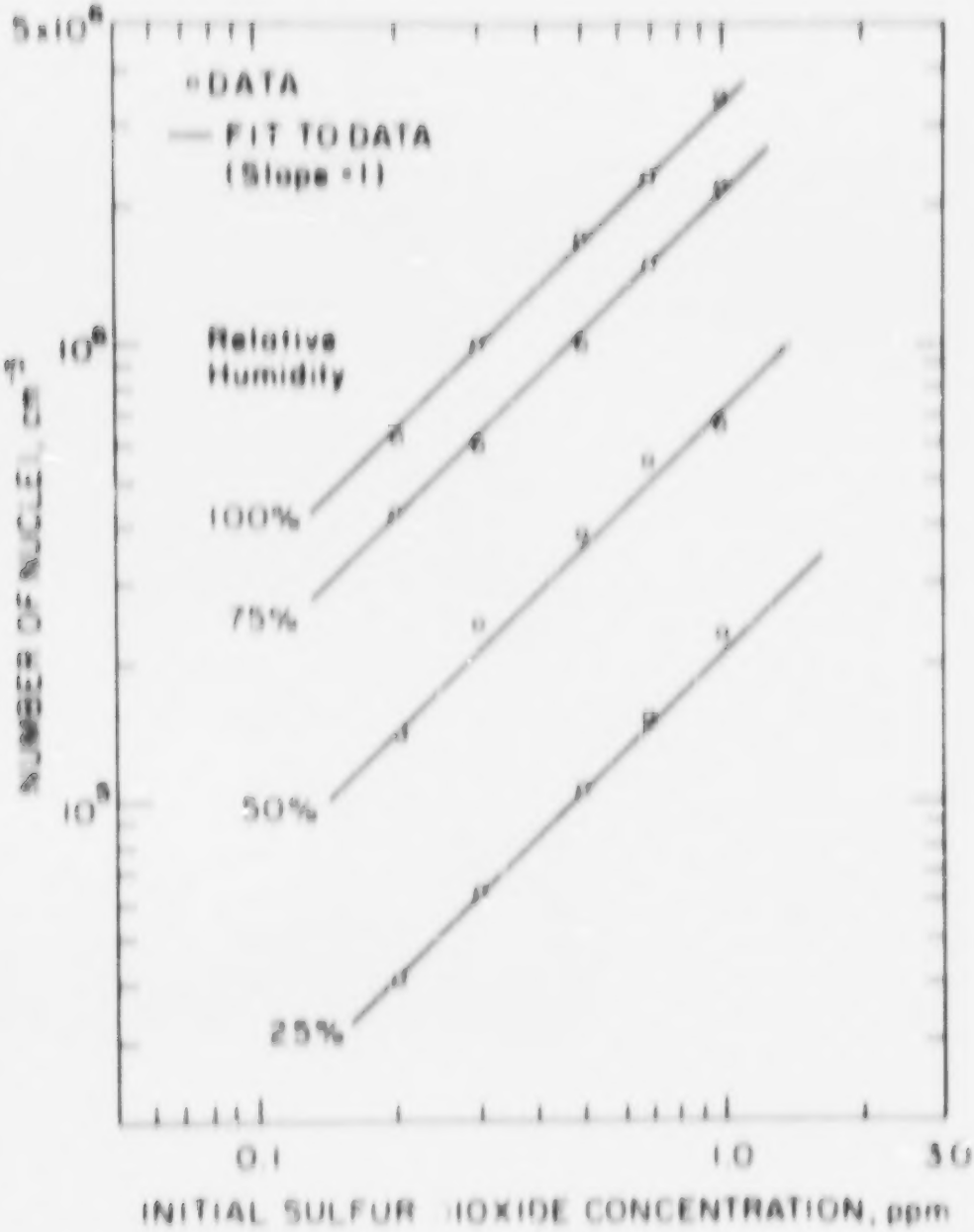

Fig. 4.2. Number of nuclei formed in sulfur dioxide-air mixtures

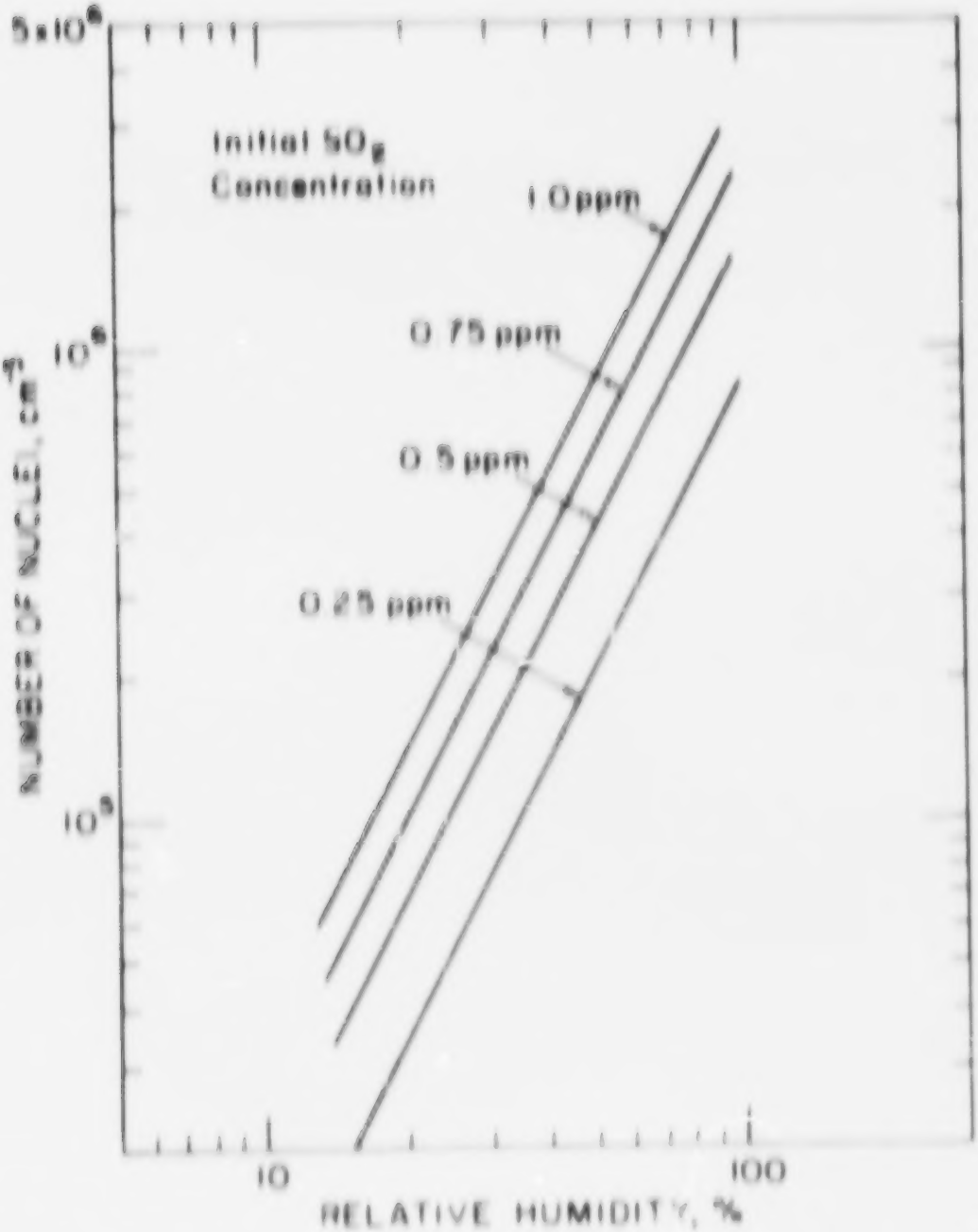
5x10^6
10^6
10^5
NUMBER OF NUCLEI, cm^-3
Initial SO2 Concentration
1.0ppm
0.75 ppm
0.5 ppm
0.25 ppm
10
100
RELATIVE HUMIDITY, %

where A is a constant. In order to test further the validity of eq. (4.1) and to obtain the value of A, all the data were compiled on an N versus $[SO_2]_0^2 [\phi]_0^2$ plot (fig. 4.4). The data correlated well with the above expression for $A = 3.11 \times 10^6$ nm. cm^{-3} ppm^{-1}. Thus, the maximum number of nuclei is given by the expression

$$N = 3.11 \times 10^6 [SO_2]_0^2 [\phi]_0^2 \qquad (4.2)$$

where $[SO_2]_0$ is in ppm and $[\phi]_0$ is in percent.

It should be noted that eq. (4.2) was determined from the data obtained under specific experimental conditions. As the light intensity inside the tunnel was not varied during these experiments, eq. (4.2) does not indicate the effect of the light intensity on nuclei production. However, Grobicki and Nebel [29] have found that the maximum amount of aerosols produced in a propylene-nitric oxide-sulfur dioxide-air mixture was not affected by a change in the light intensity. The light intensity merely affected the time required to produce the maximum number of nuclei. It is expected, therefore, that a change in the light intensity would not alter eq. (4.2), but would change the irradiation time required to produce the maximum number of nuclei.

It would be of interest now to compare the present data with results of other investigations. Results of direct measurements of the number of nuclei formed in sulfur dioxide-air mixtures were reported in references [13,14,40,48,49]. The conditions of these experiments are listed in table 4.1. The present results can be compared with those obtained by Renzetti and Doyle [49] and Raemond et. al. [40]. The number of nuclei obtained by Renzetti and Doyle for 0.24 ppm sulfur dioxide at 50% relative humidity ranged from 5×10^4 to 8×10^5 nuclei cm^{-3}.

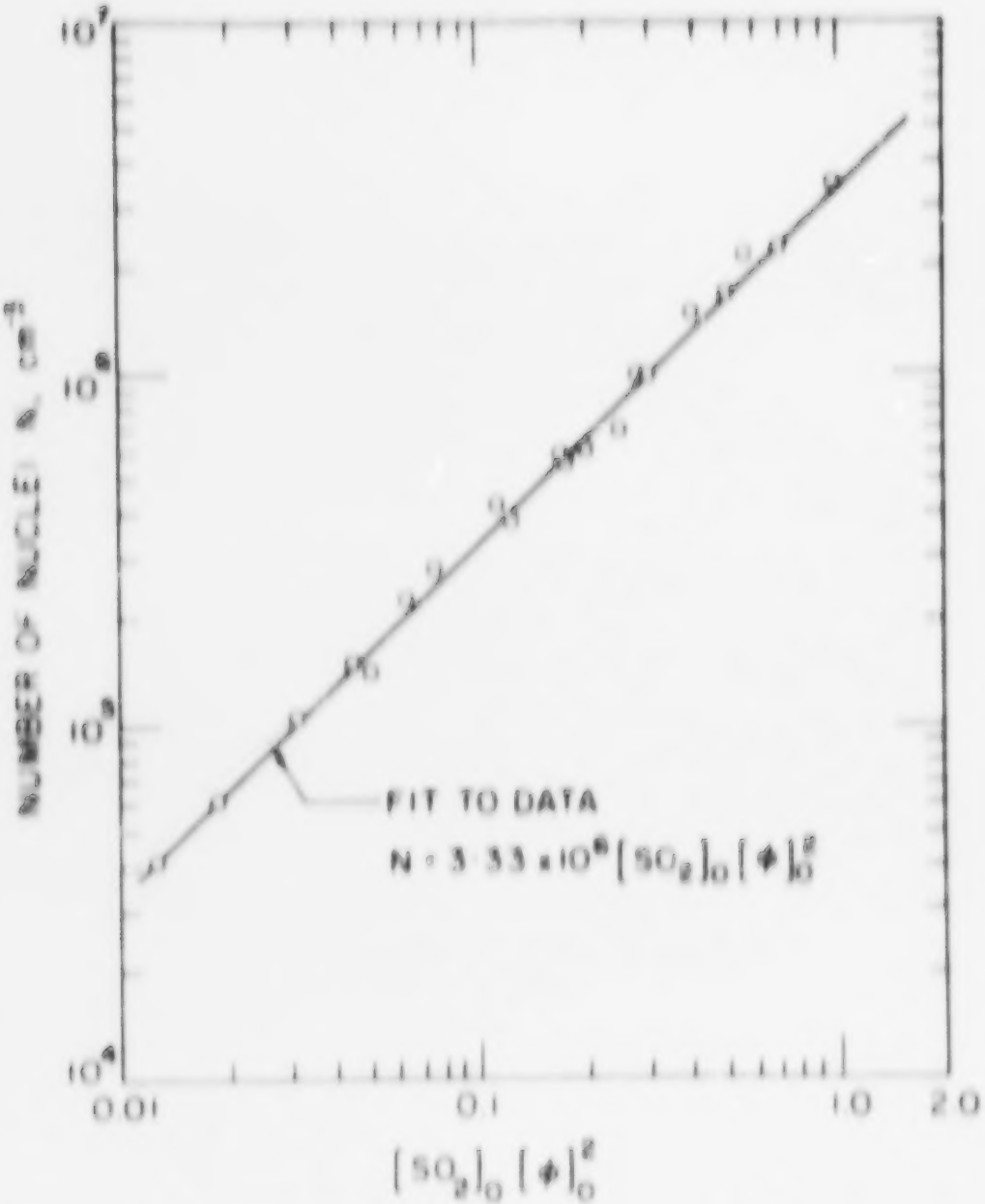
FIT TO DATA
$N = 3.33 \times 10^{6} [SO_2]_0 [\phi]_0^2$
0.01
0.1
1.0
2.0
$[SO_2]_0 [\phi]_0^2$

Table 4.1 Summary of Experimental Conditions Used by Different Investigators

Reference	Experimental Apparatus			
	Volume, m^3	Material	Light Source	Type
Cox and Pemmett [13]	0.216	Aluminum Chamber	Sunlight	S
Cox [14]	0.385	Pyrex Flask	Mercury Lamp	S
Gerhard and Johnstone [24]	0.008	Lucite Chamber	Sun Lamp	S
Leighton et. al. [40]	0.25 1.7	Teflon Bags	Fluorescent Lamps	S
	420	Steel Chamber	Fluorescent Lamps	S
Dunn et. al. [45]	0.014	Saran Bags	Fluorescent Lamps	S
Heicklen and Doyle [44]	0.05	Pyrex Flask	Mercury Lamps	F

S Static type experiment
F Flow type experiment

for this sulfur dioxide concentration and relative humidity, the number of nuclei calculated from eq. (4.2) is 2×10^5 nuclei cm^{-3}. Hence, the value obtained in the present study lies within the spread of Renzetti and Doyle's data. The amounts of nuclei measured by Eucken et. al. were two to four times higher than the values obtained in this investigation. The reason for this is unclear. The discrepancy between the two results might possibly be due to the fact that the present data were obtained from flow type experiments while Eucken et. al. performed their measurements in static type experiments.

The results of Cox and Penkett [11], Quon et. al. [40], and Cox [10] cannot be compared with the present data. Cox and Penkett did not report the humidity in their results; Quon et. al. performed measurements before the maximum amounts of nuclei were produced. The data obtained by Cox were obtained for much higher initial sulfur dioxide concentrations (5 to 1000 ppm) than those used in the present study (0.2 to 1 ppm).

Some indirect comparisons with other existing data can be made to confirm the present results. Gerhard and Johnstone [24] performed static type experiments in a 0.098 m^3 Lucite chamber irradiated by a sun lamp, and collected and measured the amount of sulfuric acid formed in sulfur dioxide-air mixtures. If it is assumed that most of the nuclei formed in the present study were composed of sulfuric acid, then the number of nuclei should be proportional to the amount of sulfuric acid collected by Gerhard and Johnstone. The variation of sulfuric acid with the initial sulfur dioxide concentration, as reported in reference [24], is presented in Fig. 4.5. Similar to the number of nuclei formed (see eq. 4.2), the amount of sulfuric acid collected varies linearly with the initial sulfur dioxide concentration.

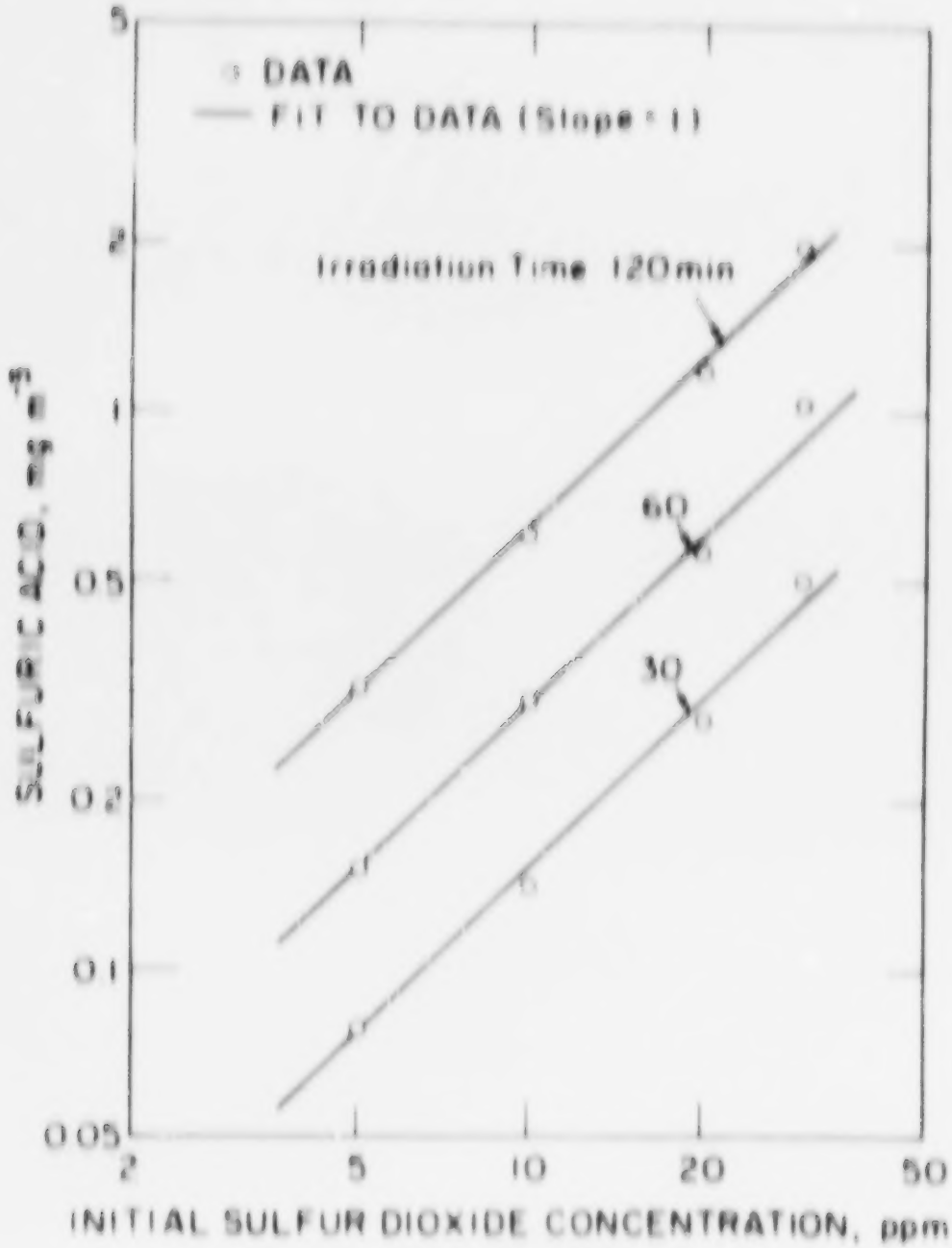

Fig. 11. Formation of sulfuric acid in sulfur dioxide-air mixtures. (From Cox and Penkett [23].)

Renzetti and Doyle [49] measured the amount of light scattered from a sulfur dioxide-air mixture undergoing photochemical reaction. Their data are reproduced in Fig. 4.6. Although there is considerable spread in Renzetti and Doyle's data, the amount of light scattered (which is proportional to the number of nuclei formed) appears to vary linearly with the initial sulfur dioxide concentration, further supporting the validity of eq. (4.2).

The information available on the effect of the relative humidity on the number of nuclei formed is conflicting. Renzetti and Doy'e observed that the amount of light scattered increased with relative humidity. Cox [14] also reported that the number of nuclei formed increased with humidity. Katz and Gale [39] observed an increase in the conversion rate of sulfur dioxide to sulfur trioxide (or sulfuric acid) as the humidity was increased. These results thus support the present data which show an increase in nucleation rate as well as the number of nuclei formed with relative humidity. In contrast to these results, Gerhard and Johnstone [34] found that the sulfur dioxide conversion rate did not change with relative humidity. The results of Owen et. al. [46] indicated that the number of nuclei formed was independent of relative humidity. The data obtained by Eriksen et. al. [30] did not show any dependence of the conversion rate of sulfur dioxide on relative humidity. However, Eriksen et. al. found that the rate of change of the total volume of the aerosols depended on relative humidity. The effect of humidity on the nuclei formation in sulfur dioxide-air mixtures would thus need further studies.

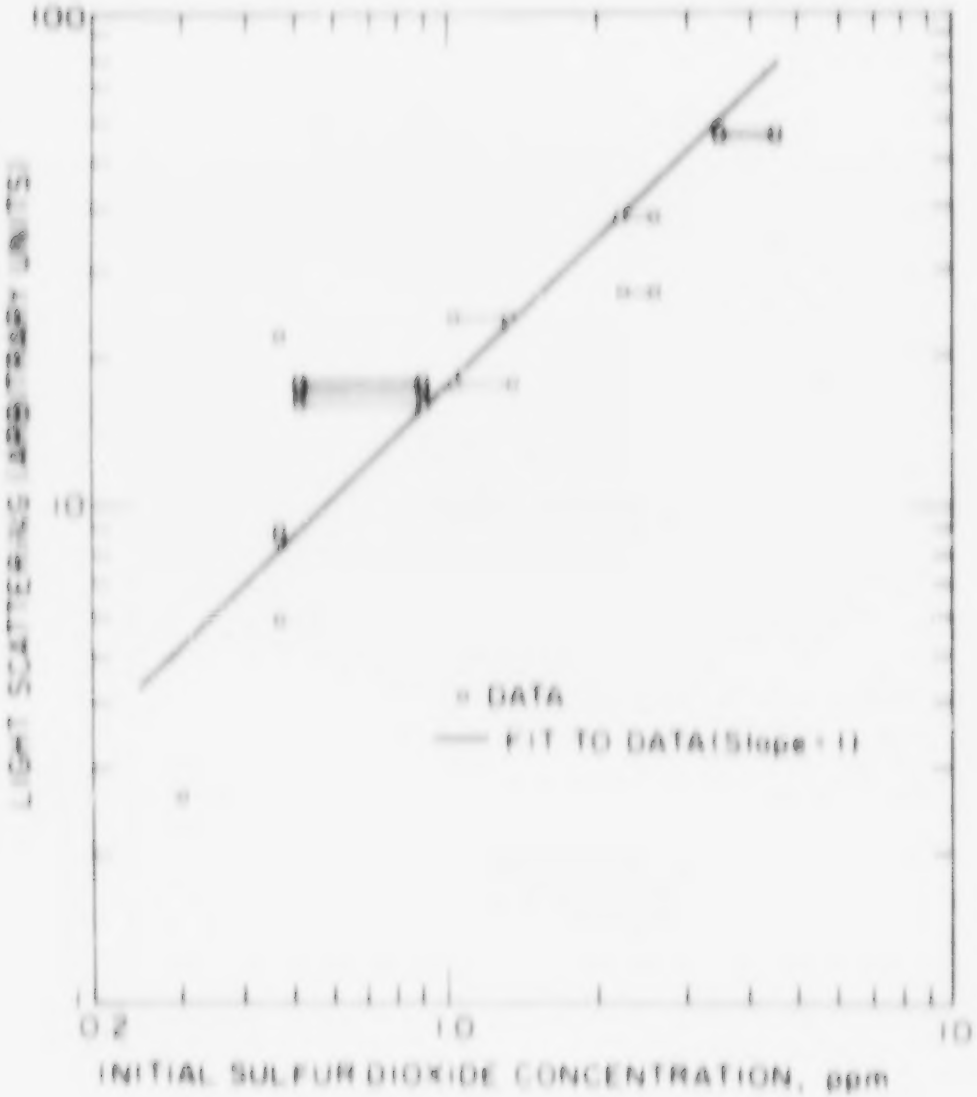

FIG. 5-6. Amount of light scattered from sulfur dioxide-air mixtures. Data from Benzelt and Boyle [49]

CHAPTER V

OZONE AND PARTICULATE FORMATION IN C_6H_{10}-NO_2-AIR MIXTURES

Photochemical reactions in a cyclohexene-nitrogen dioxide-air mixture depend on several parameters, including a) the initial concentration of cyclohexene, b) the initial concentration of nitrogen dioxide, c) the ultraviolet light intensity, and d) the length of time the mixture is irradiated. The major goal of this study was to evaluate the first two of these effects, namely, the influence of the initial concentrations of cyclohexene and nitrogen dioxide on the amounts of ozone, condensation nuclei and aerosols formed. Therefore, throughout the tests, the light intensity was kept at the constant value of k_1=0.33 ks^{-1}, and the flowrate was maintained at 40 $cm^3\ s^{-1}$. All the results discussed below apply to these conditions.

One might also expect the relative humidity to affect the formation of ozone, nuclei and aerosols. Bufalini and Altshuller [10] and Stephens and Price [58] have found, however, that the amount of ozone formed was not influenced by the relative humidity. The effects of the humidity on nuclei and aerosol formation have not yet been established. In the present study, a relative humidity of 50% was used. According to the results of Bufalini and Altshuller and of Stephens and Price, the use of a constant relative humidity would not affect the amount of ozone formed. The relative humidity might influence the nuclei and aerosol formation, but its effect was not explored here.

The initial concentrations of cyclohexene and nitrogen dioxide were varied in a systematic manner. Initially, five concentrations of cyclohexene (0.5, 1, 2, 3, and 5 ppm) and five concentrations of nitrogen

dioxide (0.5, 1, 2, 3, and 5 ppm) were permutated to provide twenty-five different mixture composition combinations. As the measurements progressed, it became evident that additional mixture compositions were needed to provide more information in certain areas of particular interest. Hence, measurements were also made with additional mixtures. A complete set of the experimental conditions and of the data obtained are given in Appendix D. The data from a typical series of tests are presented in Fig. 5.1. The results in this figure show the amounts of ozone, nuclei and aerosols formed along the irradiation tunnel. Since the flowrate in the tunnel was constant, the horizontal axis in Fig. 5.1 represents both the distance along the tunnel and the length of time the mixture has been irradiated.

As can be seen from Fig. 5.1, the amounts of ozone, nuclei and aerosols first increase, reach a peak and then decrease along the tunnel. Here, we shall be concerned with the "peaks" which represent the maximum amounts of ozone, nuclei and aerosols formed. Our interest in the maximum values is motivated by the general concern about the maximum amounts of ozone, nuclei and aerosols formed in the atmosphere due to photochemical reactions. In all subsequent discussions, the term "amount" was used to denote the peak values, which were determined by plotting all the data in a manner similar to those shown in Fig. 5.1, and by estimating the peaks from these plots. The results thus obtained are tabulated in Appendix E.

5.1 The Effects of Mixture Composition on Ozone Formation

The typical behavior of ozone along the tunnel is illustrated in Fig. 5.1. Although this figure represents only one set of data, similar

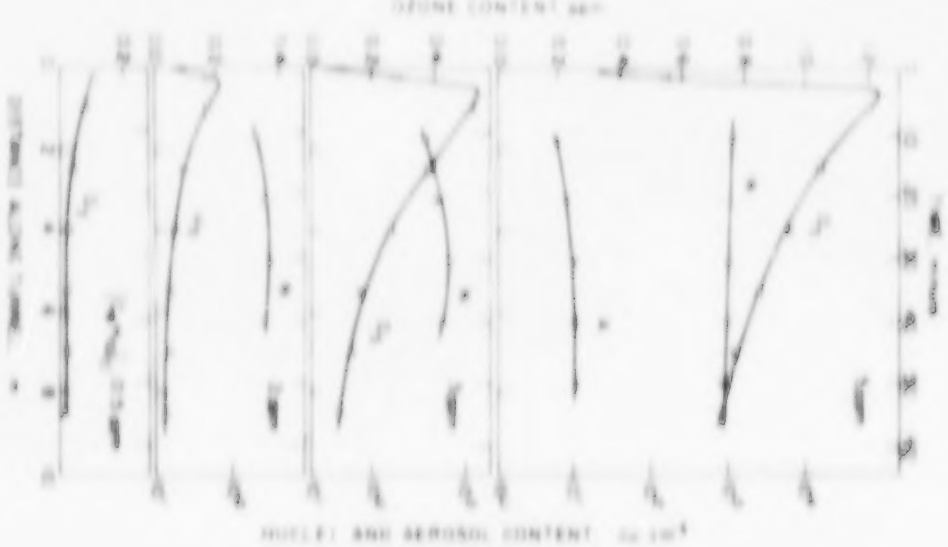

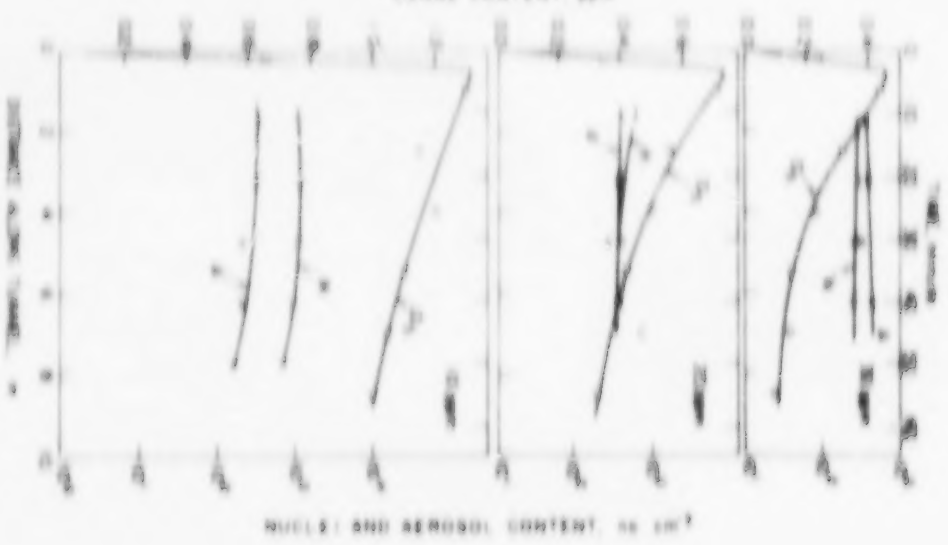

trends were observed with other initial concentrations of cyclohexene and nitrogen dioxide. For all mixture combinations, the amount of ozone along the tunnel first increased, reached a peak and then decreased. In order to describe these results quantitatively, it would be necessary to know in detail the reaction mechanism in the mixture and the corresponding reaction equations. To date, many different sets of reaction equations have been proposed [15,19,32,46,61,62], but the validity and accuracy of the various sets are still of considerable debate. Nevertheless, it is possible to explain, at least qualitatively, the observed behavior of the ozone formation by the relatively simple kinetic scheme introduced by Eschenroeder and Martinez [19]. These investigators suggested twelve reactions for describing the photochemical processes occurring in hydrocarbon-nitrogen oxides-air mixtures. The reaction equations proposed by Eschenroeder and Martinez are listed in Table 5.1 (eqs. 5.1-5.12).

According to eqs. (5.1) and (5.2), ozone and nitric oxide are formed by the photodissociation of nitrogen dioxide. The ozone reacts with the nitric oxide and the hydrocarbon (eqs. 5.3 and 5.10). These reactions tend to deplete the ozone. However, simultaneously, the nitric oxide reacts with various free radicals (denoted by RO_2, eq. 5.11), and this reaction proceeds at a much faster rate than the reactions of ozone with the nitric oxide and the hydrocarbon. The net result is an excess amount of ozone in the system; hence, the observed increase in the ozone content in the first part of the tunnel. As the photochemical reaction progresses, the nitrogen dioxide is depleted by reacting with the free radicals (eqs. 5.4 and 5.12). As the amount of nitrogen dioxide diminishes, so does the amount of ozone formed resulting in an eventual decrease in the ozone content along the tunnel.

Table 5.1 The Reaction Mechanism Proposed by Eschenroeder and Martinez [19]

It is now possible to evaluate the maximum amount (referred to simply as the "amount") of ozone produced for different initial concentrations of cyclohexene ($[C_6H_{10}]_0$) and nitrogen dioxide ($[NO_2]_0$). The amount of ozone produced as a function of the initial concentrations of cyclohexene and nitrogen dioxide is shown in figs. 5.2 and 5.3. For a given initial nitrogen dioxide concentration, the amount of ozone first increased with increasing cyclohexene concentration. An increase in the cyclohexene concentration beyond a certain value resulted in a decrease in the amount of ozone (fig. 5.2). Similar behavior was observed when the initial cyclohexene concentration was kept constant and the concentration of nitrogen dioxide was varied (fig. 5.3). Such an interrelation between the amount of ozone formed and the initial concentrations of the hydrocarbon and the nitrogen oxides has also been noticed by other investigators [2,5,6,7,25,41,50], and plausible qualitative explanations of these phenomena have been offered in references [25,50,55]. A brief explanation of these phenomena may be given by referring again to eqs. (5.1)-(5.12). First, we consider the case when the initial nitrogen dioxide concentration is kept constant and the initial concentration of cyclohexene is varied (fig. 5.2). As discussed above, the photodissociation of nitrogen dioxide yields ozone and nitric oxide (eqs. 5.1 and 5.2). Ozone is depleted by reactions with the nitric oxide and the hydrocarbon (eqs. 5.3 and 5.10). In addition to reacting with ozone, the nitric oxide also reacts with the free radicals (eq. 5.11), and this reaction proceeds faster than the reactions depleting ozone. Thus, an increase in the hydrocarbon concentration results in a decrease in the amount of nitric oxide available for the depletion of ozone. Consequently, the amount

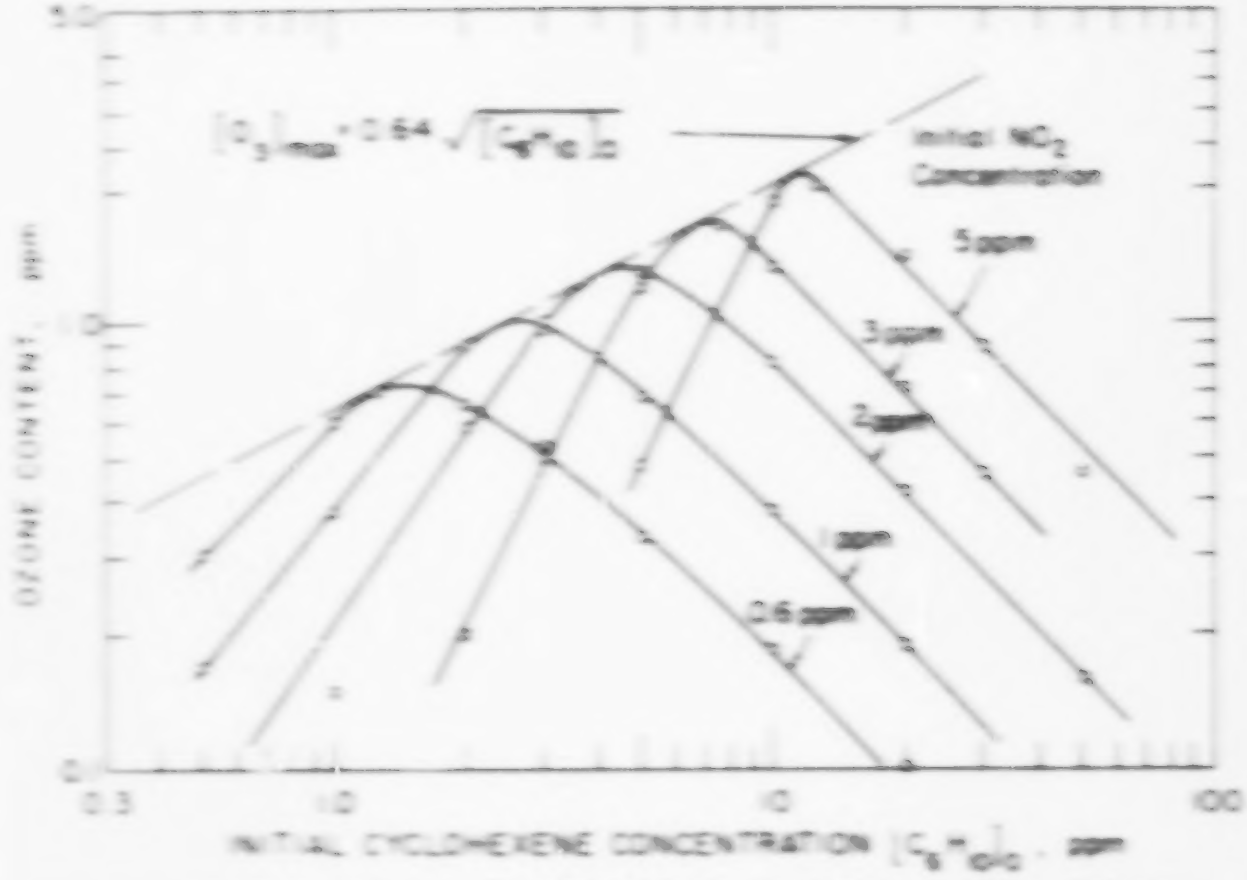
5.0
1.0
0.1
0.3
1.0
10
100
$[O_3]_{max} = 0.64\sqrt{[C_6H_{10}]_0}$
Initial NO_2 Concentration
5 ppm
3 ppm
2 ppm
1 ppm
0.6 ppm
OZONE CONTENT, ppm
INITIAL CYCLOHEXENE CONCENTRATION $[C_6H_{10}]_0$, ppm

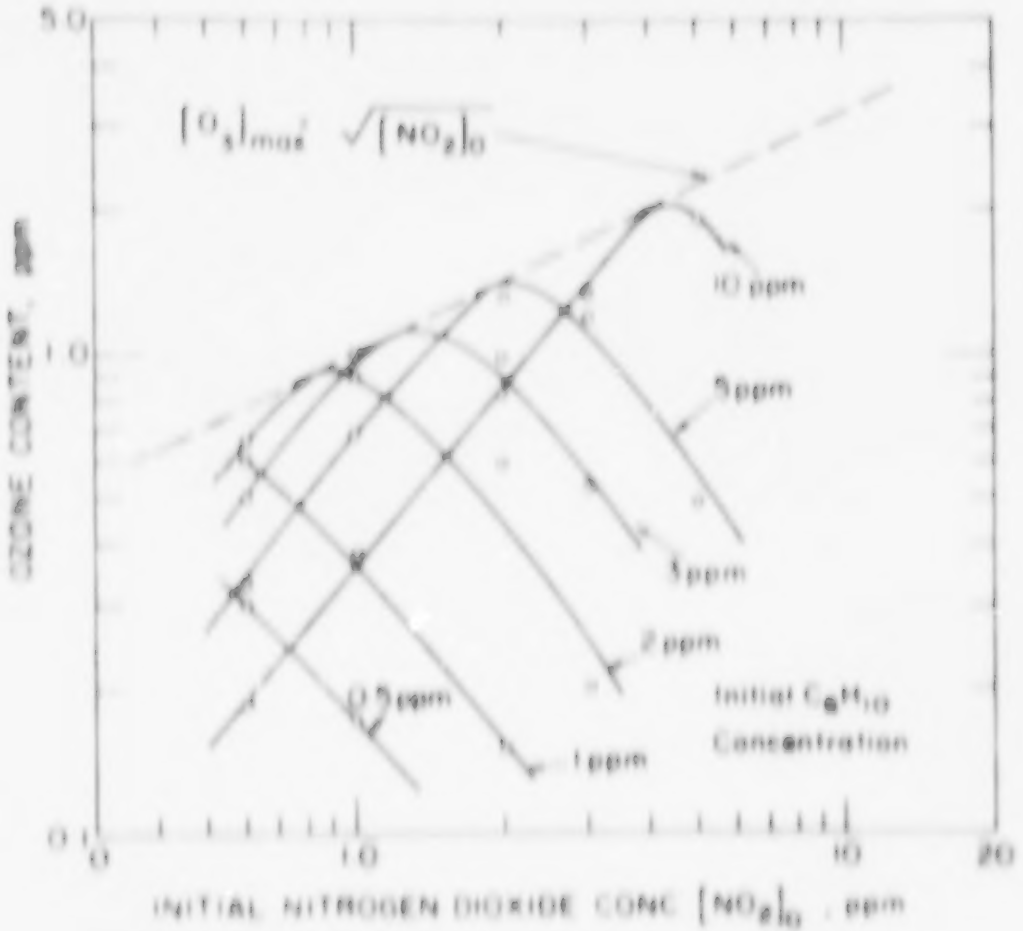

Fig. 1.1. Ozone content in cyclohexane-nitrogen dioxide-air mixtures, relative humidity: 10%, light intensity $k_1 = 0.33$ min^{-1}

of ozone formed increases with initial increase in the hy[illegible] tration. However, once there is a sufficient amount of [illegible] sent in the mixture to react with all the available nitr[illegible] any additional hydrocarbon will react with ozone. Under [illegible] tions, an increase in the hydrocarbon concentration results in a decrease in the ozone content.

The formation of ozone can be explained similarly when the initial concentration of the hydrocarbon is kept constant while the initial concentration of nitrogen dioxide is varied (Fig. 5.3). As the nitrogen dioxide concentration is increased, both the amounts of nitric oxide and nitric oxide are increased (eqs. 5.1 and 5.2). Because the [illegible] of nitric oxide with the free radicals (eq. 5.11) proceeds at a [illegible] the reactions depleting ozone (eqs. 5.3 and 5.10), more ozone is left in the mixture. This explains the increase in the ozone content with the initial increase in the nitrogen dioxide concentration. [illegible] tial nitrogen dioxide concentration is increased to [illegible] the hydrocarbon present in the mixture reacts with [illegible] produced by the nitrogen dioxide, then any further [illegible] rogen dioxide concentration provides some excess nit[illegible] with the ozone. More ozone is depleted due to this [illegible] formed due to the increase in the nitrogen dioxide. [illegible] the ozone content is reduced when the nitrogen dio[illegible] increased.

The results presented in Fig. 5.2 and 5.3 were [illegible] formation of ozone in cyclohexane-nitrogen dioxide [illegible] attempt is now made to generalize these results [illegible] information regarding the ozone production by other [illegible]

It is recognized [15,46,55] that, in a reaction described by N reaction equations, the amount of ozone formed depends on: a) the initial concentration of nitrogen dioxide $[NO_2]_0$; b) the initial concentration of the hydrocarbon $[HC]_0$, and c) the rate constants k_i (i=1 to N); i.e.

$$[O_3] = f([NO_2]_0, [HC]_0, k_1, k_2, \ldots, k_N) \qquad (5.13)$$

The terms in eq. (5.13) may be nondimensionalized, and eq. (5.13) may be expressed as

$$\frac{[O_3]}{[O_3]_c} = f\left(\frac{[HC]_0}{[NO_2]_0}, k_1^*, k_2^*, \ldots, k_{N-1}^*\right) \qquad (5.14)$$

where $k_1^*, k_2^*, \ldots, k_{N-1}^*$ represent N-1 dimensionless groups formed from the different rate constants, and $[O_3]_c$ is some characteristic ozone concentration in the mixture. To select $[O_3]_c$, it is recalled that in a nitrogen dioxide-air mixture the amount of ozone formed is (Section III)

$$[O_3]^2_{pss} = \frac{k_1}{k_3}\left([NO_2]_0 - [O_3]_{pss}\right) \qquad (3.10)$$

In most practical situations, $[O_3]_{pss}$ is negligible compared to $[NO_2]_0$, in which case eq. (3.10) becomes

$$[O_3]_{pss} \approx \sqrt{\frac{k_1}{k_3}[NO_2]_0} \qquad (5.15)$$

Representing $[O_3]_c$ by this expression, eq. (5.14) can be rewritten as

$$\frac{[O_3]}{[O_3]_c} = \frac{[O_3]}{[O_3]_{pss}} \cdot \frac{[O_3]_{pss}}{\sqrt{\frac{k_1}{k_3}[NO_2]_0}} = f\left(\frac{[HC]_0}{[NO_2]_0}, k_1^*, k_2^*, \ldots, k_{N-1}^*\right) \qquad (5.16)$$

For a hydrocarbon-nitrogen dioxide-air mixture which contains just one type of hydrocarbon, the values of the k_i's are constants, and $[O_3]/\sqrt{\frac{k_1}{k_3}[NO_2]_0}$ depends only on the ratio of the initial concentrations of the hydrocarbon and the nitrogen dioxide, i.e.,

$$\sqrt{\frac{[\,\cdot\,]}{\frac{k_1}{k_2}[NO_2]_0}} \qquad \frac{[\,\cdot\,]_0}{[NO_2]_0} \qquad (5.17)$$

Equation (5.17) relates the amount of ozone formed to the initial nitrogen dioxide concentration and the initial concentration ratio.

In many previous experiments, instead of nitrogen dioxide, nitric oxide was used in the initial gas-air mixture. With nitric oxide in the initial gas-air mixture, the production of ozone occurred at a later time than with nitrogen dioxide, but the maximum amount of ozone generated was found to be the same for both nitric oxide and nitrogen dioxide. It is noted, further, that some investigators reported measurements of 'oxidant' instead of ozone. The term oxidant designates certain pollutants formed during the photochemical reaction. These pollutants are so named because they will oxidize some specific chemical reagents (e.g. a solution of neutral-phosphate-buffered potassium iodide) which are not readily oxidized by oxygen [53]. Although the oxidant measured includes other chemical compounds as well as ozone (e.g. peroxyacyl nitrates), ozone is generally the largest amount (by volume) present in the measured oxidant, and the data reported for ozone and oxidant were usually very similar [8,59].

For the reasons outlined above, results obtained with nitrogen dioxide or with nitric oxide, and results reported in terms of ozone or oxidant may be discussed together, and compared directly.

According to eq. (5.17), for a given type of hydrocarbon and fixed initial concentration of the hydrocarbon and the nitrogen dioxide, the amount of ozone varies directly with the square root of k_1

$$[\,\cdot\,] \propto \sqrt{k_1} \qquad (5.18)$$

It is recalled from Section III that k_1 is proportional to the light intensity (eq. 3.1). Hence, the ozone content varies with the square root of the light intensity. Barton and Bolze [31], Altshuller et. al. [5], and Grosjlicki and Nebel [29] measured the effect of light intensity on the amount of ozone (or oxidant) formed in various hydrocarbon-nitrogen oxide-air mixtures. The results reported by these investigators also confirm that the amount of ozone (or oxidant) varies with the square root of the light intensity. The computer solution obtained by Niki et. al. [46] for the photochemical reactions in a propylene-nitrogen oxide-air mixture also confirms the validity of eq. (5.10).

Equation (5.12) also shows that, for a given type of hydrocarbon, the data points should fall on a common curve on a $[O_3]/\sqrt{\frac{k_1}{k_3}[NO_2]_0}$ versus $[HC]_0/[NO_2]_0$ plot. Such a plot for the present data is given in Fig. 5.3. It is seen that, within experimental error, the data follows a single curve. This lends support to the validity of eq. (5.12). In order to test further the validity of this equation, the data reported by other investigators have been plotted in a graph similar to Fig. 5.4. These results, presented in Fig. 5.5, were for eight different types of hydrocarbons. The data given in Fig. 5.5 were all obtained in chambers irradiated artificially by either fluorescent lights [2,5,6,41,58] or by mercury lamps [50]. The measurements were made either in a static type chamber [2,6,41,58] or in a flow type tube [5,58]. Scott [50] irradiated 1-methylheptane-nitrogen dioxide-air mixtures in a long path infrared absorption cell. Altshuller and Cohen [2] tested ethylene-nitric oxide-air mixtures in Teflon bags. Altshuller et. al. [6] and Kopczynski et. al. [41] used the same aluminum irradiation chamber and tested n-butane-nitric oxide-air mixtures [6] and aldehyde-nitric oxide-air mixtures [41].

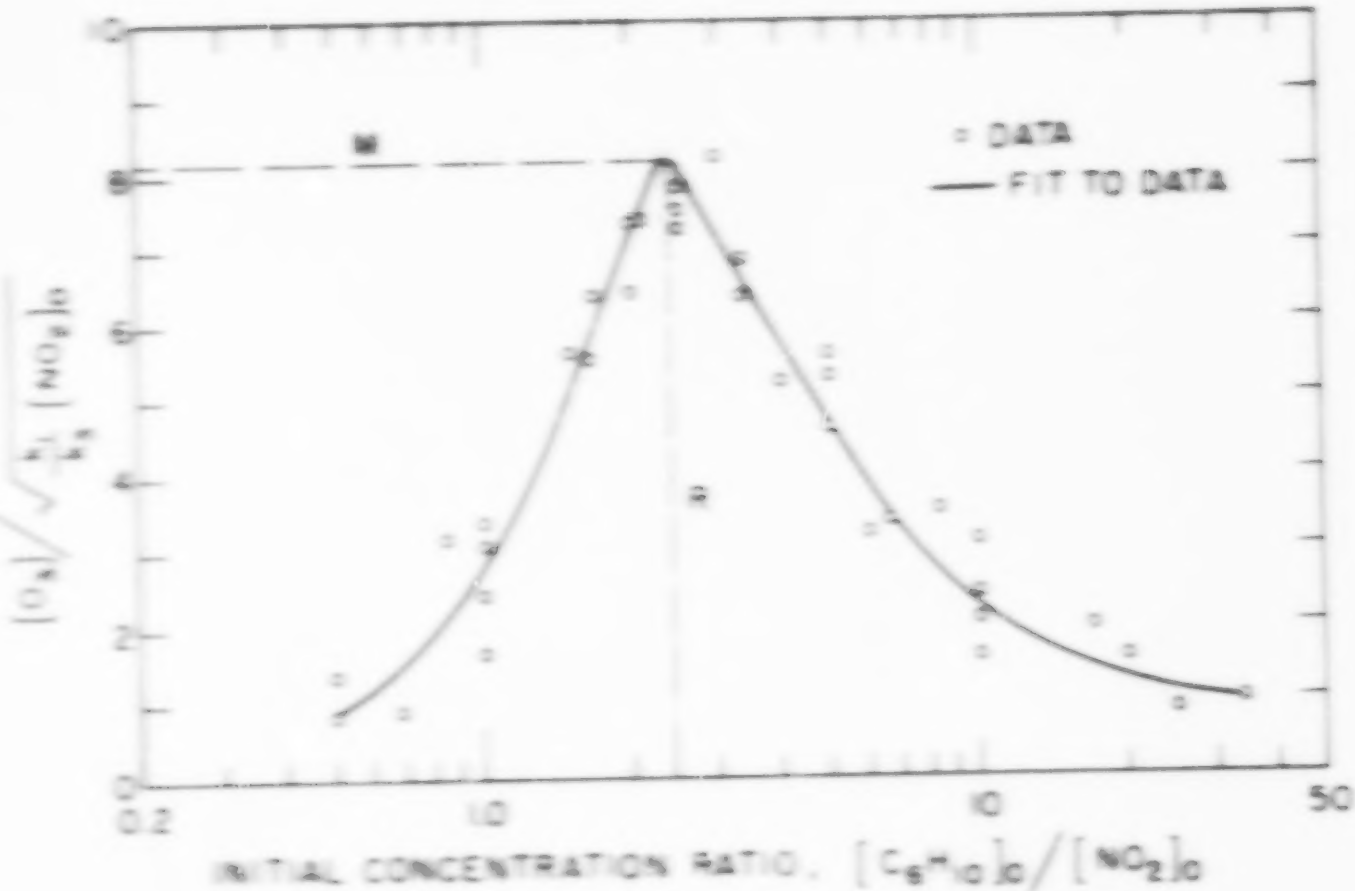
DATA
FIT TO DATA
M
0
2
4
6
8
10
0.2
1.0
10
50
INITIAL CONCENTRATION RATIO, $[C_6H_{10}]_0/[NO_2]_0$
$\frac{[O_3]}{\sqrt{\frac{k_1}{k_4}[NO_2]_0}}$

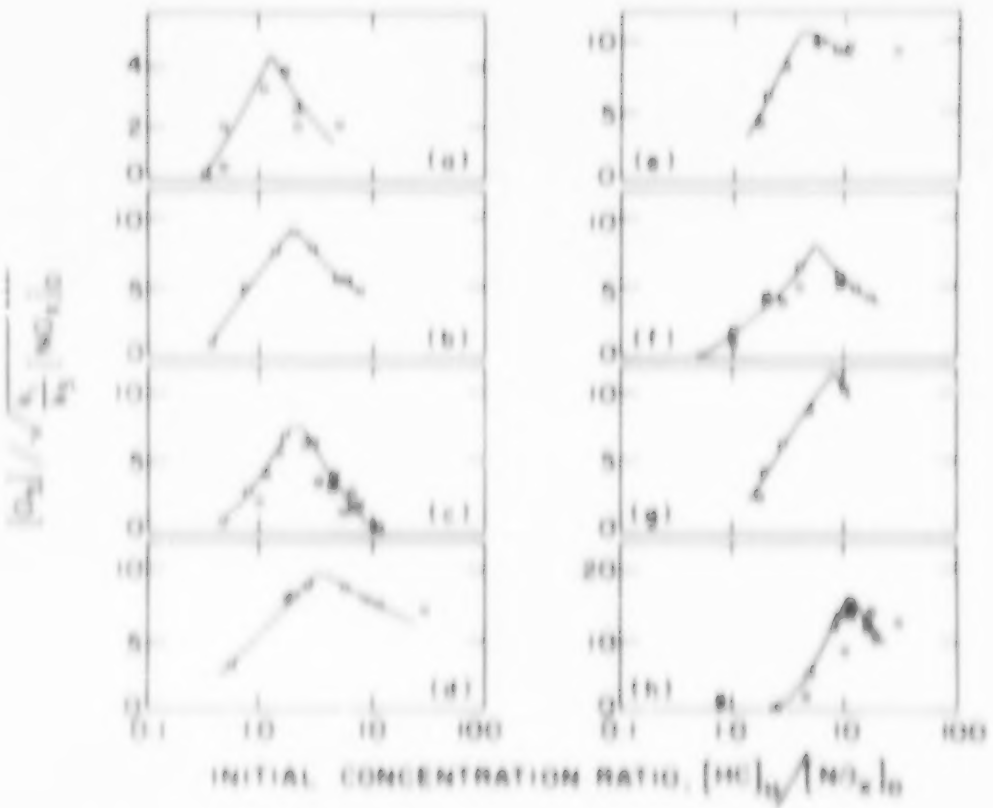

Fig. 6-5. Normalized ozone content in hydrocarbon-nitrogen oxides-air mixtures. (a) Ethylene, Altshuller and Cohen [2]. (b) 3-methylheptane, Scott [30]. (c) (trans)-butene, Stephens and Price [26]. (d) Propionaldehyde, Topczynski, et. al. [31]. (e) Acetaldehyde, Topczynski, et. al. [31]. (f) Propylene, Altshuller et. al. [5]. (g) Formaldehyde, Topczynski, et. al. [31]. (h) n-butane, Altshuller et. al. [6]

flow type experiments were performed by Altshuller et. al. [1] for propylene-nitric oxide-air mixtures in an aluminum chamber, and by Stephens and Price [58] for cis-2-butene-nitric oxide-air mixtures in a Pyrex tube. Generally, fewer data points were taken in the previous experiments than in the present study. Nevertheless, the previous data, summarized in Fig. 5.5 also indicate that the data can be correlated according to eq. (5.1f).

In addition to the investigations quoted above, ozone (or oxidant) measurements were reported in [7,10,25,31,50,51]. The results of these investigations [7, 8,25,31,50,51] could not be included in Fig. 5.5 because either there was not enough information given to plot the graph [10,11], or the amount of ozone (or oxidant) measured was not given directly [7,25,50,51]. The amount of ozone (or oxidant) was measured by Bufalini and Altshuller [10] and by Barton and Bolze [31]. However, Bufalini and Altshuller reported the nitrogen dioxide dosage instead of the initial concentration of nitrogen dioxide. Barton and Bolze did not report the maximum amount of the oxidant generated. The amount of ozone (or oxidant) was reported indirectly by Altshuller et. al. [7], Glasson and Tuesday [25], Haagen-Smit [50], and by Romanovsky et. al. [51]. Altshuller et. al. reported the oxidant decay, Glasson and Tuesday the initial formation rate of ozone. Haagen-Smit measured the crack depths of rubber strips. Romanovsky et. al. presented their results in the form of ozone contour maps.

An attempt can now be made to estimate, at the maximum possible amount of ozone formed in a hydrocarbon-nitrogen dioxide-air mixture, and at the concentration ratio at which this maximum occurs, (at the

maximum of the $[O_3]/\frac{k_1}{k_3}[NO_2]_0$ versus the concentration ratio curve be M, and the concentration ratio corresponding to this point be R (see fig. 5.4 and 5.5), i.e.

$$R = \left.\frac{[C_3]_{max}}{\frac{k_1}{k_3}[NO_2]_0}\right\} \text{ at } [C_3] = [C_3]_{max} \qquad (5.19)$$

and

$$R = \left.\frac{[NO]_0}{[NO_2]_0}\right\} \qquad (5.20)$$

In principle, the values of M and R can be obtained from the appropriate reaction equations (e.g. eqs. 5.1-5.12). In practice, this is a formidable, if not an impossible task owing to the complexity of the equations. The data summarized here, however, provide some information about M and R. Equations (5.19) and (5.20) may be rearranged to the form

$$[C_3]_{max} = M\frac{k_1}{k_3}\sqrt{\frac{k_1}{k_3}}\sqrt{[NO]_0} \qquad (5.21)$$

$$[C_3]_{max} = R\sqrt{\frac{k_1}{k_3}}\sqrt{[NO_2]_0} \qquad (5.22)$$

The maximum amounts of ozone formed ($[O_3]_{max}$) in figs. 5.2 and 5.3 are represented by the envelopes of the ozone versus cyclohexene and the ozone versus nitrogen dioxide curves (dotted lines in figs. 5.2 and 5.3). From figs. 5.2 and 5.3, the equations of these curves (envelopes) may be determined, and are

$$[C_3]_{max} = 0.58\sqrt{[C_6H_{10}]_0} \qquad (5.23)$$

$$[C_3]_{max} = \sqrt{[NO_2]_0} \qquad (5.24)$$

Comparing eqs. (5.21) and (5.23), and noting that $\sqrt{k_1/k_3} = 0.122$ ppm$^{1/2}$ (Section III), the following expression is obtained

$$M = 1.1\sqrt{R} \tag{5.25}$$

The above relationship between M and R was derived entirely from the present data using cyclohexene. In order to estimate the relationship between M and R for other types of hydrocarbons, M was plotted as a function of R for the nine different hydrocarbons for which values of M and R could be estimated (Figs. 5.4 and 5.5). The results, given in Fig. 5.6, show that in all cases M varies approximately with the square root of R with the proportionality constant being ≈ 5.3. Therefore, the relationship given by eq. (5.25) appears to be valid not only for cyclohexene but for other types of hydrocarbons as well. Substituting eq. (5.25) into eq. (5.21) and recalling that $k_3 = 0.425$ ppm^{-1} s^{-1} (Section III), eq. (5.2) becomes

$$(c_3)_{max} = 0.11\sqrt{k_1/k_3}\sqrt{(R)_0} \tag{5.26}$$

or

$$\frac{(c_3)_{max}}{\sqrt{(R)_0}} = 0.11\sqrt{k_1/k_3} \tag{5.27}$$

Accordingly, the maximum amount of ozone formed depends only on the initial concentration of the reactive hydrocarbon but not on its type. Equation (5.27) is plotted in Fig. 5.7, together with the experimental data. There is reasonable correlation between the data and the curve given by eq. (5.27). In Fig. 5.7 the carbon weights of propylene and ozone are plotted in the early mixing to various stages of the dilute tubes

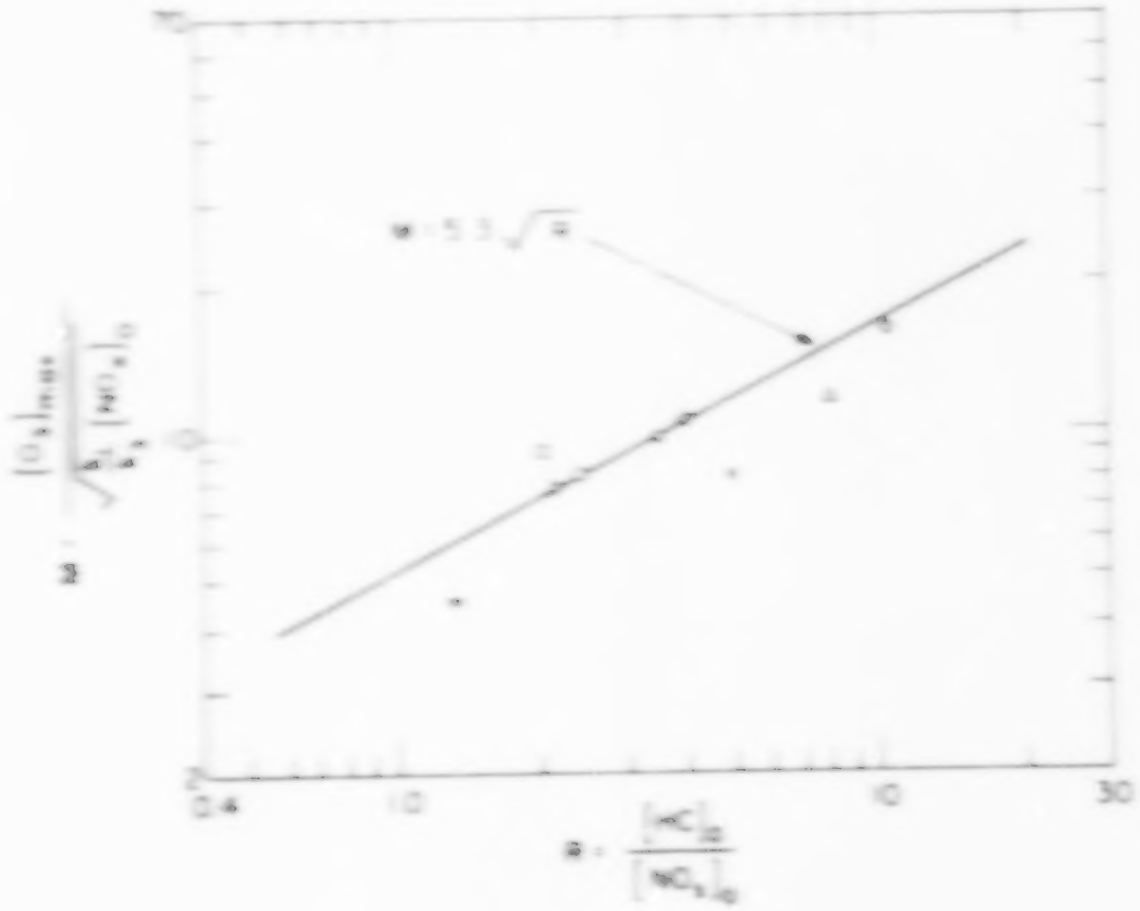
$\Phi = 5.3\sqrt{\alpha}$
$\Phi = \frac{[O_2]_{max}}{\sqrt{\frac{k_1}{k_3}[RH]_0}}$
$\alpha = \frac{[\ ]_0}{[RH]_0}$
0.4
1.0
10
30

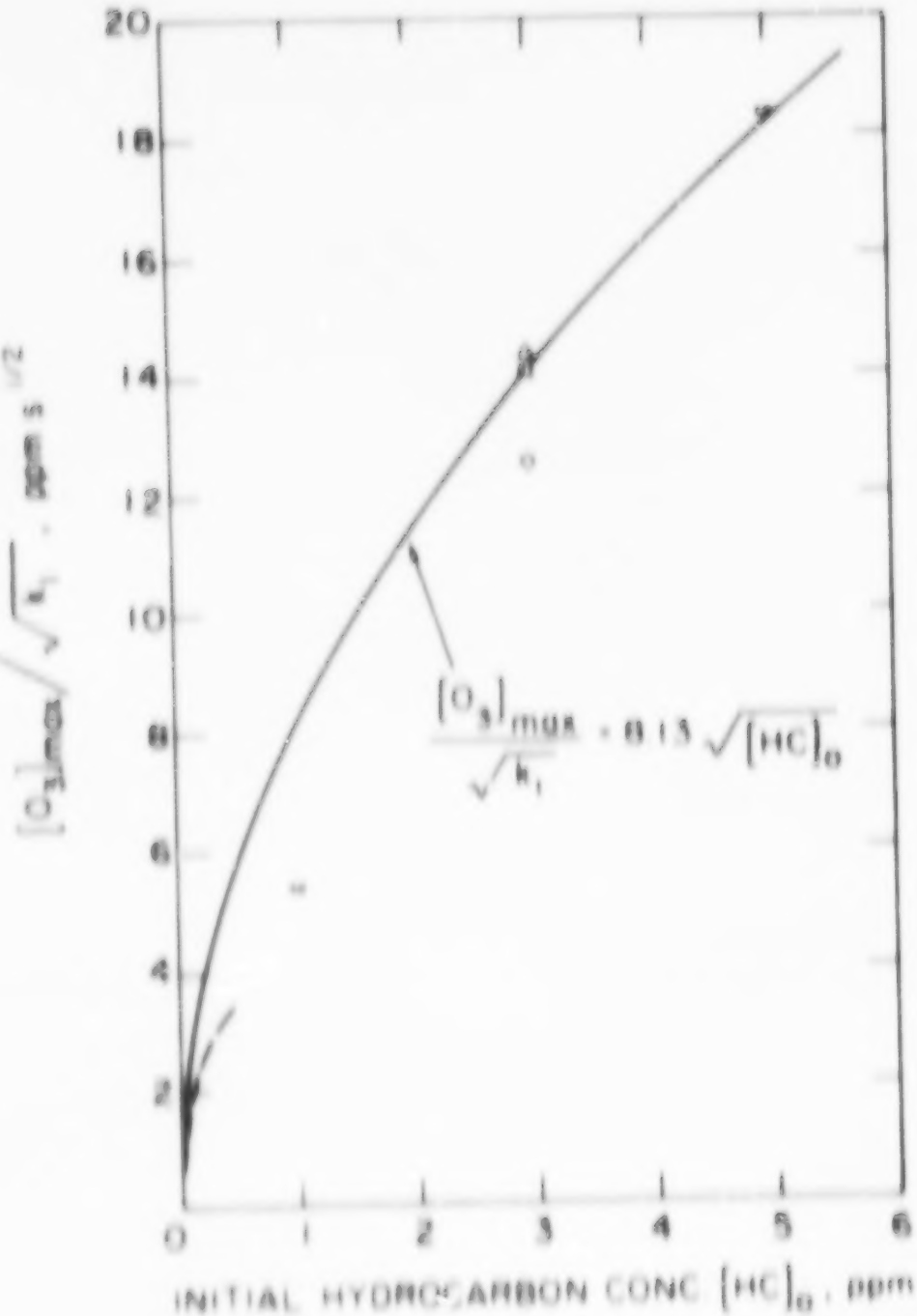
20
18
16
14
12
10
8
6
4
2
0
1
2
3
4
5
6
$[O_3]_{max}/\sqrt{k_1}$, ppm s$^{1/2}$
$\frac{[O_3]_{max}}{\sqrt{k_1}} = 8.15\sqrt{[HC]_0}$
INITIAL HYDROCARBON CONC $[HC]_0$, ppm

were also included. These atmospheric measurements were reported by the U.S. Department of Health, Education and Welfare [70] and gave the oxidant content as a function of non-methane hydrocarbon concentration in ppm C. In order to include the atmospheric data in Fig. 5.7, an average carbon number of five was assumed for these non-methane hydrocarbon mixtures and k_1 was taken to be 9 hr^{-1} (see Table 3.1). It is interesting to note that eq. (5.27), which was based on the data obtained from mixtures containing only one type of hydrocarbon, also yields reasonable results for mixtures containing several types of hydrocarbons such as those present in the atmosphere.

The maximum amount of ozone that can be formed for a given concentration of nitrogen dioxide depends on R (eq. 5.22). Since it is easier to determine R than M, eq. (5.22) is written as (see eqs. 5.23 and 5.26)

$$[O_3]_{max} = 0.11\sqrt{k_1/R}\,[NO_2]_0 \tag{5.28}$$

or

$$\frac{[O_3]_{max}}{\sqrt{k_1 R}} = 0.11[NO_2]_0 \tag{5.29}$$

Therefore, the maximum amount of ozone depends on R which is different for different types of hydrocarbons. However, the ratio $[O_3]_{max}/\sqrt{k_1 R}$ is independent of the type of the hydrocarbon and depends only on the initial concentration of the nitrogen dioxide. Equation (5.29) is presented in Fig. 5.8 together with the available data deduced from Figs. 5.4 and 5.5. It is seen that there is reasonable agreement between the curve given by eq. (5.29) and the existing data.

The foregoing discussion illustrated that in order to determine the maximum amounts of ozone produced in a given hydrocarbon-nitrogen dioxide

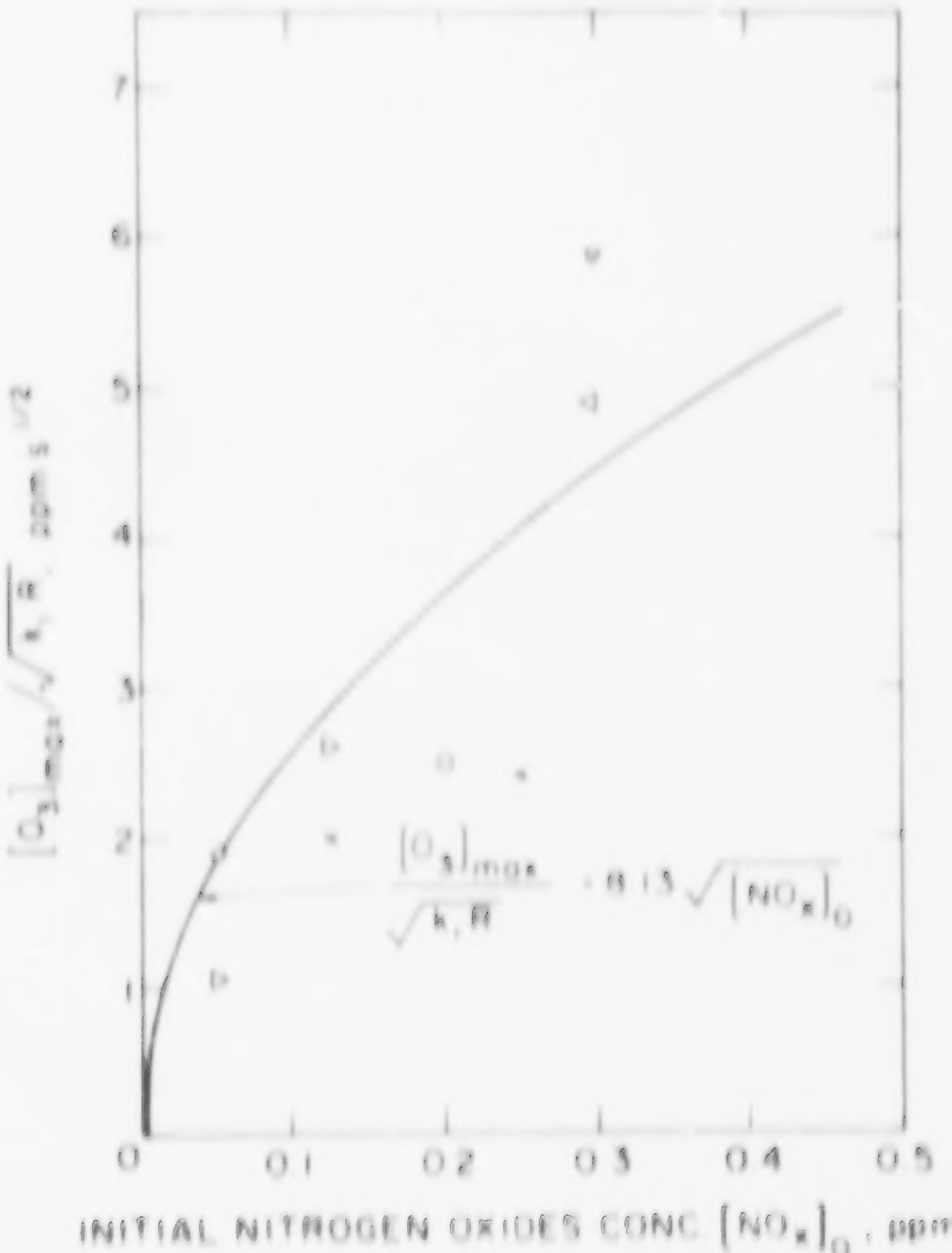

Fig. 2-1. Maximum amount of ozone as a function of the initial nitrogen oxides concentration. ○ present result, ▲ cis-2-butene-nitrogen oxides [50], ▽ propionaldehyde, Cronkowski et al. [51], ◇ acetaldehyde, Cronkowski et al. [51], ▷ propylene, Altshuller et al. [52], ◁ butylene, Altshuller et al. [6]

air mixture, the values of M and N for that hydrocarbon are needed. It would be desirable, therefore, to be able to estimate the values of M and N for different types of hydrocarbons. The values of M and N depend on all the rate constants in a complex manner. An inspection of the reaction equations (eqs. 5.1 to 5.12), indicated that the rate constants which would most likely influence M and N were k_8, k_9, and k_{10}. In addition, M and N might also be related to the conversion rate, k_{NO}, of nitric oxide to nitrogen dioxide [1,13,14,28,31]. Therefore, an attempt was made to correlate N with each of these rate constants. To facilitate this correlation, the suggestion of Glasson and Tuesday [28] was followed and a dimensionless relative rate constant called "reactivity", $\hat{k}_i$, is defined as

$$\hat{k}_i = \frac{k_i}{k_{i,propylene}} \qquad (5.10)$$

where $k_{i,propylene}$ is the rate constant of propylene. The results, presented in Table 5.2 show only weak correlations between N and the reactivities $\hat{k}_8$, $\hat{k}_{10}$, and $\hat{k}_{NO}$, but indicate a strong correlation between N and $\hat{k}_9$. Therefore, a graph of N versus $\hat{k}_9$ was plotted (Fig. 5.9), and the following approximate relationship between N and $\hat{k}_9$ was obtained

$$N = \frac{}{\hat{k}_9} \qquad (5.11)$$

The value of N can be found from this expression for any given hydrocarbon. This N value may then be used in eqs. (5.7b) and (5.8b) to calculate the maximum amount of ozone formed.

Finally, in Fig. 5.10, an ozone contour map is presented on the basis of the cyclohexene data. The general features of this map were similar to those reported for propylene-nitric oxide-air mixtures [51]

Table 5.2 Reactivities of different hydrocarbons ($\hat{k} = k/k_{ref}$)

Hydrocarbon	Initial Concentration Ratio, R[a]	$\hat{k}_b$	Reactivity $\hat{k}_a$	$\hat{k}_{10}$	$\hat{k}_{90}$
n-Butane	10.5	0.060[c]	0.28[c]	------	0.3[c]
Formaldehyde	8	0.05[c]	0.9[c]	------	0.7[c]
Propylene	5	1.0	1.0	1.0	1.0
Acetaldehyde	4	0.15[c]	0.9[c]	------	0.7[c]
Propionaldehyde	1.5	0.2[c]	1.0[c]	------	1.0[c]
Cyclohexene	2.3	------	------	5.2	1.0[d]
Cis-2-Butene	2.1	3.6[e]	------	2.0	2.0[d]
3-Methylheptane	1.0	0.06[e]	------	------	0.21[d]
Ethylene	1.3, 11[f]	0.2[c]	0.1[c]	0.33	0.3[c]

a ------ from Figs. 5.3 and 5.5

b ------ from Table 36 reference [41]

c ------ from reference [46]

d ------ from reference [76]

e ------ from reference [54]

f ------ from reference [75]

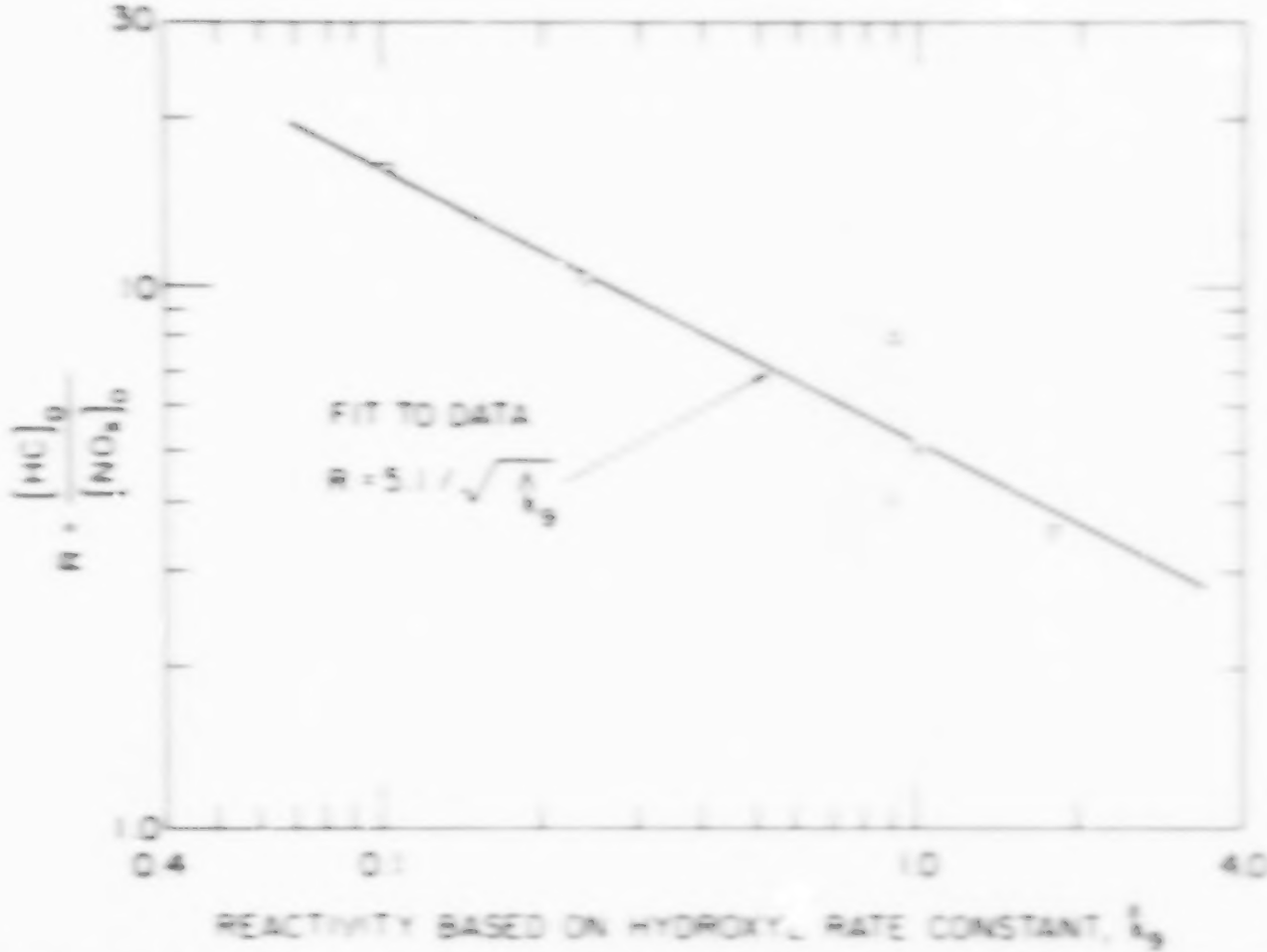

Fig. 5.4. Variation in the concentration ratio R (at which the ozone content is maximum) with the reactivity k_9. ○ ethylene, Altshuller and Cohen [22]; ● n-butane, Altshuller et al. [6]; △ formaldehyde, Kuczynski et al. [41]; ▲ propylene, Altshuller et al. [6]; ◇ acetaldehyde, Kuczynski et al. [41]; ▼ propionaldehyde, Kuczynski et al. [41].

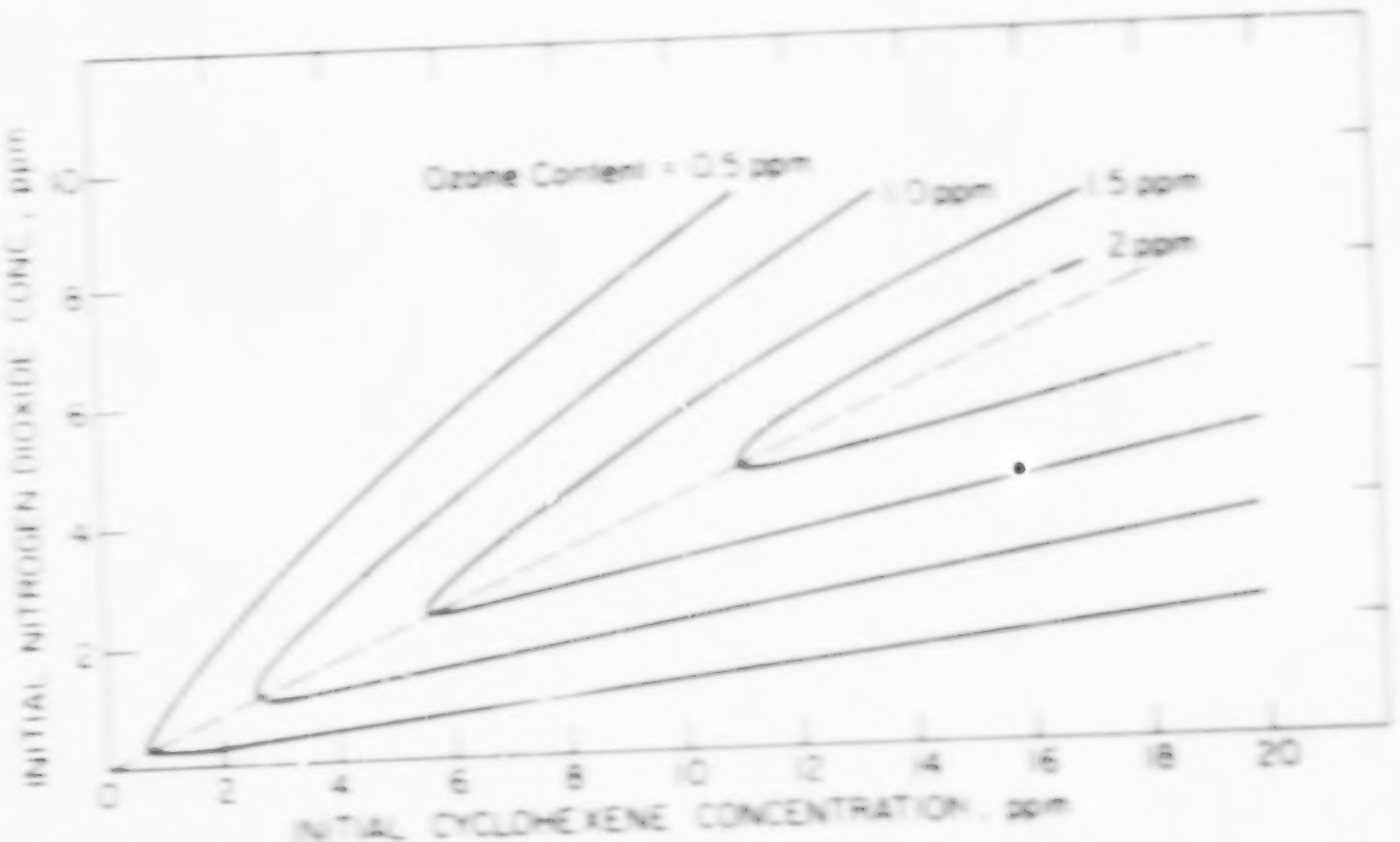
Ozone Content = 0.5 ppm
1.0 ppm
1.5 ppm
2 ppm
INITIAL NITROGEN DIOXIDE CONC., ppm
INITIAL CYCLOHEXENE CONCENTRATION, ppm
0
2
4
6
8
10
12
14
16
18
20

and for mixtures of non-methane hydrocarbons in the atmosphere [10] (Figs. 5.10 and 5.11). There was one notable difference between the maps obtained with one single hydrocarbon (e.g. cyclohexene or propylene) and with mixtures of hydrocarbons. When only a single hydrocarbon was used, each curve had reasonably well defined 'knolls', which could be connected by a straight line. For the atmospheric data, a straight line could not be drawn through the knolls either because the measurements were inaccurate, or because the many different types of hydrocarbons in the atmosphere distorted the slope of the curve.

5.2 The Effects of Mixture Composition on Particulate Formation

The nuclei and the aerosol contents in the tunnel are given in Fig. 5.1 for a typical set of initial cyclohexene and nitrogen dioxide concentrations. For other initial concentrations of nitrogen dioxide and cyclohexene, the number distribution of the nuclei and the aerosols along the tunnel exhibited similar trends, i.e. the numbers first increased, reached maximum values and then decreased slightly. Thus, in general, the nuclei and the aerosol formation followed a pattern similar to the process of ozone formation. However, the nuclei and aerosol contents changed at slower rates than the ozone content; in fact, the number of nuclei and aerosols varied only slightly past the third sampling station which was 1.75 m from the entrance of the tunnel. Since the nuclei and the aerosol counts at the tunnel entrance were nearly zero, most of the nuclei and the aerosols were formed in the region between the entrance and the third sampling station. According to the data in Fig. 5.1, ozone was also generated at the fastest rate in this region.

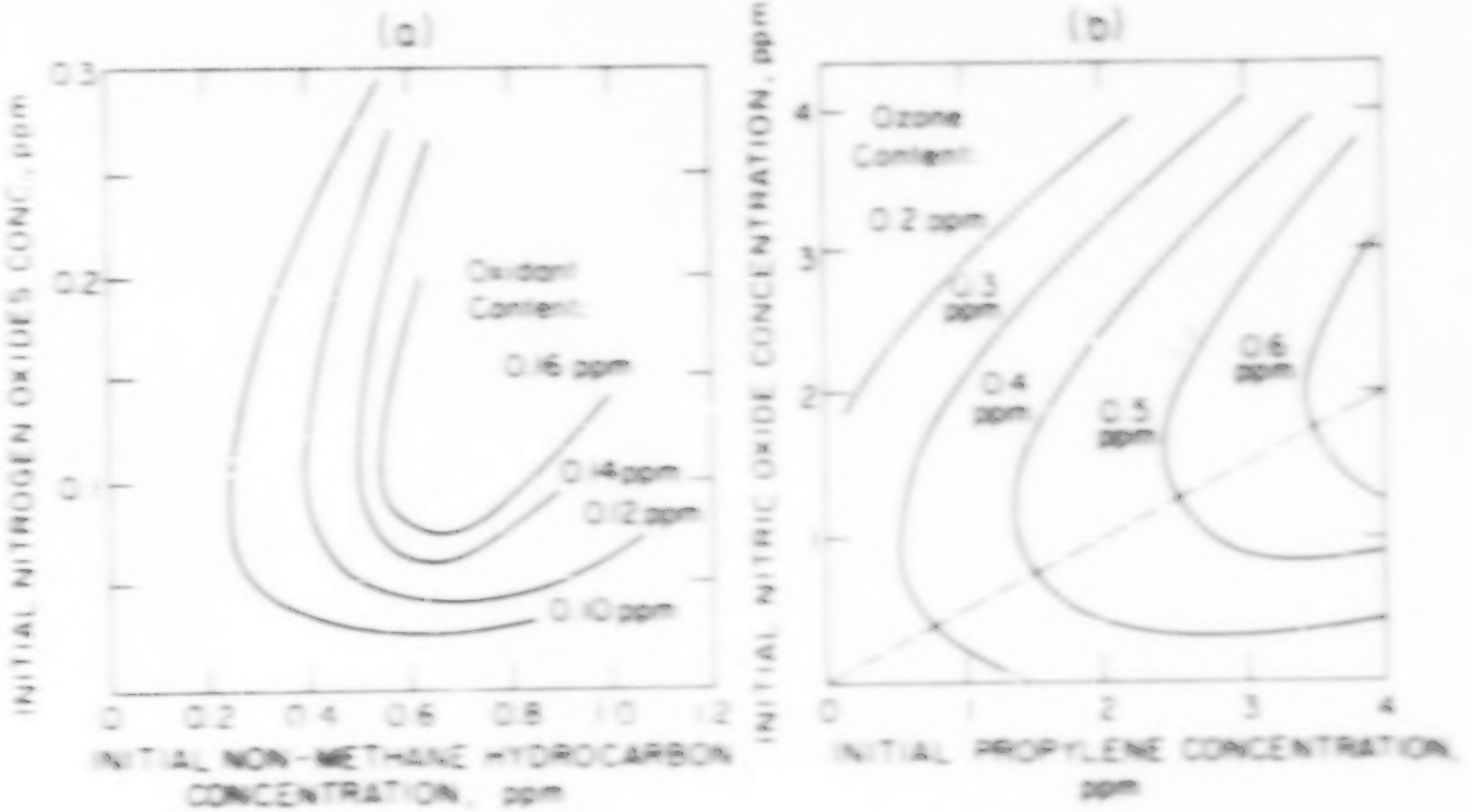
(a)
INITIAL NITROGEN OXIDES CONC., ppm
0.3
0.2
0.1
0
Oxidant Content:
0.16 ppm
0.14 ppm
0.12 ppm
0.10 ppm
0 0.2 0.4 0.6 0.8 1.0 1.2
INITIAL NON-METHANE HYDROCARBON CONCENTRATION, ppm
(b)
INITIAL NITRIC OXIDE CONCENTRATION, ppm
4
3
2
1
0
Ozone Content:
0.2 ppm
0.3 ppm
0.4 ppm
0.5 ppm
0.6 ppm
0 1 2 3 4
INITIAL PROPYLENE CONCENTRATION, ppm

Initially, nuclei were produced by the interaction of some of the primary reactants which were the byproducts of the photochemical reactions [18,49,51,61]. The nuclei then interacted both with gaseous molecules and with each other, resulting in an increase in the size of the nuclei. Eventually, the nuclei reached a size which became detectable on the aerosol counter. These "nuclei" were then designated as aerosols. The number of nuclei and aerosols decreased along the tunnel due to coagulation, diffusion, and deposition. Since the number of nuclei and aerosols remained reasonably constant along the tunnel, it appeared that in the present system the formation and the depletion of nuclei and aerosols proceeded at nearly the same rates. Here, we were not concerned with the details of these two processes but were only interested in the maximum number of nuclei and aerosols generated for each combination of nitrogen dioxide and cyclohexene concentrations. The maximum numbers of nuclei and aerosols deduced from all the data are listed in Appendix I.

The maximum number (referred to simply as the "number") of nuclei produced for different initial concentrations of cyclohexene and nitrogen dioxide is given in Fig. 5.12. In comparing this figure with Fig. 5.2, it can be seen that the variation in the nuclei content with the initial concentrations of nitrogen dioxide and cyclohexene is remarkably similar to the variation of the ozone content with the initial concentrations of nitrogen dioxide and cyclohexene. For example, similar to ozone, for a given initial nitrogen dioxide concentration, the number of nuclei produced first increased with the cyclohexene concentration, reached a peak and then decreased with further increase in the initial cyclohexene concentration. Moreover, for a given initial nitrogen dioxide concentration, the amounts of the ozone and the nuclei produced

reached their respective maximum values at approximately the same initial cyclohexene concentration (5 p.p.m. for $[NO_2]_o$ = 2 ppm, $[O_3]_{max}$ occurs at $[Light]_o$ = 4.5 ppm and the maximum number of nuclei $[N]_{max}$ at $[Light]_o$ = 4.5 ppm).

The similarities in the heights of the nuclei and the ozone levels even more evident if the number of nuclei is plotted against the initial concentration ratio $([Light]_o/[NO_2]_o)$ (Fig. 5.13). It is seen that the maximum number of nuclei always occurs at a concentration ratio of about 2.4, which is the same ratio at which the ozone content is a maximum in the mixture (Fig. 5.4).

The maximum number of nuclei produced for a given initial cyclohexene concentration is represented by the dotted line in Fig. 5.12. The equation of this line is

$$[N]_{max} = A_1 [Light]_o^{1/2} \qquad (5.10)$$

A_1 is a numerical constant having the value of 130 cm^{-3} $ppm^{-1/2}$. Again, similar to ozone, a) the maximum number of nuclei may be expressed independently of the initial nitrogen dioxide concentration, and b) the maximum number of nuclei varies with the square root of the initial cyclohexene concentration. The maximum number of nuclei produced for a given initial nitrogen dioxide concentration may also be evaluated from the data (Fig. 5.12). The results show that

$$[N]_{max} = A_2 [NO_2]_o \qquad (5.11)$$

where A_2 = 835 cm^{-3} $ppm^{-1/2}$. As in the case of ozone (see eq. 5.4), the maximum number of nuclei varies directly with the square root of the initial nitrogen dioxide concentration.

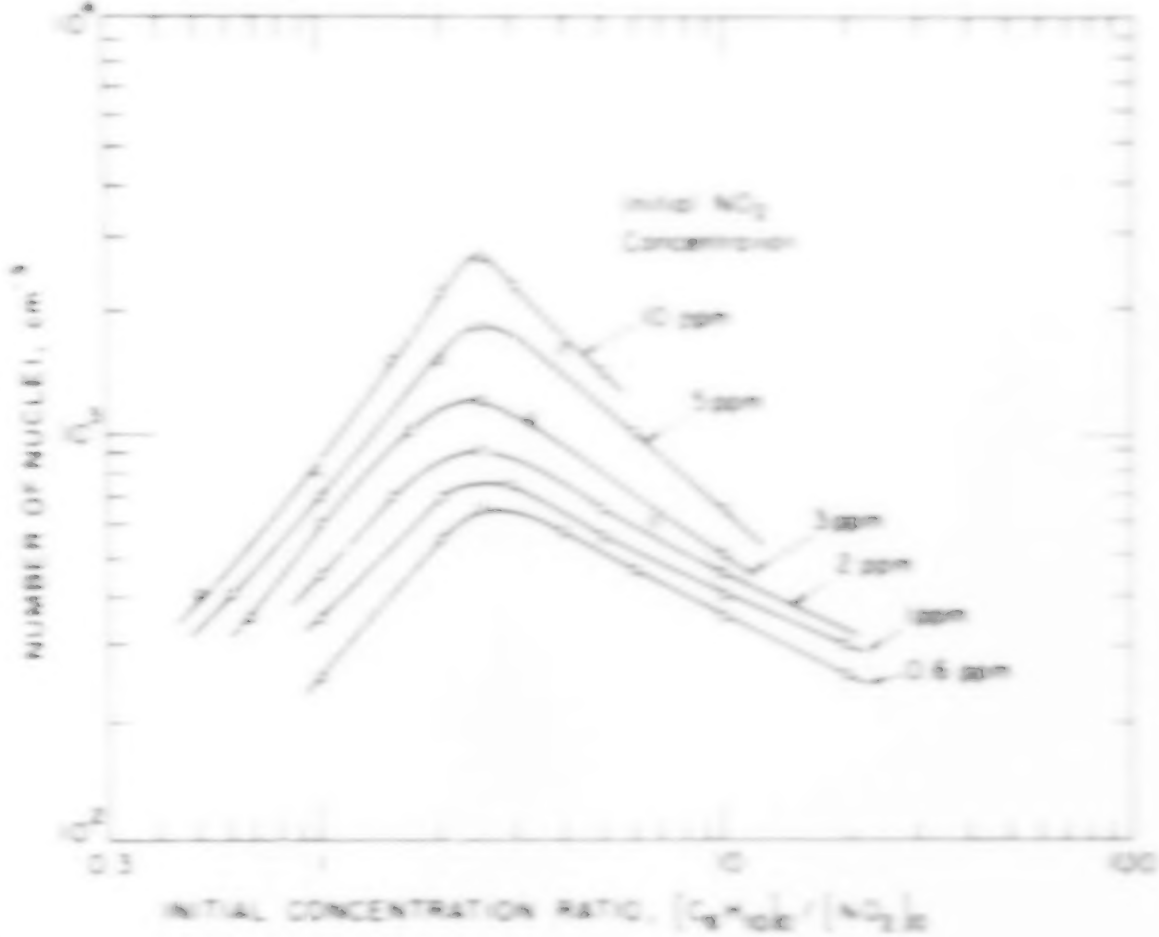
Initial NO_2 Concentration
10 ppm
5 ppm
3 ppm
2 ppm
1 ppm
0.5 ppm
0.3
1
10
100
INITIAL CONCENTRATION RATIO, $[C_8H_{16}]_0 / [NO_2]_0$

by fluorescent lamps. They reported that for a mixture containing 2 ppm of nitrogen dioxide and 1.5 ppm of cyclohexene, the number of nuclei produced was about $700\ cm^{-3}$. They did not report either the light intensity or the relative humidity inside their Pyrex tube. However, for the corresponding mixture composition, the present data indicate a nuclei count of $600\ cm^{-3}$ (Fig. 5.12) which is in good agreement with the value obtained by Stevenson, et al.

The number of aerosols as a function of the initial cyclohexene and nitrogen dioxide concentrations is shown in Fig. 5.14. For a given initial nitrogen dioxide concentration, the aerosol content at first increased sharply with increasing concentrations of cyclohexene. At about 100 aerosols $per\ cm^3$, the aerosol content gradually levelled off with further increase in the initial cyclohexene concentration. Figure 5.14 does not provide much information on the number of aerosols formed. When the aerosol content is plotted against the initial concentration ratio $([light]_o/[NO_2]_o)$, the data points all collapse onto one common curve (Fig. 5.15). In contrast to the nuclei (Fig. 5.13) and ozone (Fig. 5.4) formation, the number of aerosols produced appear to depend only on the initial concentration ratio. The effects of the initial nitrogen dioxide concentration on the aerosol content seem to be small. The apparent lack of influence of the nitrogen dioxide concentration on the aerosol production may be due to the fact that the fluctuations in the aerosol measurements (Fig. 5.12) may be larger than the effects of the changes in the nitrogen dioxide concentrations on the number of aerosols produced.

It is interesting to note that the aerosol content becomes appreciable only when the initial concentration ratio $([light]_o/[NO_2]_o)$ is larger than about 2.5, the same value at which the amounts of ozone and

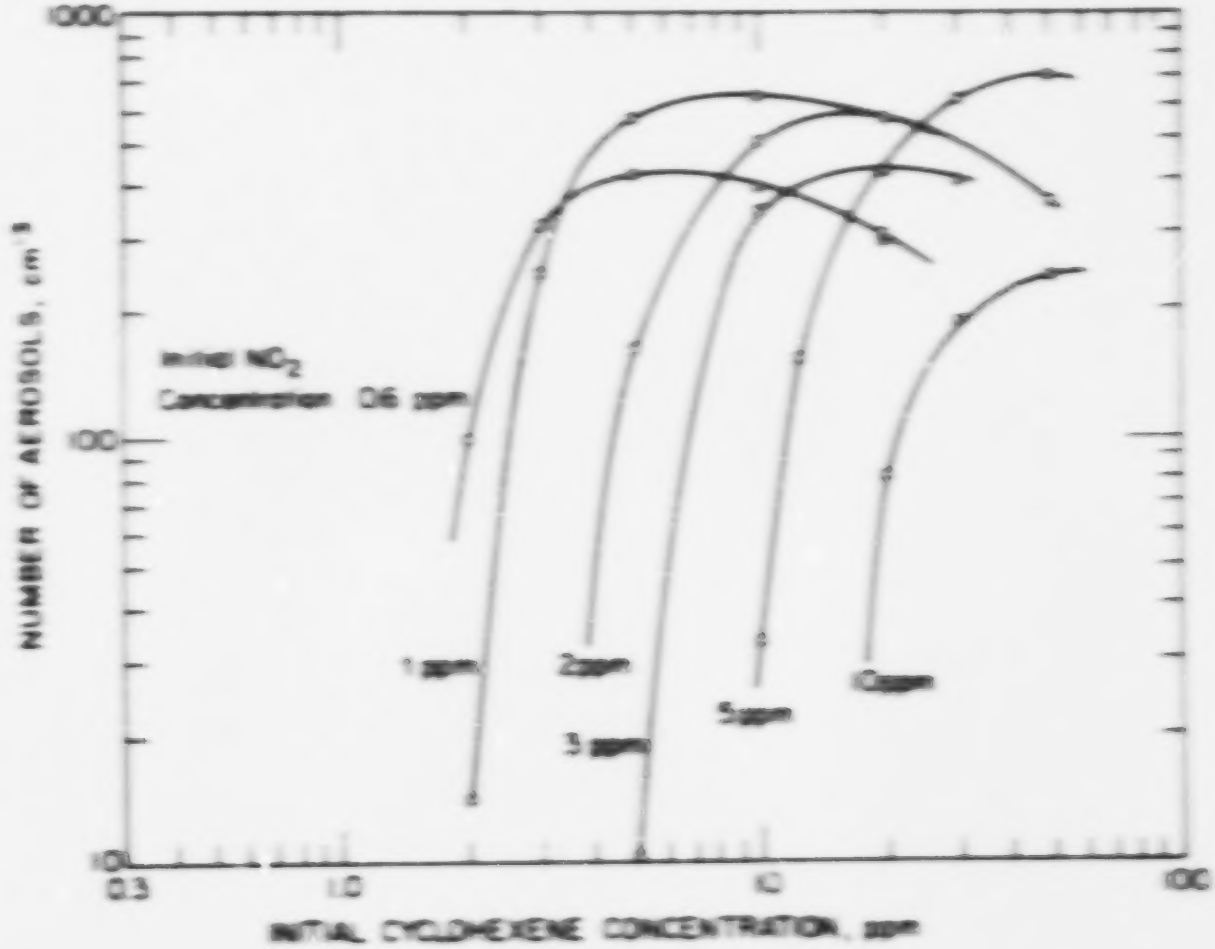

Fig. 5.14. Aerosol content in cyclohexene-nitrogen dioxide-air mixtures. Relative humidity 30%. Light intensity $k_1 = 0.33$ min^{-1}

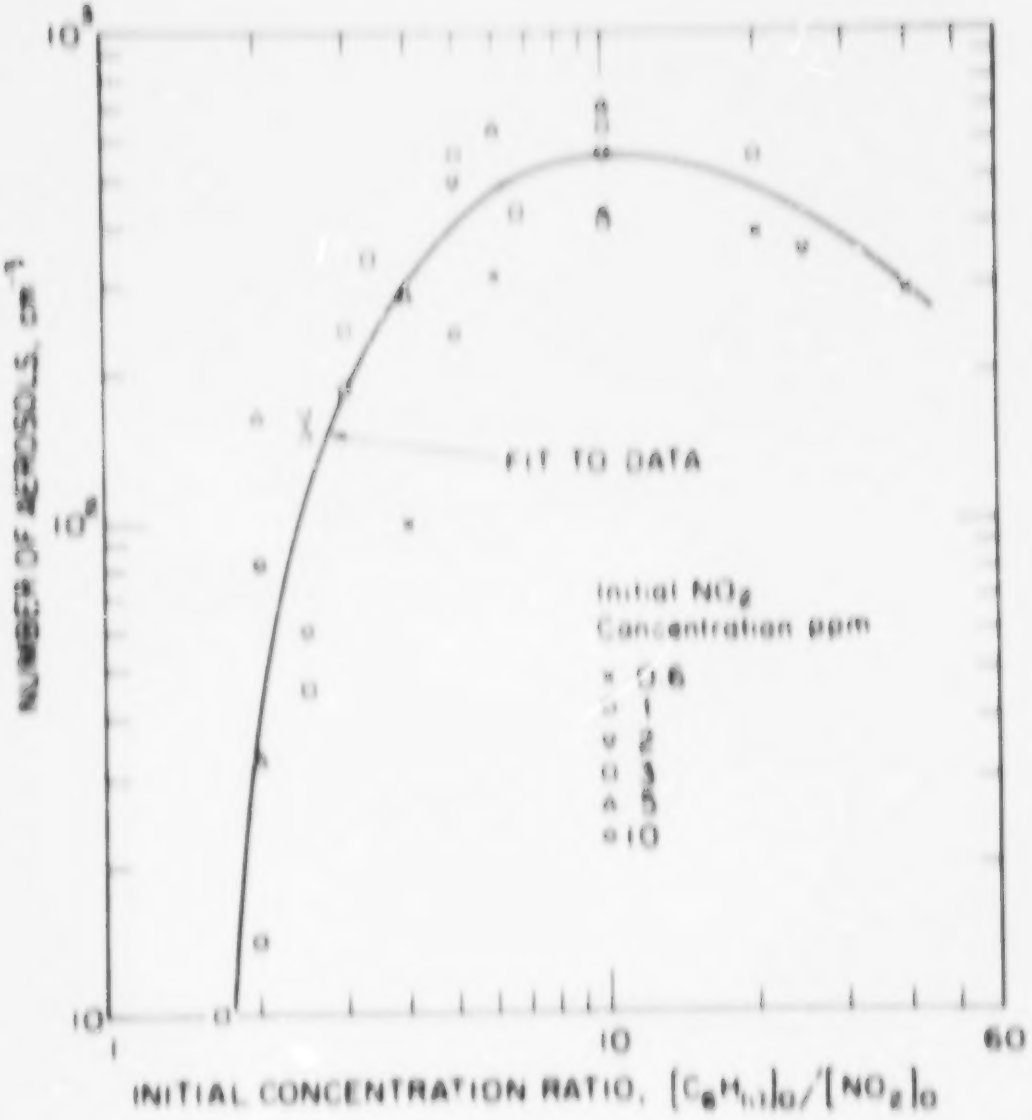

Fig. 5.15 Aerosol content as a function of the initial concentration ratio in cyclohexene-nitrogen dioxide-air mixtures. Relative humidity 50%. Light intensity $I_1 = 6.33\ ks^{-1}$

nuclei reach their maximums (see Figs. 5.4 and 5.13). When the ratio is below 2.4, only about 50 aerosols cm^{-3} are generated in the mixture. This is a small number compared to the nearly 600 aerosols cm^{-3} generated when the concentration ratio is ≈ 10.

It would be desirable now to compare the present aerosol data with the results of other investigators. Direct comparison between the results of the present and previous investigations is not possible because different light intensities and different relative humidities were used in different experiments. The effects of the light intensity and the relative humidity on aerosol formation in hydrocarbon-nitrogen oxides-air mixtures have not been studied in the past. Some indications of these two effects may be deduced from the aerosol studies performed with hydrocarbon-nitrogen oxides-sulfur dioxide-air mixtures. Grobicki and Nebel [29] investigated the effect of the light intensity on aerosol formation in propylene-nitric oxide-sulfur dioxide-air mixtures. They found that the light intensity had no effect on the maximum amount of aerosols produced. The light intensity merely affected the time required to produce the maximum amount of aerosols.

The effect of the relative humidity on the amount of aerosols generated in hydrocarbon-nitrogen oxides-sulfur dioxide-air mixtures has been studied by Grobicki and Nebel [29], Harkins and Nicksic [30], Prager et. al. [47], Schuck et. al. [53], and by Wilson and Levy [64]. Some of the results showed an increase in the amount of aerosols with increasing humidity [53], while some showed a decrease [29,30,64]. Furthermore, some of the data showed no apparent relationship between the amount of aerosols generated and the relative humidity [47].

Comparisons between the present and existing aerosol data are not possible not only because the light intensities and the relative humidities were different in the tests, but also because the number count of the aerosols was not reported in most previous investigations.

In most of the past measurements, the light scattering method was employed which provided the amount of light scattered by the aerosols in some arbitrary unit, but did not yield directly the number of aerosols per unit volume [29,47,49,59]. One notable exception was the test by Renzetti and Doyle [49] who performed flow type experiments in a 0.05 m^3 Pyrex flask irradiated by mercury arc lamps. They recorded the number of aerosols produced to be 290 cm^{-3} in a mixture containing 1 ppm nitric oxide and 1 ppm cyclohexene at a relative humidity of 50%. The present data, shown in Fig. 5.15, indicate that the number of aerosols is in the range of 100 to 300 cm^{-3}. Renzetti and Doyle's data fall within the spread of the present results.

A direct quantitative comparison is not feasible between the present data and the data obtained by light scattering methods. A qualitative comparison between the present results and the data obtained by light scattering methods is possible, because the amount of light scattered is proportional to the number of aerosols in the mixture. Measurements of light scattering in hydrocarbon-nitrogen oxides-air mixtures were reported in references [29,47,49,59]. Renzetti and Doyle [49] performed flow type experiments in a 0.05 m^3 Pyrex flask irradiated by mercury lamps, using 1 ppm hydrocarbon, 1 ppm nitric oxide, and 50% relative humidity in all their tests. Prager et. al. [47] performed static type experiments in a long-path infrared absorption cell irradiated by mercury lamps. Prager et. al. kept the mixture compositions at

10 ppm hydrocarbon, 5 ppm nitric oxide, and 100 ppm water vapor (= 0.3% relative humidity). Grobicki and Nebel [29] tested gas-air mixtures in a 0.5 m^3 stainless steel chamber irradiated by fluorescent lamps. The mixture composition was fixed at 4 ppm hydrocarbon and 2 ppm nitric oxide. Stevenson et. al. [59] performed flow type experiments in a 0.125 m^3 Pyrex tube irradiated by fluorescent lamps and measured the aerosol light scattering in cyclohexene-nitrogen dioxide-air mixtures (at 3.5 ppm cyclohexene and 2 ppm nitrogen dioxide, and at 1.83 ppm cyclohexene and 1 ppm nitrogen dioxide). Altogether, over 40 different types of hydrocarbons were tested by these previous investigators [29,47,49,59]. However, in each experiment, only one set of initial hydrocarbon and nitrogen oxides concentrations was tested. Hence, an aerosol light scattering versus initial concentration ratio curve could not be plotted for any of these hydrocarbons, with the exception of cyclohexene for which light scattering was measured by four different investigators [29,47,49,59]. For cyclohexene, the aerosol light scattering against the concentration ratio could be plotted. This plot, given in Fig. 5.16, may be compared with the present data shown in Fig. 5.15. It is seen that these two figures exhibit certain common features. First, both the aerosol light scattering and the aerosol number count indicate that when the initial concentration ratio is increased from 2 to 5 the amount of aerosols produced is increased by a factor of ten (i.e. the aerosol content is increased from 40 to 400 cm^{-3}; the light scattering from 3 to 30). Second, the light scattering measurements support the present observations that: a) few aerosols are produced when the concentration ratio is below 2.4, and b) the number of aerosols produced depends mainly on the concentration ratio and very little on the initial nitrogen dioxide concentration.

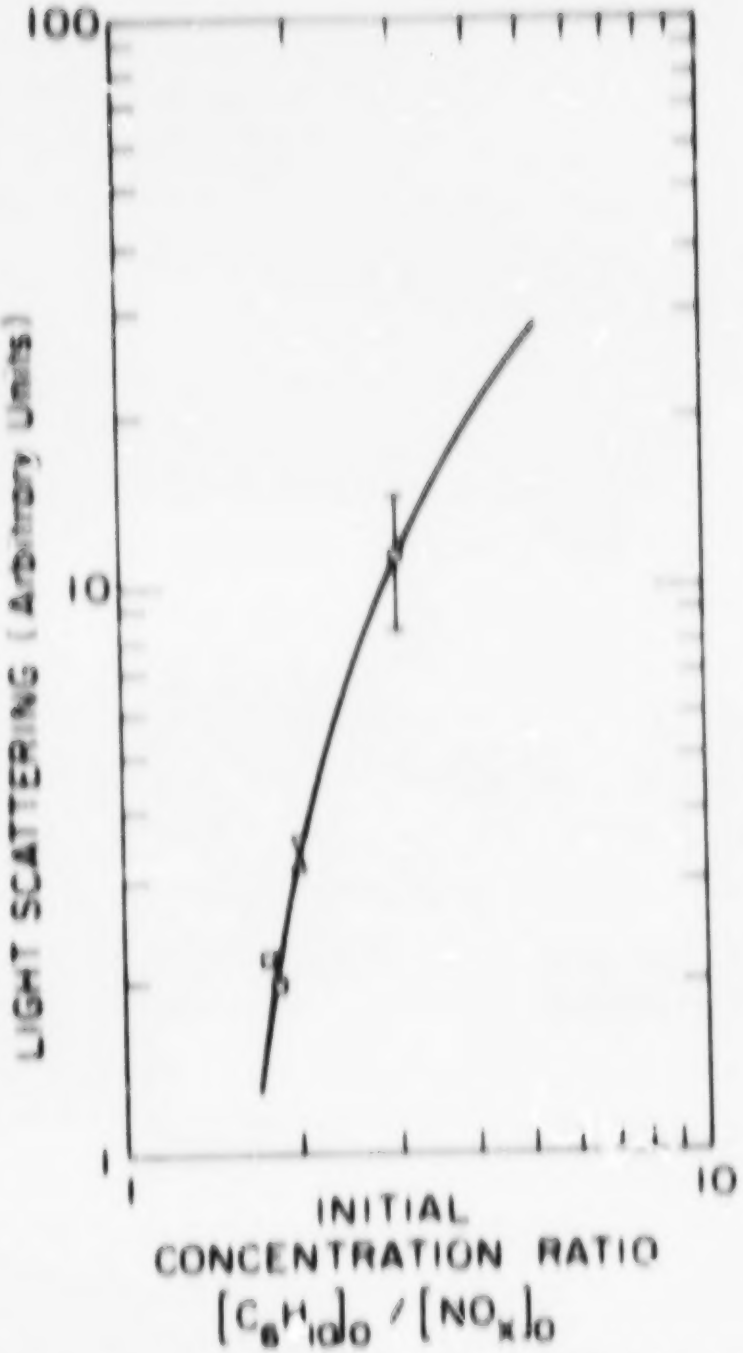

Fig. 5.16. Light scattering from aerosols produced in cyclohexene-nitrogen oxides-air mixtures. □ Stevenson et. al. [53]; ▲ Groblicki and Jebel [23]; ● Trager et. al. [37]; ◐ Renzetti and Doyle [41]

In addition to the total number of aerosols, the size distributions of the aerosols were also determined for several mixture compositions. The results of these aerosol size measurements obtained at two different sampling stations (#3 and #11) are shown in fig. 5.17. The data are expressed in terms of the dimensionless parameters (see Section II)

$$\eta = \left(\frac{\pi}{12\,\ln^2\sigma_g}\right)^{1/3} \frac{D}{D_g} \tag{2.5}$$

$$\psi = \frac{\Delta n / \Delta t}{n^2 \left(\frac{\pi}{12\,\ln^2\sigma_g}\right)^{1/3}} \tag{2.4}$$

With the use of these parameters, all aerosol size measurements should fall on one common curve [21, 45]. Moreover, in the size range where the aerosol is in a state of dynamic equilibrium (i.e. the rate of gain of aerosols by coagulation is equal to the rate of loss of aerosols due to coagulation, diffusion and sedimentation), ψ should vary inversely with the fourth power of η [11,22,38,45], i.e.,

$$\psi \propto \eta^{-4} \tag{2.6}$$

The results in fig. 5.17 show that, on a graph of ψ versus η, the present data follow a common curve and the slope of this curve is nearly -4. The slope of the curve becomes somewhat steeper for larger values of η (i.e., larger aerosols). These results agree very closely with the results of Husar and Whitby [35] (solid line in fig. 5.17) who monitored the growth of aerosols due to photochemical reactions in atmospheric air contained in a 22.5 m^3 polyethylene bag. Husar and Whitby did not report the composition of the atmospheric air.

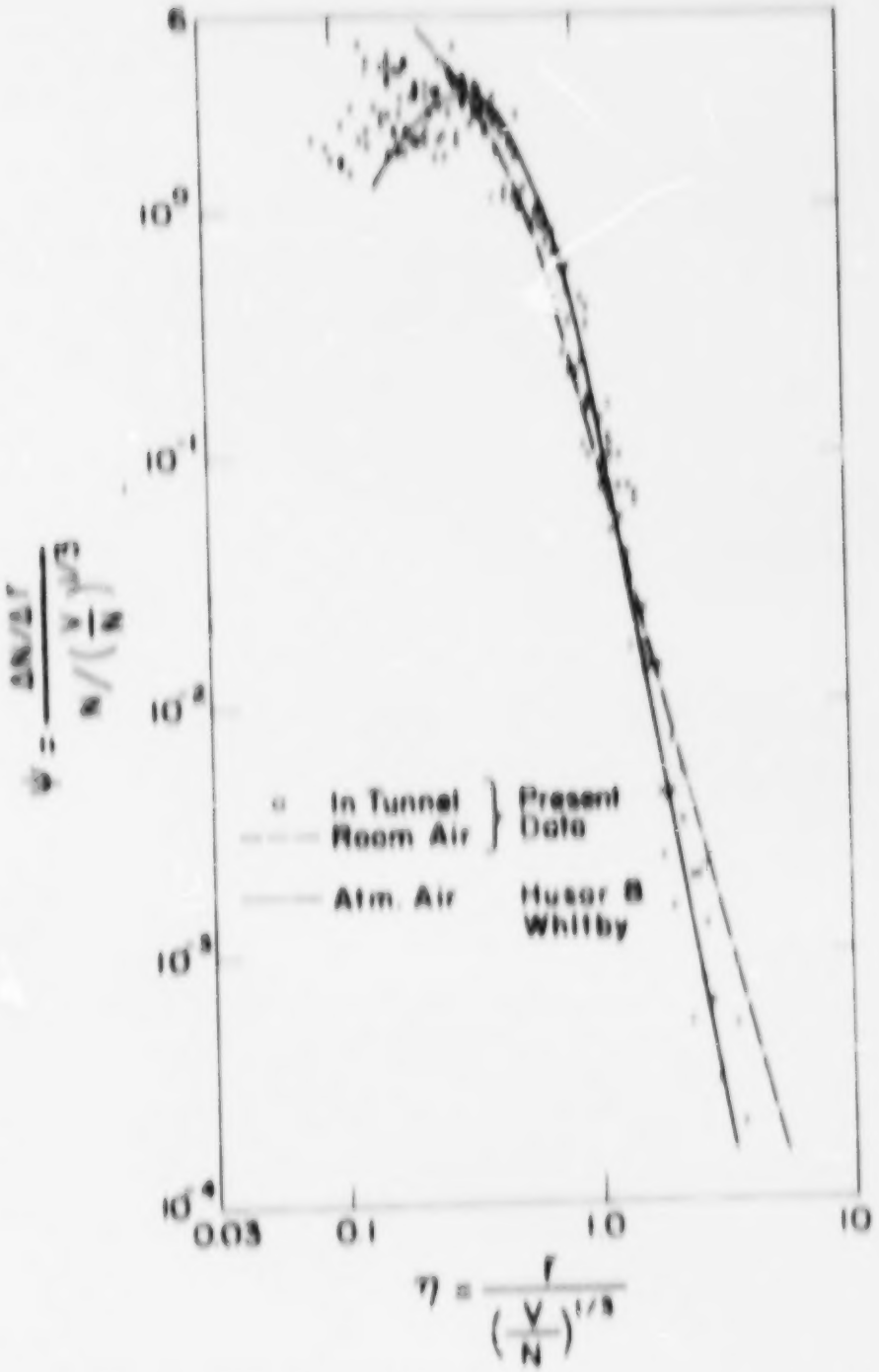

Fig. 5.12. Aerosol size distribution obtained in the tunnel for cyclohexene-nitrogen dioxide-air mixtures, ○ in the tunnel, present study, ○ - - room air, present study, —— atmospheric air, Husar and Whitby [35]

The size distribution of the aerosols in the room where the present tests were performed (see Fig. 2.6) is also included in Fig. 5.17 (dotted line). It appears that the size distributions (expressed in terms of ψ and η) of the aerosols produced by the photochemical reactions, either in a tunnel or in a bag, do not differ markedly from the size distribution of the aerosols in the natural atmosphere. The aerosol size distributions in the present tunnel, in Husar and Whitby's test, and in the atmosphere all agree very well with each other when presented on a ψ versus η plot.

The size distributions (expressed in terms of ψ and η) seem to be unaffected by the mixture composition, the light intensity or the relative humidity.

CHAPTER VI

CONCLUDING REMARKS

The experiments performed in this investigation provide new information on the particulate formation in sulfur dioxide-air mixtures and on the ozone and particulate formation in cyclohexene-nitrogen dioxide-air mixtures.

The results obtained during the photooxidation of sulfur dioxide-air mixtures showed that, for initial sulfur dioxide concentrations ranging from 0.2 to 1 ppm and relative humidities ranging from 25 to 100%, the maximum number of nuclei varied directly with the sulfur dioxide concentration and with the square of the relative humidity. The present results obtained at sulfur dioxide concentrations less than 1 ppm are in general agreement with the data reported by earlier investigators.

Aerosol measurements were also made in sulfur dioxide-air mixtures; the amounts of aerosols produced in the mixture were found to be negligible.

The maximum amount of ozone formed in cyclohexene-nitrogen dioxide-air mixtures was shown to be directly proportional to a) the square root of the initial cyclohexene concentration, b) the square root of the initial nitrogen dioxide concentration, and c) the square root of the light intensity. Using the results of the present study and the data obtained by previous investigators for different types of hydrocarbons, correlations were developed which indicated quantitatively, the maximum amount of ozone which can be formed with different types of hydrocarbons.

Nuclei measurements in cyclohexene-nitrogen dioxide-air mixtures showed that the maximum number of nuclei varied directly with the square root of both the cyclohexene and the nitrogen dioxide concentrations.

The production of aerosols in cyclohexene-nitrogen dioxide-air mixtures appeared to depend only on the ratio of the initial concentrations

of cyclohexene and nitrogen dioxide. Within the accuracy of the measurements, the amount of aerosols formed seemed to be insensitive to the nitrogen dioxide concentration.

The aerosol size distributions in cyclohexene-nitrogen dioxide-air mixtures were also measured for several mixture compositions. The size distributions were found to follow closely Friedlander's universal self-preserving curve.

During the experiments with cyclohexene-nitrogen dioxide-air mixtures, the light intensity and the relative humidity were kept constant. The effects of these two parameters on the amount of ozone formed could be assessed by utilizing the results of previous investigations. The effects of the light intensity and the humidity on nuclei and aerosol formation could not be evaluated because of the lack of relevant data. Hence, the influence of light intensity and relative humidity on particulate formation merit further investigations.

Finally, it is noted that static type experiments were also performed in a 0.6 m x 1.8 m and 1.2 m tall Plexiglas irradiation chamber. The results obtained from these tests were unrepeatable and were scattered widely. The exact reasons for the scatter in the data are unknown. It is strongly suggested, however, that the scatter was caused by the fact that the chamber could not be cleaned thoroughly before each test. Although the chamber was flushed with clean air several times prior to each test, such flushing did not seem to clean the system adequately. This conclusion is supported by the observation that in the flow type experiments, up to seven days of continuous flushing was needed to achieve a 'clean' chamber (Section III).

APPENDIX A

LITERATURE SURVEY

In the experiments performed in the past to study photochemical reactions, the following procedure was generally used. The gas mixture was introduced into a container. The mixture was then irradiated and some products of the reaction were monitored. The source of irradiation was either natural sunlight or artificial ultraviolet light. The gas mixtures either stayed inside the container during the entire experiment (static type experiment) or flowed through the container at a steady rate (flow type experiment).

In this survey, only those experiments are summarized in which the measurements of ozone (or oxidant, see below) and particulates were of primary interest. Accordingly, this survey is divided into two parts. The first part describes experiments in which the measurement of ozone (or oxidant) was the major concern. The second part describes experiments in which the production of particulates were investigated. The results of the various studies are presented in chronological order.

Ozone

Here the results of those previous investigations are included in which the amount of either ozone or oxidant was measured. This is because the formation processes of the oxidant and of the ozone are very similar [8,69]. Moreover, in a major portion of the existing literature measurements of the oxidant and not ozone were reported. It is, therefore, both desirable and advantageous to include these reports in the survey.

Haagen-Smit [50] was among the first to study the photochemical reaction in hydrocarbon-nitrogen oxides-air mixtures. He investigated the formation of ozone in a series of static type experiments in which the gas mixture was placed in a 0.005 m^3 Pyrex flask irradiated by fluorescent lights. The gas mixture tested was 3-methyheptane and nitrogen dioxide diluted in dry oxygen. Haagen-Smit varied the initial concentrations of 3-methyheptane (0.1 to 10,000 ppm) and of nitrogen dioxide (0.04 to 400 ppm). In the report, he also presented measurements in which natural sunlight and air were used instead of the fluorescent lights and oxygen. In all these experiments, the amounts of ozone generated were inferred from the crack depths of the rubber strips placed inside the flask and irradiated for ten hours.

Scott [47] performed static type experiments in which the gas mixture was placed in a long-path infrared absorption cell irradiated by a mercury lamp. The experiments were performed for two initial concentrations of 3-methyheptane (3 and 40 ppm). The initial nitrogen dioxide concentration was varied from 0.1 to 8 ppm. For each mixture composition, the amount of ozone generated was monitored as a function of the irradiation time (up to six hours).

Barton and Bolze [29] performed a series of static type experiments in which the hydrocarbon-nitrogen dioxide-air mixture was placed in a 62 m^3 glass chamber irradiated by natural sunlight. The initial concentrations were usually 0.3 and 0.6 ppm for the hydrocarbon and 0.6 and 1.2 ppm for the nitrogen dioxide. Barton and Bolze tested over thirty different types of hydrocarbons which included paraffins, straight and branched olefins, cyclo-olefins, diolefins, aromatics as well as commer-

ctal solvents. Besides measuring the oxidant and the nitrogen oxides concentrations during the tests, eye irritation measurements were also taken.

Altshuller and Cohen [2] performed static type experiments in 0.09 m^3 teflon bags irradiated by fluorescent lamps. They studied the photochemical reactions in ethylene-nitric oxide-air mixtures by varying the initial concentrations of ethylene (0.1 to 5 ppm) and of nitric oxide (0.2 to 10 ppm). In addition to measuring the amount of oxidant generated, Altshuller and Cohen also monitored the concentrations of ethylene, nitrogen dioxide, carbon monoxide, and formaldehyde during the tests.

Glasson and Tuesday [25] performed static type experiments. The hydrocarbon-nitric oxide-air mixture was placed in a long-path infrared absorption cell irradiated by fluorescent lights. Glasson and Tuesday varied the initial concentration of nitric oxide from 0.05 to 3 ppm. For the five hydrocarbon tested (propylene, ethylene, trans-2-butene, isobutane, and m-xylene), the initial concentrations most often used were 1 and 2 ppm. In their experiments, Glasson and Tuesday measured the formation rate of ozone, the oxidation rate of hydrocarbon and the concentration of peroxyacetyl nitrate.

Romanovsky et. al. [51] performed static type experiments in a 12 m^3 glass aluminum chamber irradiated by fluorescent lamps. The mixture investigated was propylene and nitric oxide in air. The initial concentration of propylene was varied from 0 to 8 ppm and that of nitric oxide was varied from 0 to 4 ppm. During the experiments, the amounts of oxidant, nitrogen oxides, propylene, and formaldehyde were monitored and eye irritation was also studied.

Altshuller et. al. [5] performed both static type and flow type experiments in a 95 m^3 aluminum chamber irradiated by fluorescent lamps. In the propylene-nitric oxide-air mixture studied, the initial concentration of propylene was varied from 0.25 to 1 ppm and the nitric oxide initial concentration was varied from 0.125 to 4 ppm. The concentrations of oxidant, nitrogen dioxide, carbon monoxide, methyl nitrate, and the aldehydes were all monitored.

Stephens and Price [58] performed flow type experiments in a 0.141 m^3 Pyrex tube irradiated by fluorescent lamps. The initial concentration of cis-2-butene was varied from 0 to 2.4 ppm while the nitric oxide concentrations used were 0.05, 0.125, 0.25, and 0.5 ppm. Stephens and Price measured the amounts of oxidant, nitrogen dioxide, methyl nitrate, and peroxyacetyl nitrate during these tests.

Bufalini and Altshuller [10] performed static type experiments in which hydrocarbon-nitric oxide-air mixtures were placed in a 0.077 m^3 Pyrex flask irradiated by fluorescent lamps. The hydrocarbons tested were 2-3 dimenyl-2-butene, 1-butene, n-butane, and 1,3,5-trimethylbenzene. The initial concentrations of the hydrocarbon were varied such that the ratio of the hydrocarbon concentration to the nitric oxide concentration ranged from 0 to 5. The parameters measured included the amount of oxidant formed, the percent of hydrocarbon reacted, and the nitrogen dioxide dosage produced.

Altshuller et. al. [6] performed static type experiments in which paraffinic hydrocarbon-nitric oxide-air mixtures were placed in a 95 m^3 aluminum chamber irradiated by fluorescent lamps. Of the eight paraffins studied, n-butane was most frequently tested. The initial concentration of n-butane was kept at 3 and 6 ppm while the nitric oxide concen-

tration was varied from 0 to 2.4 ppm. In their experiments Altshuller et. al. monitored the amounts of oxidant, nitrogen dioxide, aldehydes, peroxyacetyl nitrate, and methyl nitrate, and also studied the eye irritation effect as well as the damage incurred in Pinto Bean plants.

Using the apparatus in reference [6], Altshuller et. al. [7] also studied the photochemical reaction in aromatic hydrocarbon-nitric oxide-air mixtures. The initial concentrations of the two aromatics studied (toluene and m-xylene) were kept at 1.5, 3, and 4.5 ppm while the nitric oxide initial concentration was varied from 0.2 to 1.5 ppm. Altshuller et. al. measured the dosages of the oxidant, nitrogen dioxide and peroxyacetyl nitrate and evaluated eye irritation effects.

Kopczynski et. al. [41] used the same apparatus as Altshuller et. al. [6,7]. Kopczynski et. al. investigated the photochemical reaction in aldehyde-nitric oxide-air mixtures. The initial concentrations of the three aldehydes tested (formaldehyde, acetaldehyde and propionaldehyde) were kept at 3 ppm while the initial nitric oxide concentration was varied from 0.1 to 1.6 ppm. In this investigation the concentrations of the oxidant, hydrocarbon, nitrogen dioxide and peroxyacetyl nitrate were monitored and the eye irritation effect was studied.

In general, the results of all the previous investigations showed that, for a given initial hydrocarbon concentration, the amount of ozone produced first increased with the initial nitrogen oxides concentration, reached a peak, and then decreased with further increase in the nitrogen oxides concentration. When the initial nitrogen oxides concentration was kept fixed and the initial hydrocarbon concentration was varied, the amount of ozone produced also first increased with the initial

hydrocarbon concentration, reached a peak, and then decreased with further increase in the initial hydrocarbon concentration. Comprehensive quantitative comparisons and correlations of the results were not attempted in these investigations.

Particulates

Particulate formation has been studied in many different types of gas-air mixtures and the particles formed have been generally classified under two categories. "Condensation nuclei" are particles whose diameters lie between 2 nm and 0.1 μm and "aerosols" are particles whose diameters are greater than 0.1 μm. Condensation nuclei were usually detected and measured by condensation nuclei counters (e.g. General Electric Condensation Nuclei Counter). Aerosols were frequently detected and measured by aerosol light scattering photometers (e.g. Royco Particle Counter).

The formation of particles during the photooxidation of sulfur dioxide-air mixtures were studied by several investigators [11,14,17, 24,40,48,49]. Gerhard and Johnstone [24] performed static type experiments in a 0.008 cm^3 Lucite chamber irradiated by a sun lamp. The initial sulfur dioxide concentrations were 5, 10, 20, and 30 ppm. The relative humidity was varied from 32 to 91% and the length of irradiation time from 15 minutes to 6 hours. Gerhard and Johnstone measured the amount of sulfuric acid drops collected on a high velocity impactor.

Dunham [17] performed two static type tests to demonstrate the photooxidation mechanism in sulfur dioxide-air mixtures. In the first test, sulfur dioxide was introduced into a quartz tube containing ozone-rich air, while the ultraviolet light was turned off. In the second test, a sulfur dioxide-air mixture in the quartz tube was irradiated by

an ultraviolet light. Dunham found that nuclei was formed only in the second test and concluded that nuclei formation was due to the photo-oxidation of sulfur dioxide.

Renzetti and Doyle [49] performed flow type experiments in a 0.05 m^3 Pyrex flask irradiated by mercury lamps. The initial sulfur dioxide concentration was varied from 0 to 0.5 ppm. Relative humidities of 0 and 50% were used. The residence time of the gas-air mixture inside the flask was kept at either 17 or 27 minutes. Particulate formation was measured by an aerosol counter photometer and a nuclei counter.

Quon et. al. [48] performed a series of static type experiments in 0.014 m^3 Saran bags irradiated by fluorescent lamps. The initial sulfur dioxide concentration was varied from 0.202 to 0.647 ppm, the relative humidity from 13 to 77%, and the length of the irradiation time from 30 to 240 seconds. The amount of nuclei formed was measured by a condensation nuclei counter.

Cox and Penkett [13] performed static type experiments in a 0.216 m^3 aluminum chamber irradiated by natural sunlight. Sulfur dioxide at various initial concentrations (0.08 to 0.76 ppm) were tested. Cox and Penkett did not report the relative humidity in the tests.

Cox [14] performed flow type experiments in a 0.005 m^3 Pyrex flask irradiated by a mercury lamp. The initial sulfur dioxide concentration was varied from 5 to 1000 ppm. The relative humidities tested were 1, 5, 24, and 80%. The residence time of the gas mixture inside the flask was fixed at 150 seconds. The number of nuclei formed was measured during the tests.

Eschmond et. al. [40] performed a series of static type experiments in three different chambers irradiated by fluorescent lamps. Two of the chambers were 0.25 and 1.7 m^3 teflon bags, the third one was a 600 m^3 steel chamber whose interior surfaces were lined with a specially formulated fluoro-epoxy polymer. Various initial sulfur dioxide concentrations (from 0.049 to 2.88 ppm) and relative humidities (from 11 to 77%) were used in the experiments. The particulates produced were measured by a Whitby Aerosol Analyzer and a General Electric Condensation Nuclei Counter.

The results from the investigations described above all agreed that the number of nuclei produced increased with the initial sulfur dioxide concentration. However, the exact relationship between the number of nuclei produced and the initial sulfur dioxide concentration still remains unclear. There is also disagreement among the reports on the effect of the relative humidity on the production of the condensation nuclei. Some studies showed that the number of nuclei produced increased with humidity [14,49]; others found that there was no humidity effect [24,48].

Experiments on particulate formation in hydrocarbon-nitrogen oxides-air mixtures were reported in references [29,47,49,59]. Using the apparatus described before, Renzetti and Doyle [49] studied aerosol production in 18 different types of hydrocarbons. The same initial concentration (3 ppm hydrocarbon, 1 ppm nitric oxide and 50% relative humidity) was used in each test for each hydrocarbon. Renzetti and Doyle used an aerosol counter photometer to measure the amount of light scattered by the aerosols.

Frager et. al. [47] performed static type experiments in a long-path infrared absorption cell irradiated by mercury lamps, with 10 ppm hydrocarbon, 5 ppm nitrogen dioxide and 100 ppm water vapor. Altogether Frager et. al. tested 17 different types of hydrocarbons for aerosol production. They used a Sinclair-Phoenix smoke photometer to measure the amount of light scattered by the aerosols.

Stevenson et. al. [59] performed flow type experiments in a 0.125 m^3 Pyrex tube irradiated by fluorescent lamps. Selected initial concentrations of five hydrocarbons and nitrogen dioxide were tested. The amounts of particulates formed were measured by a nuclei counter and a Sinclair-Phoenix smoke photometer.

Groblicki and Nebel [29] performed static type experiments in a 0.5 m^3 stainless steel chamber irradiated by fluorescent lamps. Five different hydrocarbons were used in the hydrocarbon-nitric oxide-air mixture for the production of particulates. The initial hydrocarbon and nitric oxide concentrations were always 4 ppm and 2 ppm respectively. Groblicki and Nebel used a condensation nuclei counter and a Sinclair-Phoenix smoke photometer in their particulate measurements.

A total of over 40 different types of hydrocarbons were studied for particulate formation in the investigations listed above [29,47,49,59]. The general conclusion reached by the previous studies was that only highly branched olefins, cyclo-olefins and diolefins were capable of producing large quantities of particles.

Investigations were made to study the effect of adding sulfur dioxide to hydrocarbon-nitrogen oxides-air mixtures [27,29,47,49,51,59]. Groblicki and Nebel [29], Frager et. al. [47], Renzetti and Doyle [49], and Stevenson et.al. [59] all introduced known concentrations of sulfur

dioxide into the hydrocarbon-nitrogen oxides-air mixtures and measured the amounts of particulates formed. Schuck et. al. [53] performed static type experiments in a 14.7 m^3 glass chamber irradiated by a combination of mercury lamps and fluorescent lamps. Schuck et. al. measured the aerosol light scattering produced in an air mixture containing 1 ppm 2-methyl-2-butene, 1 ppm nitric oxide, and 0.1 ppm sulfur dioxide at various relative humidities. Other types of hydrocarbons (ethylene, acetylene, isobutylene, and formaldehyde) were also tested for particulate formation. Goetz and Fueschel [27] performed flow type experiments in which 1-octene-nitrogen dioxide-sulfur dioxide-air mixtures were placed in a 0.010 m^3 glass tube irradiated by fluorescent lamps. The initial concentrations of 1-octene and nitrogen dioxide were kept at 80 and 60 ppm respectively. The initial sulfur dioxide concentrations used were 2, 15, and 60 ppm and the relative humidity was changed from 15 to 70%. Goetz and Fueschel measured the aerosols by means of a Royco Particle Counter and an aerosol spectrometer.

The results of these investigations showed that, in general, sulfur dioxide would enhance the production of particulates in a hydrocarbon-nitrogen oxides-air mixture.

There have been very few experiments performed to determine the chemical compositions of the photochemical particles. The particulates formed in sulfur dioxide-air mixtures have been found to be sulfuric acid [13,14,24,48]. The exact chemical compositions of the particulates formed in hydrocarbon-nitrogen oxides-air mixtures and in hydrocarbon-nitrogen oxides-sulfur dioxide-air mixtures are not well known, although a few measurements have indicated that the particulates are predominantly nitrates and sulfates [18,29,47].

APPENDIX B

CERTIFIED CONCENTRATION OF TEST GASES

Test Gas	Concentration, ppm	Supplier
Nitrogen Dioxide	205	Air Products & Chemicals Company
Cyclohexene	219	Matheson Gas Company
Sulfur Dioxide	208	Matheson Gas Company

APPENDIX C

ESTIMATION OF PARTICLE LOSSES DUE TO SETTLING, COAGULATION AND DIFFUSION

Particles may be lost along the irradiation tunnel and along the sampling line between the sampling stations and the particle counters. Table C.1 lists the flow conditions in the tunnel and in the sampling line. The "residence time", (defined as the average time during which the gas-air mixture stays in the tunnel or in the sampling line) is obtained by dividing the length of the tunnel or the sampling line by the corresponding mean flow velocity. The Reynolds numbers in both flow situations are low and the flows are essentially laminar (Table C.1).

C.1 Loss Due to Settling

The settling velocities of very small particles settling under the action of gravity are given in reference [23]. The distance travelled by a particle falling under the action of gravity in a certain time is equal to the product of the settling velocity and the time. Table C.2 lists the settling velocities and the vertical distances travelled by different size particles during a time interval equal to the residence time both in the tunnel and in the sampling line. Particles deposit on the lower part of the inside surface of the tube when the distance fallen is larger than the inside diameter of the tube. The inside diameters of the tunnel and the sampling line are 15.2 and 0.635 cm respectively. These distances are larger than the distances travelled by particles less than ~ 1 μm in diameter. Thus, losses due to settling is negligible for particles less than ~ 1 μm in diameter.

Table C.1 Flow Conditions in the Tunnel and in the Sampling Line

	Diameter cm	Length cm	Flowrate $cm^3 s^{-1}$	Mean Flow Velocity $cm\ s^{-1}$	Residence Time s	Reynolds Number
Tunnel	15.2	912	46	0.255	3,580	24
Sampling Line	0.635	120	4.72	14.9	8.1	59

Table C.2 Estimation of the Vertical Distance Travelled by Different Size Particles Due to Gravity During Residence Time in the Tunnel and in the Sampling Line

Particle Diameter μm	Settling velocity* $cm\ s^{-1}$	Distance Travelled, cm Tunnel	Sampling Line
$2x10^{-3}$	$7.11x10$	$4.7x10^{-3}$	$1x10^{-5}$
$4x10^{-3}$	$2.62x10$	$1.4x10^{-3}$	$2x10^{-5}$
$1x10^{-2}$	$8.61x10$	$1.4x10^{-2}$	$5x10^{-5}$
$2x10^{-2}$	$1.37x10^{2}$	$4.9x10^{-2}$	$1.1x10^{-4}$
$1x10^{-1}$	$8.61x10^{2}$	$1.1x10^{-1}$	$2x10^{-4}$
$2x10^{-1}$	$2.24x10^{3}$	$0.1x10^{-1}$	$1.0x10^{-3}$
1	$1.47x10^{4}$	$1.2x10$	$2.0x10^{-3}$
2	$1.7x10^{5}$	$4.6x10$	$1x10^{-1}$

Tunnel Diameter=15.2 cm
Sampling Line Diameter=0.635 cm

* from Table 12 in reference [2.]

C.2 Loss Due to Coagulation

The number of particles also decreases due to coagulation with the passage of time. For particles initially of the same size, it can be shown that the number of particles n_t after time t, is related to the initial number n_0 by the expression

$$\frac{n_t}{n_0} = \frac{1}{1 + Kn_0 t} \qquad (C.1)$$

where K is the coagulation constant [23]. Table C.1 lists the coagulation constants for different particle sizes. In order to compute the value n/n_0, t is assumed to be equal to the residence time and n_0 is assumed to be 10^3 particles cm^{-3}. It is found that, for every particle size, the value n/n_0 calculated from eq. (C.1) is very close to one. Hence, the loss due to coagulation is negligible for all sizes of particles that may be present in the gas-air mixture.

C.3 Loss Due to Diffusion

Particles may also be lost due to diffusion to the inside surface of a tube. An expression was given in reference [23] for the diffusion of particles in a laminar flow inside a circular tube. If n_0 is the initial particle concentration, n the particle concentration after passing through a tube of radius R and length L, U the mean flow velocity in the tube, and D the diffusion coefficient of the particle, then n/n_0 is given by

$$\frac{n}{n_0} = 1 - 2.56\mu^{2/3} + 1.2\mu + 0.177\mu^{4/3} \qquad (C.2)$$

where μ is a dimensionless parameter equal to DL/UR^2. Calculations have been made for various particle sizes using eq. (C.2) and the re-

Table C.3 Calculation of Particle Loss due to Coagulation
$n_0 = 10^3$ particles cm^{-3}, t=1,500 s (tunnel), t=0.1 s (sampling line)

Particle Diameter, μm	Coagulation Constant,* $\times 10^{10}$ $cm^3 s^{-1}$
2×10^{-3}	4.5
4×10^{-3}	6
1×10^{-2}	9
2×10^{-2}	12
1×10^{-1}	7.2
2×10^{-1}	5.2
1	1.4
2	1.2

* From table 20 in reference [23]

Table C.4 Calculation of Particle Loss due to Diffusion

Particle Diameter, μm	Diffusion Coefficient,* D $cm^2 s^{-1}$	Tunnel		Sampling Line	
			n/n_0		n/n_0
2×10^{-3}	1.28×10^{-2}	8×10^{-1}	≈ 0	1.02	≈ 0
4×10^{-3}	1.71×10^{-3}	2.2×10^{-1}	0.45	6.6×10^{-1}	0.3
1×10^{-2}	5.28×10^{-4}	3.4×10^{-2}	0.78	4.2×10^{-2}	0.74
2×10^{-2}	1.35×10^{-4}	8.4×10^{-3}	0.90	1.1×10^{-2}	0.89
1×10^{-1}	8.02×10^{-6}	5.2×10^{-4}	0.99	5.32×10^{-4}	0.98
2×10^{-1}	2.21×10^{-6}	1.3×10^{-4}	0.99	1.3×10^{-4}	0.99
1	2.78×10^{-7}	1.7×10^{-5}	≈ 1.0	2.2×10^{-5}	≈ 1.0
2	1.22×10^{-7}	7.5×10^{-6}	≈ 1.0	1.0×10^{-5}	≈ 1.0

* From table 11 in reference [23]

sults are presented in Table C.4. It is seen that the loss of aerosols (particle diameter $\geq 0.1\ \mu m$) due to diffusion is negligible. However, for the very small particles (particle diameter $\leq 0.01\ \mu m$) which fall into the condensation nuclei category, the loss due to diffusion is appreciable. Nearly all the particles whose diameters are about $0.002\ \mu m$ appear to be lost due to diffuston. A correction for this effect was not made to the present data since the size distribution of the condensation nuclei was not measured. The measurable range of the condensation nuclei counter is from $0.002\ \mu m$ to $0.1\ \mu m$. The loss due to diffusion of the larger size particles recorded by the nuclei counter is seen to be small (Table C.4).

Appendix I Estimated Peak Values of Ozone, Nuclei and Aerosols for Different Initial Mixture Compositions

$[NO_2]_0$ ppm	$[C_6H_{10}]_0$ ppm	$[O_3]$ ppm	Nuclei no. cm^{-3}	Aerosols no. cm^{-3}
0.6	0.5	0.3	250	0.0
0.6	1.0	0.6	550	0.0
0.6	1.25	0.7	650	0.0
0.6	2.0	0.65	580	99
0.6	3.0	0.50	450	310
0.6	5.0	0.33	350	424
0.6	10.0	0.185	250	389
0.6	20.0	0.1	$\leq$ 200	800
1.0	0.5	0.17	$\leq$ 200	0.0
1.0	1.0	0.375	350	0.0
1.0	2.0	0.9	700	14
1.0	3.0	1.0	750	247
1.0	5.0	0.80	550	565
1.0	10.0	0.38	400	636
1.0	20.0	0.19	300	565
2.0	0.5	0.0	$\leq$ 200	0.0
2.0	1.0	0.15	$\leq$ 200	0.0
2.0	2.0	0.585	450	0.0
2.0	3.0	0.90	700	2.0
2.0	5.0	1.3	900	166
2.0	10.0	0.81	650	395
2.0	20.0	0.42	450	565
2.0	50.0	0.16	$\leq$ 200	353

Appendix C (continued)

$[SO_2]_0$ ppm	$[C_6H_{10}]_0$ ppm	$[O_3]$ ppm	Nuclei no. cm^{-3}	Aerosol no. cm^{-3}
3.0	0.5	0.0	< 200	0.0
3.0	1.0	0.0	< 200	0.0
3.0	2.0	0.2	350	0.0
3.0	3.0	0.52	600	0.0
3.0	5.0	1.2	1000	10
3.0	7.5	1.67	1200	46
3.0	10.0	1.33	1100	343
3.0	20.0	0.72	600	424
3.0	30.0	0.46	500	406
5.0	0.5	0.0	< 200	0.0
5.0	1.0	0.0	< 200	0.0
5.0	2.0	0.0	< 200	0.0
5.0	3.0	0.0	400	0.0
5.0	5.0	0.48	700	0.0
5.0	10.0	1.87	1500	166
5.0	12.5	2.0	1800	152
5.0	20.0	1.42	1600	290
5.0	30.0	0.88	1000	636
5.0	50.0	0.46	650	707
10.0	0.5	0.0	< 200	0.0
10.0	1.0	0.0	< 200	0.0
10.0	2.0	0.0	< 200	0.0
10.0	3.0	0.0	< 200	0.0
10.0	5.0	0.0	400	0.0
10.0	10.0	0.0	800	0.3
10.0	15.0	0.70	1500	0.0
10.0	20.0	1.55	2200	81
10.0	25.0	1.8	2600	60
10.0	30.0	1.6	2200	187
10.0	50.0	1.05	1400	250

REFERENCES

1. Altshuller, A.P., and Cohen, I.R., "Structural Effects on the Rate of Nitrogen Dioxide Formation in the Photo-Oxidation of Organic Compound-Nitric Oxide Mixtures in Air," International Journal of Air and Water Pollution, 7, 787-797 (1963).

2. Altshuller, A.P., and Cohen, I.R., "Atmospheric Photo-oxidation of the Ethylene-Nitric Oxide System," International Journal of Air and Water Pollution, 8, 611-632 (1964).

3. Altshuller, A.P., Klosterman, L.L., Leach, F.W., Kinosel, I.J., and Sigsby, J.E., Jr., "Products and Biological Effects from Irradiation of Nitrogen Oxides with Hydrocarbons or Aldehydes Under Dynamic Conditions," International Journal of Air and Water Pollution, 10, 81-98 (1966).

4. Altshuller, A.P., "Reactivity of Organic Substances in Atmospheric Photooxidation Reactions," International Journal of Air and Water Pollution, 10, 713-733 (1966).

5. Altshuller, A.P., Kopczynski, S.L., Lonneman, W.A., Becker, F.L., and Slater, R., "Chemical Aspects of the Photooxidation of the Propylene-Nitrogen Oxide System," Environmental Science and Technology, 1, 899-914 (1967).

6. Altshuller, A.P., Kopczynski, S.L., Wilson, D., Lonneman, W., and Sutterfield, F.D., "Photochemical Reactivities of n-Butane and Other Paraffinic Hydrocarbons," Journal of the Air Pollution Control Association, 19, 787-790 (1969).

7. Altshuller, A.P., Kopczynski, S.L., Lonneman, W.A., Sutterfield, F.D., and Wilson, D.L., "Photochemical Reactivities of Aromatic Hydrocarbon-Nitrogen Oxide and Related Systems," Environmental Science and Technology, 4, 44-50 (1970).

8. Altshuller, A.P., and Bufalini, J.J., "Photochemical Aspects of Air Pollution: A Review," Environmental Science and Technology, 5, 39-64 (1971).

9. Bufalini, J.J., and Altshuller, A.P., "The Effect of Temperature on Photochemical Smog Reactions," International Journal of Air and Water Pollution, 7, 769-771 (1963).

10. Bufalini, J.J., and Altshuller, A.P., "Oxidation of Nitric Oxide in the Presence of Ultraviolet Light and Hydrocarbons," Environmental Science and Technology, 1, 669-672 (1967).

11. Carturight, L., Jayanty, R., and Stidmore, J.F., "The Study of Air Pollution with the Electron Microscope," Quarterly Journal of the Royal Meteorology Society, 90, 357-364 (1964).

12. Clyne, M.A.A., Thrush, B.A., and Wayne, R.P., "Kinetics of the Chemiluminescent Reaction between Nitric Oxide and Ozone," Transaction of the Faraday Society, 60, 359-370 (1964).

13. Cox, R.A., and Penkett, S.A., "The Photooxidation of Sulfur Dioxide in Sunlight," Atmospheric Environment, 4, 425-433 (1970).

14. Cox, R.A., "Particle Formation from Homogeneous Reactions of Sulfur Dioxide and Nitrogen Dioxide," Tellus, 26, 235-240 (1974).

15. Leonardian, E.L., Kerr, J.A., and Calvert, J.G., "The Mechanism of Photochemical Smog Formation," in Advances in Environmental Science and Technology, edited by Pitts, J.N., Metcalf, R.L., and Lloyd, A.C., 4, 1-262 (1974), John Wiley & Sons, New York.

16. Dimitriades, B., "Methodology in Air Pollution Studies Using Irradiation Chambers," Journal of the Air Pollution Control Association, 17, 460-466 (1967).

17. Dunham, S.G., "Detection of Photochemical Oxidation of Sulfur Dioxide by Condensation Nuclei Techniques," Nature, 188, 51-52 (1960).

18. Endow, N., Doyle, G.J., and Jones, J.I., "The Nature of Some Model Photochemical Aerosols," Journal of the Air Pollution Control Association, 13, 141-147 (1963).

19. Eschenroeder, A.Q., Martinez, J.R., "Concepts and Applications of Photochemical Smog Models," in "Photochemical Smog and Ozone Reactions," edited by Gould, R.F., Advances in Chemistry Series, 113, 107-148 (1972), American Chemical Society, Washington, D.C.

20. Ford, H.W., Doyle, G.J., and Endow, N., "Rate Constants at Low Concentrations. II Reaction between Nitric Oxide and Ozone in Air at Room Temperature," Journal of Chemical Physics, 28, 1337 (1957).

21. Friedlander, S.K., "Similarity Considerations for the Particle-Size Spectrum of a Coagulating, Sedimenting Aerosol," Journal of Meterology, 17, 479-483 (1960).

22. Friedlander, S.K., and Pasceri, R.E., "Measurement of the Particle Size Distribution of the Atmospheric Aerosol: I. Introduction and Experimental Methods," Journal of Atmospheric Science, 22, 571-576 (1965).

23. Fuchs, N.A., "The Mechanics of Aerosols," The Macmillan Company, New York (1964).

24. Gerhard, E.R., and Johnstone, H.F., "Photochemical Oxidation of Sulfur Dioxide in Air," Industrial and Engineering Chemistry, 47, 972-978 (1955).

25. Glasson, W.A., and Tuesday, C.S., "Inhibition of the Atmospheric Photooxidation of Hydrocarbons by Nitric Oxide," Research Publication GMR-479, General Motors Research Laboratories, Warren, Michigan (1965).

26. Glasson, W.A., and Tuesday, C.S., "Hydrocarbon Reactivities in the Atmospheric Photooxidation of Nitric Oxide," Environmental Science and Technology, 4, 916-924 (1970).

27. Goetz, A., and Fuenchel, R., "Basic Mechanisms of Photochemical Aerosol Formation," Atmospheric Environment, 1, 265-304 (1967).

28. Goetz, A., and Kleinst, G.J., "Formation and Degradation of Aerocolloids by Ultraviolet Radiation," Environmental Science and Technology, 6, 143-151 (1972).

29. Grabitski, F.J., and Jebel, G.J., "The Photochemical Formation of Aerosols in Urban Atmospheres," in "Chemical Reactions in Urban Atmospheres," edited by Tuesday, C.S., 241-264 (1971), American Elsevier Publishing Company, New York.

30. Harkins, J., and Nicksic, S.W., "Studies on the Role of Sulfur Dioxide in Visibility Reduction," Journal of the Air Pollution Control Association, 17, 218-221 (1967).

31. Hanton, E.I., Jr., and Goltz, L.F., "Eye Irritation from Solar Radiation of Organic Compounds and Nitrogen Dioxide," Report No. 23, Air Pollution Foundation, San Marino, California (1958).

32. Hecht, T.A., and Seinfeld, J.H., "Development and Validation of a Generalized Mechanism for Photochemical Smog," Environmental Science and Technology, 6, 47-57 (1972).

33. Heuss, J.M., and Glasson, W.A., "Hydrocarbon Reactivity and Eye Irritation," Environmental Science and Technology, 2, 1109-1116 (1968).

34. Holmes, J.R., O'Brien, R.J., Bradtree, J.R., Hecht, T.A., and Seinfeld, J.H., "Measurement of Ultraviolet Radiation Intensity in Photochemical Smog Studies," Environmental Science and Technology, 7, 519-523 (1973).

35. Hyser, R.B., and Whitby, K.T., "Growth Mechanisms and Size Spectra of Photochemical Aerosols," Environmental Science and Technology, 7, 241-247 (1973).

36. Jaffe, R.D., and Smith, F.L., Jr., "Factors Affecting Reactions in Smog Chambers," Lockheed Missiles & Space Company, Inc., Sunnyvale, California. Presented at the 67th Annual Meeting of the Air Pollution Control Association, Denver, Colorado, June 13, 1974.

37. Johnston, H.S., and Crosby, D.J., "Kinetics of the Fast Gas-Phase Reaction between NO_2 and Nitric Oxide," Journal of Chemical Physics, [illegible] (1956).

38. Junge, C.E., "Atmospheric Chemistry," in Advances in Geophysics, edited by Landsberg, H.E., and Van Mieghem, J., 4, 1-101 (1958), Academic Press, New York.

39. Katz, M., and Sale, S.B., "Mechanism of Photooxidation of Sulfur Dioxide in Atmosphere," Proceedings of the Second International Clean Air Congress, edited by England, H.M., and Beery, W.T., 336-343 (1971), Academic Press, New York.

40. Koppand, W.C., Kittleson, D.B., Yang, J.Y., and Berberian, M.L., "Determination of the Formation Mechanisms and Compositions of Photochemical Aerosols," Calspan Corporation, Buffalo, New York. First Annual Summary Report, 31 August 1973. Prepared for Environmental Protection Agency, Durham, North Carolina and Coordinating Research Council, New York, NewYork.

41. Kopczynski, S.L., Altshuller, A.P., and Sutterfield, F.D., "Photochemical Reactivities of Aldehyde - Nitrogen Oxide Systems," Environmental Science and Technology, 8, 969-970 (1974).

42. Latty, J.L., "A Smog Chamber Study Comparing Blacklight Fluorescent Lamps with Natural Sunlight," Environmental Science and Technology, 5, 1218-1220 (1971).

43. Leighton, P.A., "Photochemistry of Air Pollution," Academic Press, New York (1961).

44. Littlan, D., "Formation and Destruction of Ozone in a Simulated Natural System (Nitrogen Dioxide + α -Pinene + Ir)," in "Photochemical Smog and Ozone Reactions," edited by Gould, R.F., Advances in Chemistry Series, 113, 211-211 (1972), American Chemical Society, Washington, D.C.

45. Liu, B.Y.H., and Whitby, K.T., "Dynamic Equilibrium in Self-Preserving Aerosols," Journal of Colloid and Interface Science, 26, 161-163 (1968).

46. Niki, H., Daby, E.E., and Weinstock, B., "Mechanisms of Smog Reactions," in "Photochemical Smog and Ozone Reactions," edited by Gould, R.F., Advances in Chemistry Series, 113, 16-57 (1972), American Chemical Society, Washington, D.C.

47. Prager, M.J., Stephens, E.R., and Scott, W.E., "Aerosol Formation from Gaseous Air Pollutants," Industrial and Engineering Chemistry, 58, 521-524 (1966).

48. Quon, J.E., Siegel, B.P., and Gulbert, H.E., "Particle Formation from Photooxidation of Sulfur Dioxide in Air," Proceedings of the Second International Clean Air Congress, edited by England, H.M., and Beery, W.T., 330-335 (1971), Academic Press, New York.

49. Renzetti, N.A., and Doyle, G.J., "Photochemical Aerosol Formation in Sulfur Dioxide-Hydrocarbon Systems," International Journal of Air Pollution, 2, 327-345 (1960).

50. Rogers, L.B., ed., "Proceedings of the Conference on Chemical Reactions in Urban Atmospheres," Report No. 15, Air Pollution Foundation, Los Angeles, California, 1956.

51. Romanovsky, J.C., Ingels, R.F., and Gerdom, R.J., "Estimation of Smog Effects in the Hydrocarbon-Nitric Oxide System," Journal of the Air Pollution Control Association, 17, 454-459 (1967).

52. Schofield, K., "An Evaluation of Kinetic Rate Data for Reactions of Neutrals of Atmospheric Interest," Planetary and Space Science, 15, 643-670 (1967).

53. Schuck, E.A., Doyle, G.J., and Endow, N., "A Progress Report on the Photochemistry of Polluted Atmospheres," Report No. 31, Air Pollution Foundation, San Marino, California, 1966.

54. Schuck, E.A., and Stephens, E.R., "Oxides of Nitrogen," in Advances in Environmental Science and Technology, edited by Pitts, J.N., and Metcalf, R.L., 1, 73-117 (1969), John Wiley & Sons, New York.

55. Seinfeld, J.H., Hecht, T.A., and Roth, P.F., "Existing Needs in the Experimental and Observational Study of Atmospheric Chemical Reactions," Report No. EPA-R4-73-021, Systems Applications, Inc., Beverly Hills, California, Prepared for U.S. Environmental Protection Agency, 1973.

56. Stedman, D.H., Daby, E.E., Stuhl, F., and Niki, H., "Analysis of Ozone and Nitric Oxide by a Chemiluminescent Method in Laboratory and Atmospheric Studies of Photochemical Smog," Journal of the Air Pollution Control Association, 22, 260-263 (1972).

57. Stedman, D.H., and Niki, H., "Photolysis of NO_2 in Air as Measurement Method for Light Intensity," Environmental Science and Technology, 7, 735-739 (1973).

58. Stephens, E.R., and Price, P.A., "Atmospheric Photochemical Reactions in a Tube Flow Reactor," Atmospheric Environment, 3, 673-686 (1969).

59. Stevenson, H.J.R., Sanderson, D.E., and Altshuller, A.P., "Formation of Photochemical Aerosols," International Journal of Air and Water Pollution, 3, 367-375 (1965).

60. Tuesday, C.S., "The Atmosphere Photooxidation of trans-Butene-2 and Nitric Oxide," in "Chemical Reactions in the Lower and Upper Atmosphere," edited by Cadle, R.D., 1-49 (1961), Interscience, New York.

61. Wayne, L.G., Weisburd, M., Danchik, E., and Tokin, A., "Final Report-Development of a Simulation Model for Estimating Ground-Level Concentrations of Photochemical Pollutants," Technical Memorandum, System Development Corporation, Santa Monica, California, (1973).

66. Westberg, K., and Cohen, N., "The Chemical Kinetics of Photochemical Smog as Analyzed by Computer," AIR-7(1)(10/7)-1, The Aerospace Corporation, El Segundo, California (1967).

67. Wilson, W.E., Jr., Ferryman, T.L., and Levy, A., "A Literature Survey of Aerosol Formation and Visibility Reduction in Photochemical Smog," Battelle Memorial Institute, Columbus, Ohio, Project EF-2, August 1, 1969, Prepared for the American Petroleum Institute, Committee for Air and Water Conservation.

68. Wilson, W.E., Jr., Levy, A., and Wiener, B.B., "A Study of Sulfur Dioxide in Photochemical Smog II. Effect of Sulfur Dioxide on Oxidant Formation in Photochemical Smog," Journal of the Air Pollution Control Association, 22, 27-32 (1972).

69. Wilson, W.E., Jr., Ferryman, T.L., Levy, A., and Taliaferro, B.B., "Aerosol Formation in Photochemical Smog I. Effect of Stirring," Journal of the Air Pollution Control Association, 21, 128-132 (1971).

70. "Air Quality Criteria for Particulate Matter," National Air Pollution Control Administration, Publication No. AP-49, 1969, U.S. Department of Health, Education, and Welfare, Washington, D.C.

71. "Air Quality Criteria for Sulfur Oxides," National Air Pollution Control Administration Publication No. AP-50, January 1969, U.S. Department of Health, Education, and Welfare, Washington, D.C.

72. "Air Quality Criteria for Nitrogen Oxides," Pollution Control Office Publication No. AP-84, 1971, U.S. Environmental Protection Agency, Washington, D.C.

73. "Air Quality Criteria for Photochemical Oxidants," National Air Pollution Control Administration Publication No. AP-63, 1970, U.S. Department of Health, Education and Welfare, Washington, D.C.

74. "Air Quality Criteria for Hydrocarbons," National Air Pollution Control Administration Publication No. AP-64, 1970, U.S. Department of Health, Education and Welfare, Washington, D.C.